NERO

NUUK ECOLOGICAL RESEARCH OPERATIONS

8th Annual Report 2014

GEM

Greenland Ecosystem Monitoring

Aarhus University

DCE – Danish Centre for Environment and Energy

NUUK ECOLOGICAL RESEARCH OPERATIONS

8th Annual Report 2014

This report is dedicated to Lillian Magelund Jensen, who passed away far too early. Lillian's dedication to the work in the Greenland Ecosystem Monitoring Programme is greatly missed. All honour to her memory.

AARHUS UNIVERSITY
DCE – DANISH CENTRE FOR ENVIRONMENT AND ENERGY

Data sheet

Title: Nuuk Ecological Research Operations
Subtitle: 8th Annual Report 2014

Editors: Lillian Magelund Jensen(†), Elmer Topp-Jørgensen and Torben R. Christensen
Department of Bioscience, Aarhus University

Publisher: Aarhus University, DCE – Danish Centre for Environment and Energy
URL: http://dce.au.dk

Year of publication: 2016

Please cite as: Jensen, L.M., Topp-Jørgensen, E. and Christensen, T.R. (Eds.) 2016. Nuuk Ecological Research Operations 8th Annual Report, 2014, Aarhus University, DCE – Danish Centre for Environment and Energy. 86 pp.

Layout and drawings: Tinna Christensen and Juana Jacobsen, Department of Bioscience, Aarhus University
Front cover photo: Katrine Raundrup
Back cover photo: (top to bottom): Jakob Abermann, Louise H. Rasmussen, Bula Larsen, Thomas Juul-Pedersen and Michele Citterio

ISSN: 1904-0407
ISBN: 978-87-93129-38-2

Number of pages: 86

Internet version: The report is available in electronic format (pdf) on www.nuuk-basic.dk/Publications and on www.dce.au.dk

Supplementary notes: Nuuk Basic Secretariat
Department of Bioscience, Aarhus University
P. O. Box 358, Frederiksborgvej 399
DK-4000 Roskilde

E-mail: nuuk-basic@au.dk
Phone: +45 87158657

Nuuk Ecological Research Operations (NERO) is together with Zackenberg Ecological Research Operations (ZERO) operated as a centre without walls with a number of Danish and Greenlandic institutions involved. The two programmes are gathered under the umbrella organization Greenland Ecosystem Monitoring (GEM). The following institutions are involved in NERO:
Department of Bioscience, Aarhus University: GeoBasis, BioBasis and MarineBasis programmes
Greenland Institute of Natural Resources: BioBasis and MarineBasis programmes
Asiaq – Greenland Survey: ClimateBasis programme
University of Copenhagen: GeoBasis programme

The programmes are coordinated by a secretariat at the Department of Bioscience at Aarhus University, and are financed with contributions from:
The Danish Energy Agency
The Environmental Protection Agency
The Government of Greenland
Private foundations
The participating institutions

(†) 14 February 2016

Contents

Summary for policy makers

Elmer Topp-Jørgensen and Torben R. Christensen

The 2014 field season in the Nuuk Basic programme started 14 January and continued until 14 November. During this period 49 scientists and logisticians spent 265 'man-days' in the study area at the Kobbefjord Station.

Five helicopter landings in Kobbefjord and 102 sailing days (74 to and from Kobbefjord and 28 for Marine Basis) took place during 2014. 514 liters of gasoline and 6450 liters freshwater were consumed, while 500 kg of waste was taken to Nuuk.

In 2014, more than nine peer-reviewed papers were publish by the researchers from the Nuuk Basic programme and from externally funded research projects. Nuuk Basic participants also produced four reports, nine presentations and took part in a number of public events and outreach initiatives.

Infrastructure development

Greenland Institute of Natural Resources (GINR) received its new research boat named 'Avataq', which is expected receive final approval for operation in early 2015.

Organisational changes

Torben R. Christensen was appointed new Scientific Leader for Greenland Ecosystem Monitoring.

Data collection and significant findings

Data collection for Nuuk Basic was carried out according to the manuals for the individual sub-programmes http://nuuk-basic.dk/monitoring/.

Like Zackenberg, Kobbefjorden experienced a cold spring where April was particularly cold, 2.8 °C below average. In Nuuk, however, July temperatures were 3.0 °C warmer than normal and only 0.7 °C colder than July 2012, which was the warmest July recorded in the period 1866-2014.

The total discharge of the Kobbefjord river during the hydrological year 2013/2014 was 42.85×10^6 m^3. The peak discharge in 2014 was recorded on 14 August along with the highest ever recorded total daily precipitation (75 mm in 24 hours), showing the rapid runoff in the Kobbefjord catchments area.

Sea-ice cover in Kobbefjord developed as early as 24 October, which is the earliest registration in the seven years of monitoring in Kobbefjord. The cold spring months lead to a very late snow/ice melt and meant that the fjord was not ice-free until 1 June, which was nearly 17 days later than the normal for the six previous years.

Temperature also affect methane fluxes (a potent greenhouse gas) and interestingly, three distinct peaks appeared in the 2014 data: one in early season (25-27 June), one in mid-season (27-29 July) and one in late season (20-21 August). The early season and mid-season peaks have been observed in previous years and can possibly be explained by different sources of carbon for the methane production; i.e. old litter-derived carbon from previous growing season during first peak and recently assimilated carbon during second peak. The peak in late season has not been observed previously. The variation between years is likely related to variations in timing of snow-melt, meteorological conditions, and primary production in the fen.

In 2014, the overall number of bird observations was low for all species with fewer observations of both Lapland bunting and northern wheatears than in any previous year. The reason is unknown but could be explained by the cold spring temperatures that also affected bird numbers in Zackenberg.

Overall, the vegetation coverage in lakes has its maximum at intermediate depths due to less physical disturbance and preferable light conditions. The coverage in 2014 was lower than most of the previous years, which can be a response to cold conditions in 2013.

Isotope results from Badesø and Qassisø illustrates the differences between the food chain/food webs of the two lakes, where Badesø is holding an extra trophic level (the fish) compared to Qassi-sø. The presence of this extra trophic level forces the invertebrates to feed on a more narrow food range ($\delta^{13}C$ range).

The monthly marine monitoring program showed a seasonal pattern of physical and chemical conditions resembling previous years with the exception of an apparent lack of a deep warm coastal inflow into Godthåbsfjord, which is commonly observed during late winter.

The phytoplankton primary production showed a distinctive spring bloom and summer bloom which lasted longer than commonly observed, thus resulting in the highest integrated annual production since the first full season was recorded in 2006. The high production also resulted in some of the highest carbon vertical sinking fluxes recorded.

The phytoplankton and the zooplankton species composition showed a seasonal pattern resembling previous years, while the abundance of copepods during mid-summer was low compared to previous years.

Monitoring of benthic fauna and flora focusses on the key intertidal species the brown macroalgae 'knotted wrack' (*Ascophyllum nodosum*) and 'blue mussel' (Mytilus edulis), in relation to temperature, ice cover/light availability and tidal level. The macroalgae knotted wrack showed an almost ten-fold higher net population growth rate in 2013-14 due to an insulating layer of ice in winter, compared to the previous year (2012-13) with an ice-free winter. A lower survival of the blue mussel in the upper intertidal zone could be explained by higher maximum temperature, combined with longer air exposure.

International cooperation

Nuuk Basic plays a central role in Arctic Council's monitoring programmes; Circumpolar Biodiversity Monitoring Programme (CBMP) and Arctic Monitoring and Assessment Programme (AMAP), influencing the design of the programmes and being at the forefront of implementing protocols. CBMP has strong international linkages to global biodiversity initiatives (e.g. CBD, IPBES, GEOBON) and is the biodiversity component of the Sustaining Arctic Observing Networks (SAON). AMAP has strong international linkages to climate, ecosystem and health related initiatives, including WMO and the International Panel on Climate Change (IPCC).

In September 2014, Greenland Institute of Natural Resources (GINR) hosted the annual meeting of the marine working group of CBMP as the MarineBasis-Nuuk manager (GINR) also co-chaired of the CBMP-Marine group in 2013 and 2014. During this meeting GEM and particularly the MarineBasis-Nuuk programme was presented and promoted.

Nuuk Ecological Research Operations is engaged in numerous international scientific networks and projects to influence and implement international standards. Data is often shared in the networks to enable larger assessments and more precise predictions. All data of the 2014 season has been added to the GEM open access database, www.data.g-e-m.dk.

The Greenland Institute of Natural Resources is also involved in INTERACT (International Network for Terrestrial Research and Monitoring in the Arctic), an infrastructure network funded by the EU.

Economy

In 2014, the monitoring programme Nuuk Basic received almost 5.36 million DKK from the Danish Energy Agency and the Environmental Protection Agency for the four programmes – ClimateBasis, GeoBasis, BioBasis and MarineBasis. The funding includes means for long-term monitoring as well as analytical and strategic initiatives. On top of this, the four Nuuk Basic monitoring programmes co-funded the monitoring with more than 1.9 million DKK.

Aarhus University received 0.3 million DKK from the Danish Environmental Protection Agency for the Nuuk Basic secretariat.

A number of projects visited the Nuuk Basic area in 2014, but it is not possible to estimate the costs and income generated from these.

The Danish Environmental Protection Agency provided 0.61 million DKK in support for Nuuk Basic logistics, facilitating access for the Nuuk Basic monitoring programmes; while the external funded research projects spent approximately 2.54 million DKK on logistics handled by the station.

In 2014, one project, one researcher and six bed nights from INTERACT Transnational Access.

Executive summary

Jakob Abermann and Birger Ulf Hansen

ClimateBasis

The ClimateBasis programme is dedicated to describing the climatological and hydrological conditions in Kobbefjord. Two automatic climate stations, C1 and C2 (Station 652 and Station 653), two automatic hydrometric stations, H1 and H2 (Station 650 and Station 651), and four diver stations, H3, H4 and H5 (Stations 654, 655, 656 and 658) are located in the Kobbefjord basin.

The two climate stations are placed next to each other to ensure data continuity and fill data gaps should one of the stations fail.

The mean annual air temperature in 2014 was –0.1 °C, which is 0.3 °C below the average since the programme started in 2008. In contrast to 2013, warm summer months outweighed below average winter months. April was particularly cold with 2.8 °C below average. There was no freezing temperatures between 1 June and 26 September.

Hydrological measurements in the Kobbefjord basin started in 2006 at H1, in 2007 at H2, H3 and H4, in 2008 at H5. In 2014, a new site was chosen at Langesø, which drains into H1. Manual measurements of discharge were performed at H1 and Langesø. H1, H2 and Langesø are measuring throughout the year, while sensors at H3, H4 and H5 are set up in early spring when the rivers are free of snow and ice, and taken down in late fall before the river freezes.

For H1, which is placed at the main river in Kobbefjord, the total discharge during the hydrological year 2013/2014 was 42.85×10^6 m^3. The peak discharge in 2014 was recorded on 14 August along with the highest ever recorded total daily precipitation (75 mm in 24 hours).

GeoBasis

The 2014 season was the seventh full season for the GeoBasis programme with a field season between May and late September. However, due to cooperation with other research projects, the programme continued until late October. Data collected by the Danish Meteorological Institute showed that in 2014 the annual mean air temperature in Nuuk reached –0.6 °C, which is 0.8 °C warmer than normal. The three summer months, June-August, were all warmer than normal. The warmest month was July with 9.7 °C, which was 3.0 °C warmer than normal but 0.7 °C colder than the previous July, which was the warmest July in the period 1866-2014. The coldest month in 2014 was March with –8.8 °C, which was 1.4 °C colder than normal, but 10.8 °C warmer than the record from February 1984.

Sea-ice cover in Kobbefjord developed as early as 24 October, which is the earliest registration in the seven years of monitoring in Kobbefjord. The fjord was ice-free on 1 June, which was nearly 17 days later than the normal for the six previous years. The snow cover survey in 2014 was carried out on 8-9 April and the average snow depth for the three sites was 67 cm which was only 1 cm above the average for the three sites in the period 2009-2014. However, an average of 305 kg m^{-3} in density was well below the average of 323 kg m^{-3} for the six-year period.

At the micrometeorological station – SoilFen – in Kobbefjord in 2014, March was the coldest month with –9.4 °C, while July with 10.7 °C was the warmest month and it was 0.5 °C warmer than the average for the period 2007-2014. These measurements are in line with the air temperature measured in Nuuk located 30 km away. The M500 is placed approximately 500 m a.s.l. south of Badesø. In 2008-2014 the mean air temperature in July at the M500 station was between 6.6 °C and 10.4 °C; in

2014 it was 9.5 °C and only +0.9 °C above the average for the period. The relative humidity measured at the M500 station in the period 2008-2014 shows an annual average of 76 % with maximum values of 90-91 % during the snowmelt in April and in the cold rainy autumn from September to November. The incoming shortwave irradiance in the period 2008-2014 was between 211-295 W m^{-2} in June and in 2014 it was 232 W m^{-2} or 11 W m^{-2} below the average. The annual shortwave irradiance is 104 W m^{-2} as an average for the period 2008-2014.

In 2014, 42 water samples were collected from end May to start October which is one month shorter than previous year due to a very late snow/ice-melt. *In situ* measurements of river water temperature, conductivity and pH were conducted along with the water sampling. The minimum river water temperature was 1-2 °C from end May which was 1.0 °C lower than the previous years and the water temperature peaked with a maximum temperature of 14.8 °C at the end of July which was 1.9 °C higher and 2 weeks earlier than in 2013. The conductivity measurements showed a normal decrease in conductivity within the snow-melting period from 23-24 μSc m^{-1} to a level of 18 +/- 1.5 μSc m^{-1}. From the beginning of July and through the rest of the field season, the conductivity showed no significant trend which is normal for the period. pH showed a normal trend from 6.0 at the beginning of the field season to 7.6 at the beginning of August, followed by some variation due to rain events during the autumn.

Mean CH_4 fluxes across chambers were initially relatively high, but decreased to below 3 mg CH_4 m^{-2} h^{-1} within a few days. Interestingly, three distinct peaks appear in the measurement record: one in early season (25-27 June), one in mid-season (27-29 July) and one in late season (20-21 August). The early season and mid-season peaks have been observed in previous years and can possibly be explained by different sources of carbon for the methane production; i.e. old litter-derived carbon from previous growing season during first peak and recently assimilated carbon during second peak. The peak in late season has not been observed previously. The mid-season peak amounted to slightly above 6 mg CH_4 m^{-2} h^{-1}, a magnitude that is similar to the previous year. The variation between years is likely related to variations in timing of snow-melt, meteorological conditions, and primary production in the fen. After the late season peak, CH_4 fluxes decreased steadily and reached approximately 1 mg CH_4 m^{-2} h^{-1} in late September.

Eddy covariance measurements of the CO_2 and H_2O exchange in the fen were initiated 30 May. At the end of July, a pump broke down and due to unexpected long delivery time from the supplier, it was unfortunately not possible to resume the measurements during 2014. The fen was still snow-covered when measurements began. During the snowmelt period and pre-green season, CO_2 fluxes were generally small. Highest daily spring time emission (0.6 g C m^{-2} d^{-1}) was measured 7 June. As the vegetation developed, photosynthetic uptake of CO_2 started, and on 18 June the fen ecosystem switched from being a net source to a net sink of atmospheric CO_2 on a daily basis. The measurements during 2014 did not cover the entire net uptake period. However, between 18 June and 28 July, the fen accumulated –36.6 g C m^{-2}. Maximum daily uptake (–2.0 g C m^{-2} d^{-1}) was recorded on the last day with complete measurements (27 July). During the entire measurement period, the fen constituted a sink for atmospheric CO_2 amounting to –32.7 g C m^{-2}.

In 2011, GeoBasis installed two new energy balance stations in cooperation with the INTERACT programme. One station was located at a new site over heath vegetation and the second station was installed at the existing fen site. In 2013, GeoBasis installed a Snow Pack Analysing System (SPA) on the heath site close to the energy balance and CO_2 stations. The heath site was chosen as it is the dominating ecosystem within the drainage basin. The SPA constitutes an innovation in snow measurements as it automatically and continuously measures all relevant snow parameters such as snow depth and at three levels (10, 35 and 55 cm) snow density, snow water equivalent and contents of liquid water and ice. The remote placing of the heath site and the use of fuel cells caused numerous breaks in the time series although the station was visited frequently even outside the normal field season. In 2013, a more stable power supply was installed combining a wind generator with a nominal effect of 350 W and three 110 W solar panels. With that in place the time series recording at both the energy balance and the SPA stations have been more stable with only a few minor breaks.

The 2014 season is the seventh full year and it has provided valuable learning lessons and ensured improvements of the monitoring that will improve the programme in the following years. All methods and sampling procedures are described in detail in a new manual 'GeoBasis Manual – Guidelines and sampling procedures for the geographical monitoring programme of Nuuk Basic in Kobbefjord', which can be downloaded from http://nuuk-basic.dk/monitoring/geobasis/. All data from the GeoBasis Nuuk programme as available at http://data.g-e-m.dk/. The data will in the coming years be regularly updated after each field season.

BioBasis

Results of the eighth year of the BioBasis monitoring programme at Nuuk are presented.

Reproductive plant phenology: The reproductive phenology has been studied since 2008 on three vascular plant species: The evergreen dwarf shrub *Loiseleuria procumbens*, the herb *Silene acaulis*, and the shrub *Salix glauca*. In 2014 the recording of phenology started on 15 May and ended on 14 October. The reproductive phenology of *L. procumbens* and *S. acaulis* was comparable to that of 2013, with intermediate timing of budding, flowering and onset of senescence. However, there was a tendency to produce larger numbers of flowers in most plots. The timing of 50 % flowering was similar to previous years. The first flower buds of *S. glauca* were observed on 4 June, just two days later than the earliest year 2010 and two weeks earlier than in 2013. First flowering male and female catkins were observed on 18 June. The first female flowers with hairs were observed 17 days later than in 2013.

Vegetation greening, NDVI: The seasonal greening of the vegetation was monitored 1) in plots with *Empetrum nigrum ssp. hermaphroditum* and *Eriophorum angustifolium*, 2) in the plant phenology plots, 3) along the NERO line (Bay *et al.* 2008) and 4) in the CO_2 flux plots. *Empetrum nigrum* consistently reached high NDVI values throughout the season although the values were lower than in 2012 and 2013. All *Empetrum* plots had high NDVI values, with little variation throughout the season. *Eriophorum angustifolium* reached intermediate NDVI values compared to previous years. A peak was recorded on 18 August. Compared to the four other species, *Eriophorum* reached intermediate to high NDVI levels.
The NDVI values for *L. procumbens* were low to intermediate with only small fluctuations throughout the season. *Salix glauca* values tended to be lower in 2014 than in most other years. Low NDVI values were recorded in all four *S. acaulis* plots with little variation over time.
Along the NERO line the NDVI values were lower than in 2012 and 2013 but higher than the previous years.

Carbon dioxide exchange: Similar to earlier years, Net Ecosystem Exchange (NEE) was generally more negative (i.e. higher CO_2 uptake) in Control plots compared to plots with elevated temperature and shaded plots.
In 2014, ecosystem respiration rates (R_{eco}) from plots with elevated temperature were not consistently higher than in the control plots. Highest rates of gross primary production (GPP) were generally observed in control plots, while especially shaded plots had lower GPP rates compared with other treatments. As photosynthesis is driven by solar radiation, shading decreases GPP and build-up of biomass. Since the extensive outbreak of the larvae *Eurois occulta* in 2011, which defoliated large parts of the heath vegetation in the area, CO_2 flux magnitudes have been high in the following years. This trend was continued and further accentuated in 2014.

UV-B exclosure plots: Measurements of chlorophyll fluorescence is a measure of plant stress. The impact of ambient UV-B radiation on the vegetation was studied in a mesic dwarf shrub heath dominated by *Empetrum nigrum* and with *Betula nana* and *Vaccinium uliginosum* as subdominant species.

The exclusion of UV-B is expected to have a positive effect on the total performance index. The measurements of 2014 showed no significant positive responses. There seems to be a similar pattern through the season for the two species although the magnitude is different. This lacking of positive response is somehow unexpected; previous years have reported a positive effect on UV-B exclusion. The results may be due to other parameters influencing the performance for the plants (e.g. precipitation, cloud cover) thus inter-annual variation in light and UV-B dose.

Arthropods: In Kobbefjord, all four pitfall trap stations (each with eight traps) established in 2007 and the two window trap stations (each with two traps) established in 2010 were open during the 2014 season (4301 trap days (including 3839 pitfall trap days and 462 window trap days)). Pitfall traps were established from 20 May through 10 June and they all worked continuously until 30 September when the liquid began to freeze.

Microarthropods: Three sampling sessions for microarthropods in Kobbefjord took place at the end of June, August and September, respectively. Each sampling session consisted of three to four sampling occasions within approximately one week. The collembolan communities of the four plant communities have retained their basic characteristics (table 4.1). The *Silene* and *Loiseleuria* habitats continued to support the smallest collembolan diversity, although the total microarthropod abundance was high due to favourable conditions for opportunistic species. *Silene* was still extreme by having only 4 % collembolans and 96 % mites indicating that the replicate plots turn out to have unique environmental characteristics creating particular communities.

Bird census points: Four passerine species, Lapland bunting (*Calcarius lapponicus*), snow bunting (*Plectrophenax nivalis*), northern wheatears (*Oenanthe oenanthe*) and common redpoll (*Carduelis flammea*), were counted at 13 census points within the 32 km^2 Kobbefjord catchment area. In 2014 the overall number of observations were low for all species with fewer observations of both Lapland bunting and northern wheatears than in any previous year.

Mammals: The Kobbefjord catchment area is only sparsely populated with mammals. During the field season two sightings of caribou (possibly the same animal) and one sighting of arctic hare were recorded. There were several sightings of tracks and faeces from arctic fox, though no actual sightings were made this season.

Lakes: Water chemistry was at average levels compared to the previous monitored years. Chlorophyll levels are slightly increasing and were close to 1.0 µg Chl *a* l^{-1} in Badesø and slightly lower in Qassi-sø. The best explanation for the increasing trend in Chl *a*, is predation from fish on zooplankton causing cascading effects to phytoplankton. Zooplankton communities are generally different in Qassi-sø compared to Badesø, which is consistent with the lack of fish in Qassi-sø. Overall, the vegetation coverage has its maximum at intermediate depths due to less physical disturbance and preferable light conditions. Coverage in 2014 was lower than most of the previous years, which can be a response to cold conditions in 2013. Isotope results from Badesø and Qassi-sø illustrates the differences between the food chain/food webs of the two lakes, where Badesø is holding an extra trophic level (the fish) compared to Qassi-sø. The presence of this extra trophic level forces the invertebrates to feed on a more narrow food range ($\delta^{13}C$ range).

MarineBasis

The MarineBasis programme in Nuuk was initiated in late 2005 and this chapter presents data and results from the ninth full year of monitoring. The programme represents the marine component of the comprehensive ecosystem monitoring programme Nuuk Basic. The programme samples key oceanographic parameters including sea-ice conditions, physical and chemical oceanography, biological components of the water column and sediment as well as observations of whales and sea birds. The collected data provide essential information for understanding and describing the ecosystem. The long-time series also makes it possible to study, identify and quantify seasonal and inter-annual patterns and variability, as well as aiming to identify possible effects of climate-related changes. A parallel marine programme is operating at the high Arctic Zackenberg area (MarineBasis-Zackenberg); both programmes collaborate closely and supplement each other.

Satellite images (AMSR) showed that sea ice ('West Ice') covered most of the Baffin Bay region until May when the ice began retreating, reaching a minimum during July-September. Sea-ice formation from the north started in October, covering much of Baffin Bay by late December. Satellite images (MODIS) of the Godthåbsfjord system showed that sea ice was limited to the innermost part and smaller fjord branches, as observed in previous years. Most of the sea ice and glacial ice are melting within the fjord, but part of the ice is exported from the fjord in seasonal burst events. This seasonal pattern is monitored by a camera cross section of the fjord, unfortunately no photos were taken during 2014 but the camera system has been re-established.

Key abiotic and biotic hydrographical parameters were measured during the monthly sampling programme in the outer sill region, along with a length and cross section of the fjord. These measurements showed a deep coastal inflow of warm and saline water during winter. Tidal forces create vertical mixing at the outer sill region (Main Station, GF3) during winter and spring; as a result the water column depicts largely homogenous temperatures, salinities and phytoplankton biomass (i.e. chlorophyll *a*) with depth. Similar to previous years, an early stratification with high surface phytoplankton biomass was observed inside the fjord during the annual length section survey in May. Primary production and the biomass of phytoplankton increased in spring, due to the improving light conditions. In 2014 the long spring bloom lasted during April and May, which lead to low nutrients levels particularly in the photic zone. Increased freshwater runoff from land, along with ice melt, solar heating of the surface layer and air-sea heat exchange, strengthened the pycnocline, thus withstanding vertical mixing in the outer sill region. A second phytoplankton bloom was observed during summer, which resulted in elevated phytoplankton biomass and production values until October. The high spring and summer production resulted in the highest integrated annual primary production recorded during the programme. Decreasing freshwater runoff during autumn weakened the stratification within the fjord and vertical mixing of the water column re-established in the outer sill region.

The phytoplankton community in the outer sill region was comprised mainly of haptophytes (*Phaeocystis* sp.) and diatoms throughout the year, similar to previous years. *Phaeocystis* sp. dominated the phytoplankton community from March-June, while diatoms such as *Thalassiosira* spp. and *Chaetoceros* spp. were the dominant groups during winter, autumn and summer. Other phytoplankton groups such as dinoflagellates and silicoflagellates also contributed significantly to the seasonal species assemblages identified during 2014. The zooplankton community was characterized by a peak in Cirripedia nauplii in April followed by a peak in bivalvia larvae and increasing copepod nauplii abundances in May. Copepod nauplii peaked in July along a second peak in bivalvia larvae and high abundances of rotifers. The adult copepods emerged during spring and peaked in summer. This seasonal pattern in zooplankton community structure resembles previous years, though abundance values vary between years. The fish larvae showed interannual variation in abundances. In general, sandeel (*Ammodytes* sp.) larvae dominate the fish larvae assemblage in late winter/early spring, while arctic shanny (*Stichaeus punctatus*) larvae dominated in spring and capelin (*Mallotus villosus*) larvae in summer/autumn. American plaice usually peaks in June, while Atlantic cod larvae appears to peak in different months during spring and summer. Total abundance of fish larvae was the second highest recorded due to capelin larvae in summer, despite the absence of sandeel larvae. The length section showed higher fish larvae abundances on Fyllas Banke compared to inside Godthåbsfjord, dominated by a high number of sandeel larvae. For the first time, Atlantic cod larvae was observed on all stations on Fyllas Banke and inside Godthåbsfjord in May, while Arctic shanny still dominated the fish larvae at all stations inside the fjord.

At the Main Station (GF3) the shellfish larvae community showed the characteristic peak of *Pandalus* sp. in May and *Chionoecetes opilio* and *Hyas* spp. peaked one month later in June. Outside the months May and June, the community was mainly dominated by *Ctenophora* and *Sagitta* spp. Other jellyfish were observed in unusually low relative abundance and comprised only a minor part of the community except in January. Along the length section, larvae of the commercial species *Chionoecetes opilio* were less abundant at all stations, compared to previous years. *Sagitta* spp. and *Pandalus* sp. dominated the stations inside the fjord in May.

Vertical sinking flux of particulate material showed peak sinking fluxes of phytoplankton biomass (i.e. chlorophyll *a*) and particulate organic carbon during spring. While chlorophyll *a* sinking fluxes decreased again in June and remained low, elevated particulate organic carbon fluxes were observed in summer. The sinking material was comprised mainly by fresh algal material in spring, while the degraded material appeared to contribute more in summer.

The benthic community generally increases the oxygen uptake into the sediment during spring and summer, when primary production in the photic zone and sinking flux were highest. The recorded oxygen uptake was within the range of values previously observed in the monitoring programme.

Previous monitoring of benthic fauna and flora has established a solid baseline for future comparisons. The monitoring of benthic flora and fauna, since 2012, focuses on population dynamics of key species of the intertidal zone – the brown macroalgae 'knotted wrack' (*Ascophyllum nodosum*) and 'blue mussel' (*Mytilus edulis*), in relation to temperature, ice cover/light availability and tidal level. Temperature loggers also showed less variability during the 2013-14 winter, compared to the ice-free winter in 2012-13, because an insulating layer of ice covered the shore. The macroalgae knotted wrack showed an almost ten-fold higher net population growth rate in 2013-14 than during the previous year (2012-13). A lower survival of the blue mussel in the upper intertidal zone could be explained by higher maximum temperature, combined with longer air exposure. It is striking that due to the effect of an ice foot in winter, which modulates low winter temperatures, high temperatures in summer appear to be a significant stress factor for the blue mussel.

Two major seabird colonies in the vicinity of Nuuk are monitored for the MarineBasis programme, but additional colonies are also included in this report. The Qeqertannguit bird colony holds the largest diversity of breeding seabirds in the Nuuk area and is influenced by legal and illegal egg harvesting. Arctic tern was not observed at the island in 2014 or during 2013 and 2008. Small and mid-sized colonies of Arctic tern in Greenland are known to fluctuate considerably in population size, but the reason is poorly understood. In addition, Iceland gull also showed the fewest numbers of nesting Iceland gull observed so far in the Qeqertannguit bird colony.

In order to address the proportion of the boreal distributed common guillemot versus the arctic Brünnich's guillemot in the Nunngarussuit colony, an analysis of digital photographs is usually performed. This is interesting in the context of climate change where the proportion of common guillemot could be expected to increase in a warmer climate. Due to the distance and the quality of the photos, the two species could not be distinguished and the analysis was not performed this year.

West Greenland is a summer feeding ground for an estimated 3200 humpback whales, (*Megaptera novaeangliae*). A photo-identification programme is used to estimate the number of humpback whales present and returning to the Godthåbsfjord system. A total of 88 and 18 ID pictures were collected in Godthåbsfjord in 2013 and 2014, respectively. In the period 2007-2014 a total of 619 ID photos have been collected and with these, a total of 101 individual whales have been identified in Godthåbsfjord so far. May and early June are the months where most whales are seen in the fjord likely due to an influx of whales on their northward migration. The individuals with the highest degree of site fidelity are also the individuals that stay within the fjord for the longest periods of time during the feeding period and are therefore encountered more often.

Research projects

Two GEM relevant research projects were carried out in Kobbefjord in 2014. One on the influence of icebergs, glacial meltwater and suspended sediments on iron and nutrient concentrations and one on Food web structures of low Arctic lakes and streams.

1 Introduction

Josephine Nymand

The year 2014 was the eight year of operation of the fully implemented Nuuk Basic programme having both a marine and a terrestrial component, and it was the sixth year with complete annual time series for all sub-programmes. For the marine programme the season started on 21 January, continued until 18 December, while the field season in Kobbefjord area started 17 March and continued until 14 November, thus having a season of 329 and 242 days, respectively.

VIP visits

At the field station, we had two VIP visits during the summer season. The first visit was by the Aage V. Jensen Charity Foundation including Dorte Mette Jensen, Jens Haugbyrd, and Mette Fabricius Skov. The second visit was by the Controller and Audit General of Denmark including Helge Adam Møller MP, Henrik Thorup MP, Jens Frederik Rasmussen MP, Lennert Damsbo-Andersen MP, and Peder Larsen MP.

Furthermore, the Nordic Council of Ministers, Climate and Air Pollution Group (KoL) also visited the field station.

Another important summer visit was by the evaluation panel including Professor Steve Albon, Professor Kim Efrén, and Professor Jørn Tiede. This group conducted the evaluation of the entire GEM programme resulting in a comprehensive report for the Danish Environmental Protection Agency and the Danish Energy Agency.

International cooperation

Also in 2014, Nuuk Ecological Research Operations was involved in the EU project 'International Network for Terrestrial Research and Monitoring in the Arctic' (INTERACT). In 2014, one project (one researcher) received support for six bed nights from INTERACT Transnational Access.

Funding

Nuuk Basic is funded by the Danish Energy Agency and the Environmental Protection Agency with contributions from Greenland Institute of Natural Resources, Asiaq –Greenland Survey, Aarhus University and University of Copenhagen. Aage V. Jensen Charity Foundation has generously provided most of the necessary research infrastructure, including boats, research house, boathouse, warehouse and office, and accommodation facilities at Greenland Institute of Natural Resources in Nuuk.

Outreach

Results from the Nuuk Basic monitoring programme are continuously published in scientific papers, popular science articles and at scientific meeting and conferences. Furthermore, data from Nuuk Basic programme is freely available and was in 2014 used for reporting purposes in a number of international fora and by a number of externally funded research projects. In Nuuk the GEM researchers are contributing to education of high school student as well as undergraduate and graduate students by giving lectures and supervising small research projects in relation to field work. Researchers from GEM programmes are also participating in the Arctic Science Partnership working groups and research teams.

In 2013, more than seven scientific papers were published by the researchers from the Nuuk Basic programme and from externally funded research projects.

Further information

Further information about Nuuk Ecological Research Operations (NERO) programme and Kobbefjord Field Station are collected in previous annual reports, which can be found on the NERO web site (www.nuuk-basic.dk). On the web site, one can find much more information including manuals for the different monitoring programmes, a database holding freely available data from the monitoring, up-to-date weather information, a NERO bibliography and a collection of public outreach papers in PDF format.

The NERO programme's address is:

Nuuk Basic Secretariat
Department of Bioscience.
Aarhus University
P. O. Box 358
Frederiksborgved 399
DK-4000 Roskilde
Denmark
Phone: 45 30 78 31 61
E-mail: nuuk-basic@au.dk
Website: www.nuuk-basic.dk

Greenland Institute of Natural Resources provides the logistics in the Nuuk area:

Logistics Coordinator
Greenland Institute of Natural Resources
P.O. Box 570
Kivioq 2
3900 Nuuk
Greenland
Phone: +299 55 05 62
E-mail: heph@natur.gl
Website: www.natur.gl

2 Nuuk Basic

The ClimateBasis programme

Jakob Abermann, Per Hangaard, Dorthe Petersen, Majbritt Westring Sørensen and Stefan Wacker

The ClimateBasis programme is dedicated to describing the climatological and hydrological conditions in Kobbefjord. Two automatic climate stations, C1 and C2 (Stations 652 and 653), two automatic hydrometric stations, H1 and H2 (Stations 650 and 651), and four diver stations, H3, H4, H5 and Langesø (Stations 654, 655, 656 and 658), monitor the physical parameters related to climate and hydrology. The Langesø stations were established in 2014 through a recent collaboration with BioBasis. In 2012, a small mountain glacier on the northern side of the basin was included in the programme in the framework of a strategic initiative in order to better understand the cryospheric component of the water-cycle. Both mass balance and since 2013 also energy balance measurements are performed there.

The location of the different stations can be seen in figure 2.1. ClimateBasis is operated by Asiaq – Greenland Survey.

2.1 Meteorological data

In 2014, the climate stations in Kobbefjord were visited six times by Asiaq personnel. A full description of the climate stations is given in Iversen *et al.* (2008). In terms of hydrological fieldwork, there has been a focus on obtaining manual discharge measurements at the new station at Langesø. Nine discharge measurements have been performed there and one at H1.

This annual report describes the seventh full year of data for all climate parameters and refers to data collected in the period from 1 January to 31 Decem-

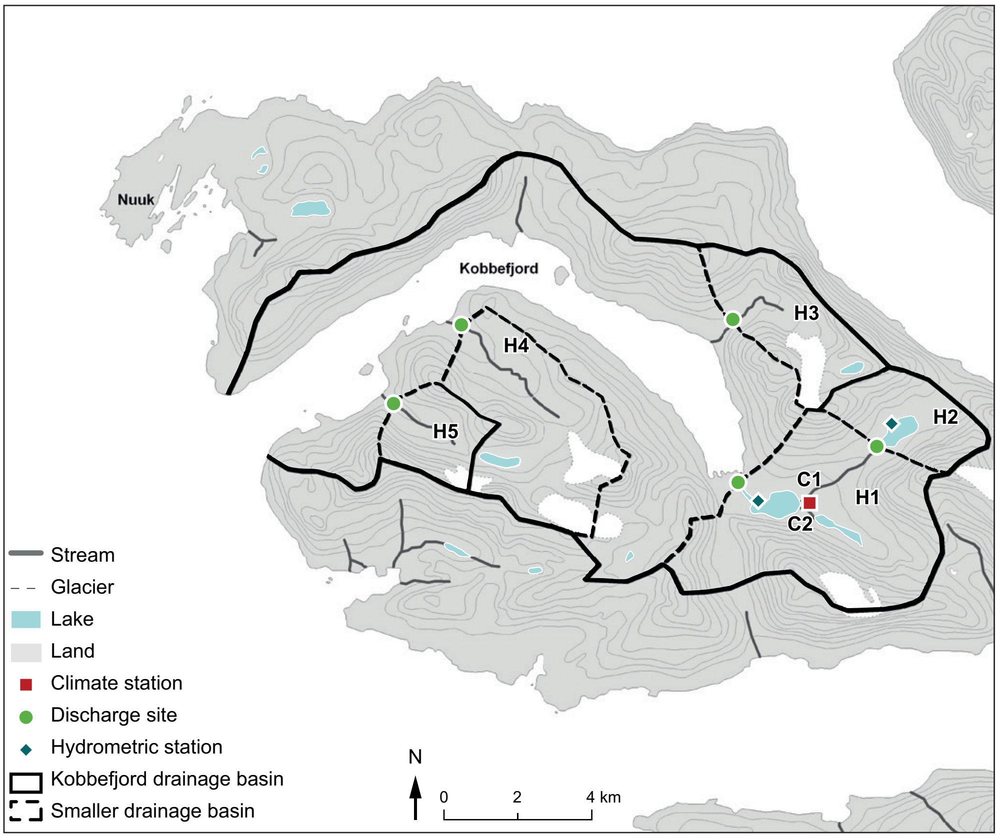

Figure 2.1 Location of the climate station (square), the hydrometric (H1, H2) and diver stations (H3, H4, H5) in Kobbefjord together with the respective drainage basins.

Figure 2.2 Variation of selected climate parameters in 2014. From above: Air temperature [°C], relative humidity [%], air pressure [hPa], snow depth [m], net radiation [Wm-2], incoming short wave radiation [Wm-2], outgoing short wave radiation [Wm-2], wind speed [ms-1] and wind direction [°]. Wind speed and direction are measured 10 m above terrain; the remaining parameters are measured 2 m above terrain.

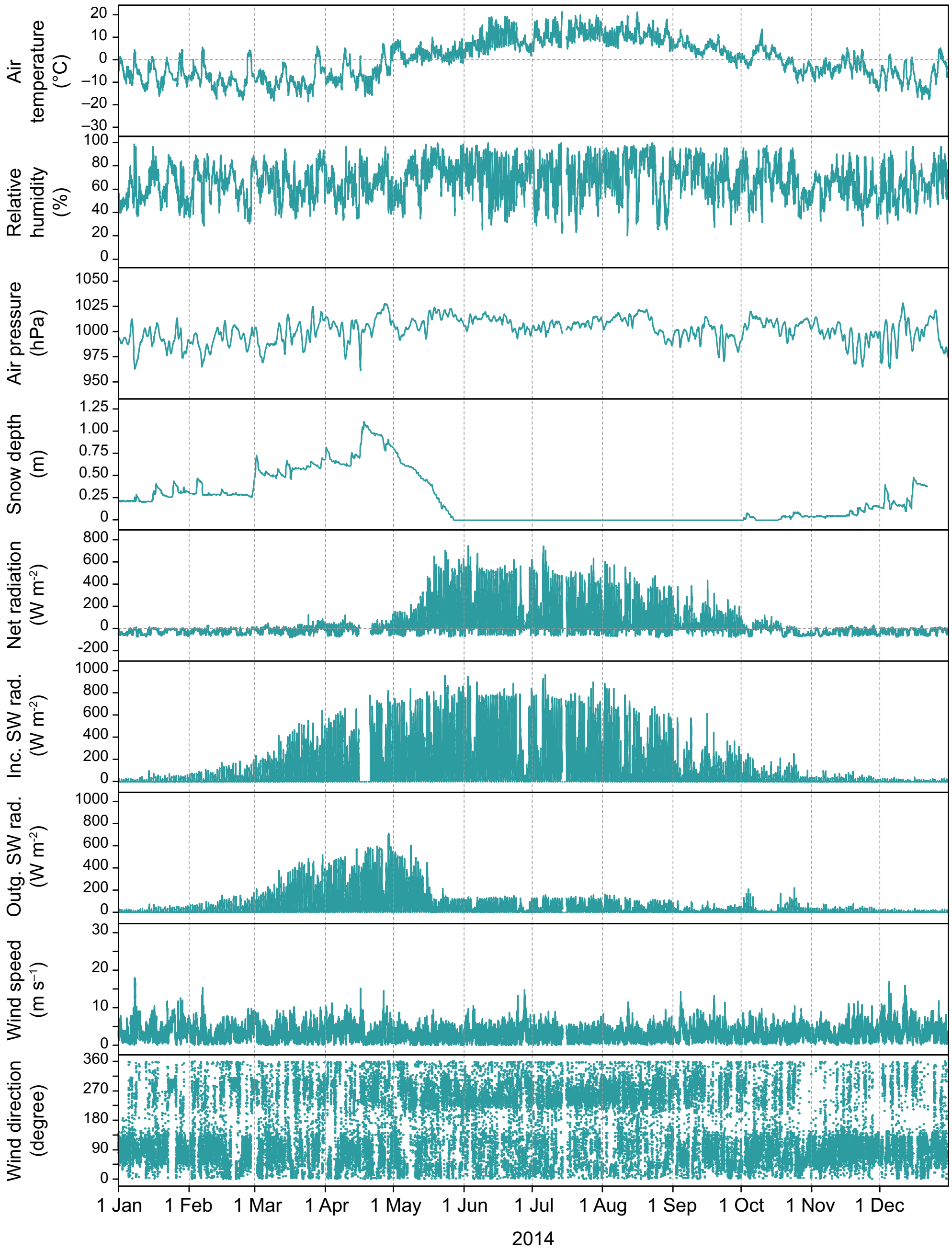

ber 2014. Figure 2.2 gives an overview of selected meteorological parameters in 2014.

The mean annual temperature in 2014 was –0.1°C, which is close to the average between 2008 and 2014 (tables 2.1 and 2.2). The highest temperature was recorded on 14 July (21.3°C) and the lowest on 25 March (–18.6°C). There was no month where not at least once positive temperatures were recorded, while there was no freezing from 1 June until the 26 September and already on 28 September the mean daily temperature was slightly below 0 °C. Winter months were generally below average with April being 2.8 °C colder than average. May to August were significantly warmer than average. Comparing Nuuk with Kobbefjord, the generally stronger continentality in Kobbefjord is a clear climatological feature with higher temperatures in summer and lower temperatures in winter (figure 2.3). In 2014 this was even more pronounced than usual with June, July and August being 2.7°C warmer in Kobbefjord than in Nuuk.

After 2013 with less snow than on average, 2014 showed the second thickest snow cover on record with up to 1.1 m on 18 April. By the end of May, snow had disappeared at the climate station and did not come back until 2 October. The

Table 2.1 Monthly mean values of selected climate parameters from January to December 2014 and the annual average.

Month Year	Rel. hum. (%)	Snow depth (m)	Air temp. (°C)	Air pressure (hPa)	Precip. (mm)	Wind (m s^{-1})	Wind dir. most frequent
Jan	61	0.27	–6.1	991	28.3	3.9	E
Feb	64	0.30	–8.4	992	4.2	3.2	E
Mar	65	0.57	–8.9	996	19.4	3.3	WNW
Apr	65	0.80	–6.0	1006	60.7	3.7	WNW
May	72	0.38	2.5	1010	26.7	2.5	WNW
Jun	72	0.00	8.4	1009	101.2	3.1	WSW
Jul	69	0.00	11.8	1006	11.9	2.7	WSW
Aug	73	0.00	10.7	1009	93.8	2.7	W
Sep	71	0.00	4.9	997	171.0	3.4	WNW
Oct	67	0.03	0.1	1007	92.7	3.2	NE
Nov	62	0.08	–3.9	995	22.5	3.1	E
Dec	65	0.30	–6.6	997	71.2	4.4	ESE
2014	67	–	–0.1	1001	703.6	3.3	–

Table 2.2 Comparison of monthly mean air temperatures 2007 to 2014 (italic text represents months with incomplete coverage).

	Air temperature °C							
Month	2007	2008	2009	2010	2011	2012	2013	2014
Jan	–	–12.0	–5.4	–3.8	–5.4	–8.7	–5.9	–6.1
Feb	–	–13.3	–6.1	–1.6	–8.7	–7.7	–7.2	–8.4
Mar	–	–8.3	–11.7	–4.5	–9.2	–11.0	–3.1	–8.9
Apr	–	–0.9	–3.2	–0.1	–9.5	–1.7	–0.8	–6.0
May	0.6	3.9	0.3	7.1	0.3	3.2	–0.4	2.5
Jun	5.3	7.9	6.4	8.8	6.2	9.4	6.6	8.4
Jul	10.8	10.9	10.6	10.7	10.0	12.1	9.7	11.8
Aug	10.6	8.7	9.3	11.7	8.7	10.0	8.8	10.7
Sep	4.0	4.4	3.8	7.8	3.9	6.6	4.7	4.9
Oct	–0.5	0.0	–0.6	2.9	–2.4	3.0	0.9	0.1
Nov	–3.5	–1.7	–7.9	1.2	–6.2	–3.0	–3.5	–3.9
Dec	–8.7	–7.8	–2.8	0.5	–7.5	–6.1	–8.2	–6.6
Year	–	–0.7	–0.6	3.4	–1.6	0.5	0.2	–0.1

record snow cover of 2011 was about 20 cm higher than 2014. Compared to previous years, relative humidity was generally low, especially in January, February and March as well as November, where all-time minima in mean monthly relative humidity were reached. Air pressure was also below average, especially in March and September, where monthly minima were reached.

Precipitation was below average in 2014 with 704 mm in total. Almost a quarter of the annual precipitation came in September (171 mm) during a number of low-pressure systems with strong winds (figure 2.2). On 14 August, 75 mm rain fell

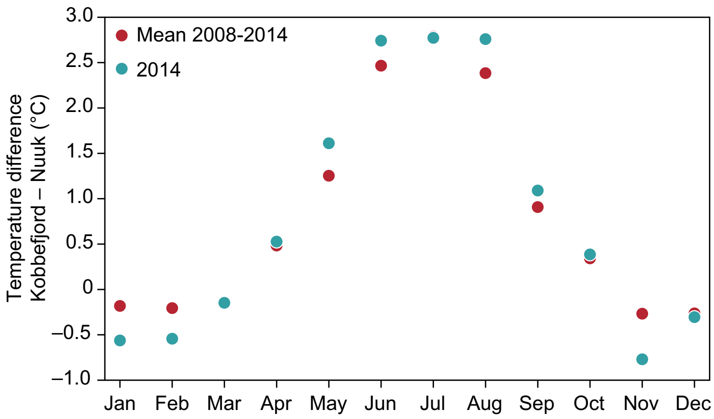

Figure 2.3 Difference in monthly average temperature Kobbefjord – Nuuk [°C]: red: mean for the period 2008-2014, turquoise: 2014.

Table 2.3 Monthly mean values of selected radiation parameters in 2014.

Month Year	Short wave rad ($W m^{-2}$)		Long wave rad. ($W m^{-2}$)		Net rad. ($W m^{-2}$)	PAR ($\mu mol\ s^{-1} m^{-2}$)	UVB ($mW m^{-2}$)
	in	out	in	out			
Jan	5.2	4.9	239.6	270.7	–30.7	13.3	0.2
Feb	21.4	18.9	231.4	261.9	–28.0	52.7	1.2
Mar	74.7	66.0	237.9	263.1	–16.5	173.4	4.3
Apr	169.7	143.1	244.5	277.8	–9.7	396.2	12.3
May	235.9	99.2	279.8	325.7	90.9	559.9	23.2
Jun	238.0	37.2	305.8	365.0	141.7	555.3	26.7
Jul	233.5	40.4	319.0	384.3	128.5	540.2	25.8
Aug	149.1	26.2	322.0	372.1	72.8	345.1	16.5
Sep	56.4	8.8	309.0	335.0	21.5	133.2	5.0
Oct	21.6	12.8	273.7	302.5	–20.1	55.0	2.3
Nov	6.9	6.0	247.3	279.9	–31.6	18.3	0.4
Dec	2.0	2.0	249.3	272.5	–23.2	5.2	0.1

during 24 hours which marks the maximum value on record.

The predominant wind direction was from E in winter, during spring WNW dominated and in the summer months an in-valley flow (from the western sector) indicates a valley wind system (table 2.1). Wind speed followed the general cycle of higher wind speed in winter than in summer and individual storms can be seen in figure 2.2. Compared to previous years, April, September and December were particularly windy with 3.7, 3.4 and 4.4 m s^{-1} on average.

Table 2.3 summarizes the radiation components on a monthly basis measured in Kobbefjord. The short-wave balance clearly determines the net radiation in summer, while the long-wave balance does so in winter. Most net radiation input happened in June with 141.7 Wm^{-2} on average being added to the surface while net radiation minimum happened in November where radiative cooling is not compensated by significant incoming shortwave radiation. Photosynthetic active radiation (PAR) peaked in May and ultraviolet B (UVB) in June, along with the maximum average shortwave incoming radiation (238.0 Wm^{-2}). The annual cycle of the net radiation was close to normal with the biggest deviation being an abnormally negative April. This is due to steady snow cover and thus a high reflectance of the surface.

2.2 River water discharge

Hydrometric stations

There were hydrological measurements carried out on six locations in the Kobbefjord catchment. Two hydrometric stations were established in 2007 and various divers are set up every year in three minor rivulets to Kobbefjord. The drainage basins of the six locations cover a total of 58 km^2 corresponding to 56 % of the 115 km^2 catchment area of Kobbefjord.

In figure 2.1 the locations of the hydrometric stations (H1, H2) and the diver stations (H3, H4, H5) are marked. For further descriptions of the stations and their respective drainage area see Jensen and Rasch (2009). For descriptions of the hydrometric stations see Jensen and Rasch (2008).

Q/h-relation

Manual discharge measurements have been carried out at station H1 (1 measurement) and Langesø (9 measurements). The purpose is to establish and validate a stage-discharge relation (Q/h-relation). It is generally recommended to base a Q/h-relation on a minimum of 12-15 discharge measurements covering the water levels normally observed at the station (ISO 1100-2, 1998). For H2, H3, H4, H5 and Langesø not enough discharge measurements have been made yet to produce a

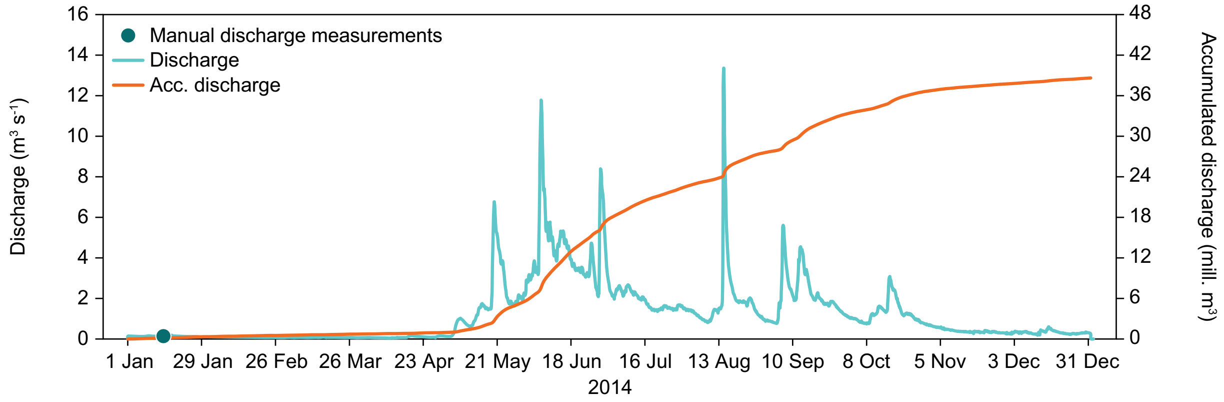

Figure 2.4 River water discharge at H1 during 2014. The turquoise line is the instantaneous discharge [m^3s^{-1}] and refers to the left axis, the red line the accumulated discharge over the calendar year [10^6 m^3] and refers to the right axis.

reliable Q/h-relation. Measurements at high-water levels are particularly missing. Therefore data from these stations are not presented yet.

A Q/h-relation was established for H1 in 2009 and based upon a total of 17 discharge measurements. The Q/h-relation was updated in 2011 in order to account for winter conditions with the outlet being affected by ice/snow. Details on that can be found in Pernosky *et al.* 2012.

River water discharge at H1

Figure 2.4 shows the discharge at H1 for 2014. Very little water has been running during the entire winter and in contrast to several other years, there was no significant winter discharge event recorded. The water level rose in the first days of May and discharge first peaked due to snowmelt and after several rainy days around May 19. Further notable peaks occurred in early and late June from where a dry summer period started with temperatures above average and little precipitation. On 8 August as little as 0.8 m^3s^{-1} discharge was recorded and only a week later, this year's maximum was reached with 37.5 m^3s^{-1}. This was associated with the all-time maximum daily total precipitation record (75.1 mm on 14 August). Right after this event, an unseen occurrence of silt was observed in Langesø. Autumn storms brought some further peaks in precipitation and runoff, respectively with the last peak on 17 October. After that, the year continued with very little discharge.

Table 2.4 summarizes the total discharge for the hydrological years from 2007/2008 until 2013/2014. The three latest seasons showed discharge above average and 2013-2014 is ranked second since 2007. Inter-annual variations are high, the maximum year showing more than double the runoff than the minimum year. Taking the drainage basin of 31 km^2 into account, the overall water loss was 1382 mm in 2013/2014.

Table 2.4 Total discharge (10^6 m^3) and mean water loss (mm) for hydrological years 2007-2008 to 2012-2014.

Hydrological year	Total discharge (million m^3)	Water loss (mm)
2007-2008	32.79	1058
2008-2009	40.83	1317
2009-2010	23.21	749
2010-2011	34.34	1108
2011-2012	49.06	1583
2012-2013	42.41	1368
2013-2014	42.85	1382

3 Nuuk Basic

The GeoBasis programme

Birger Ulf Hansen, Louise Holm Christensen, Mikkel P. Tamstorf, Magnus Lund, Maria Libach Burup, Mikhail Mastepanov, Andreas Westergaard and Torben R. Christensen

Figure 3.1 Micromet station, M1000, in March 2014 with heavy icing. The station was repaired in October 2013, but most sensors broke down less than two weeks later due to strong winds and heavy icing.

The GeoBasis programme provides long term-data of climatic, hydrological and physical landscape variables describing the environment in the Kobbefjord drainage basin close to Nuuk. GeoBasis was in 2014 operated by the Department of Geoscience and Natural Resource Management, Copenhagen University in collaboration with the Department of Bioscience, Aarhus University. In 2014, GeoBasis was funded by Danish Ministry for Climate and Energy (now Danish Ministry of Energy, Utilities and Climate) as part of the environmental support programme DANCEA – Danish Cooperation for Environment in the Arctic. A part-time position is placed in Nuuk at Asiaq – Greenland Survey. The GeoBasis programme includes monitoring of the physical variables within snow and ice, soils, vegetation and carbon flux. The programme runs from May to the end of October with some measurements all year round from automated stations (figure 3.9).

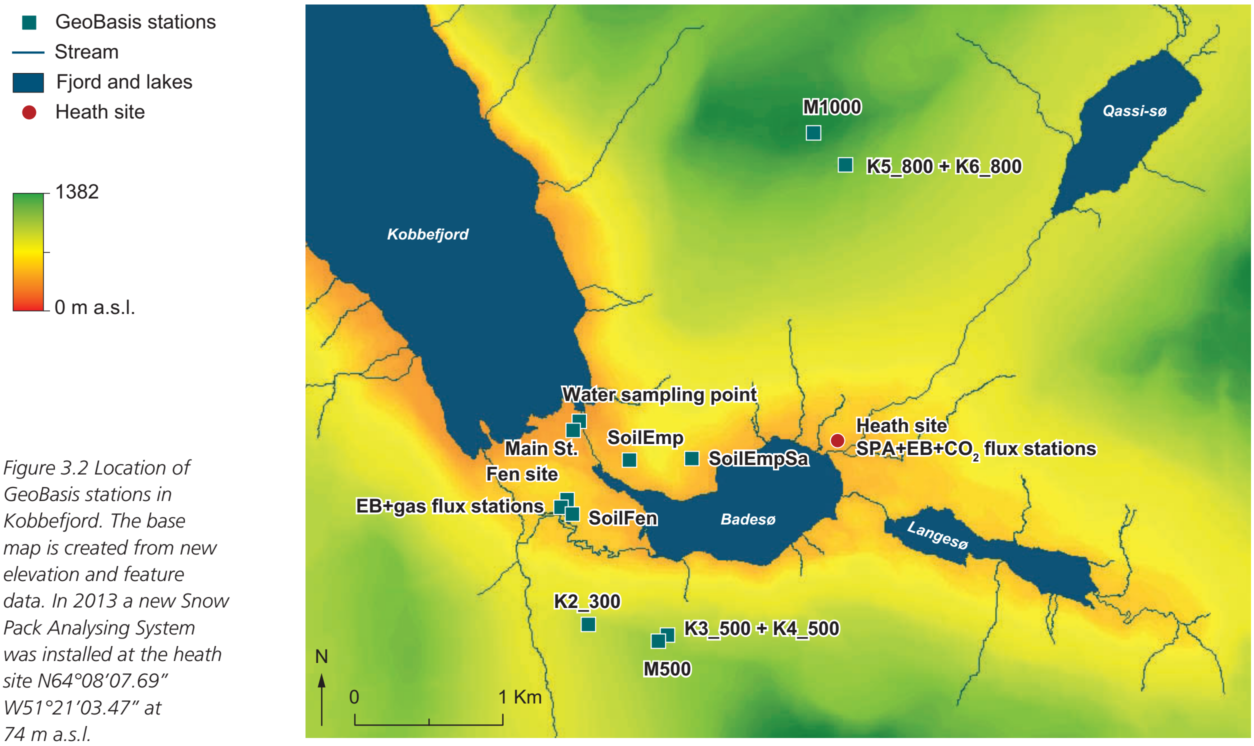

Figure 3.2 Location of GeoBasis stations in Kobbefjord. The base map is created from new elevation and feature data. In 2013 a new Snow Pack Analysing System was installed at the heath site N64°08'07.69" W51°21'03.47" at 74 m a.s.l.

The 2014 season is the seventh full season for the GeoBasis programme. In 2007, the field programme was initiated during a three-week intensive field campaign in August where most of the equipment was installed, although some installations had to be postponed until 2008. Methods and sampling procedures are described in detail in a new manual 'GeoBasis Manual – Guidelines and sampling procedures for the geographical monitoring programme of Nuuk Basic in Kobbefjord', which can be downloaded from http://nuuk-basic.dk/monitoring/geobasis/. In 2014 all data from the GeoBasis Nuuk programme were uploaded to the new GEM (Greenland Ecosystem Monitoring) database, which can be founded at http://data.g-e-m.dk/. The data will in the coming years be regularly updated after each field season.

In 2011, GeoBasis installed two new energy balance stations in cooperation with the INTERACT programme. One station was located at a new site over heath vegetation (figure 3.2) and the second station was installed at the existing fen site (Hansen *et al.* 2014). The remote placing of the heath site and the use of fuel cells caused numerous breaks in the time series although the station was visited frequently even outside the normal field season. In 2013, a more stable power supply was installed combining a wind generator with a nominal effect of 350 W and a 18 W solar panel. With that the time-series recording at both the energy balance and the SPA stations have been more stable with only a few minor breaks.

In 2013, Geobasis installed a Snow Pack Analysing System (SPA) on the heath site close to the energy balance and CO_2 stations (figure 3.2.). The heath site was chosen as it is the dominating ecosystem within the drainage basin. The SPA constitutes an innovation in snow measurements as it automatically and continuously measures all relevant snow parameters such as snow depth and at three levels (10, 35 and 55 cm), snow density, snow water equivalent and contents of liquid water and ice.

Unfortunately the micromet station, M1000, has been out of order since February 2012. Although it has been repaired several times, frequent strong winds and icing have damaged all sensors shortly after each repair (figure 3.1), so it has now been decided to close down the station during the field season 2015. In order to minimize the number of gaps in the time series from the climate station and the two flux stations at the fen location, two 350W wind generators and four new 100Ah batteries were added to the existing power supply of six 110W solar panels and eight 100Ah batteries (figure 3.9).

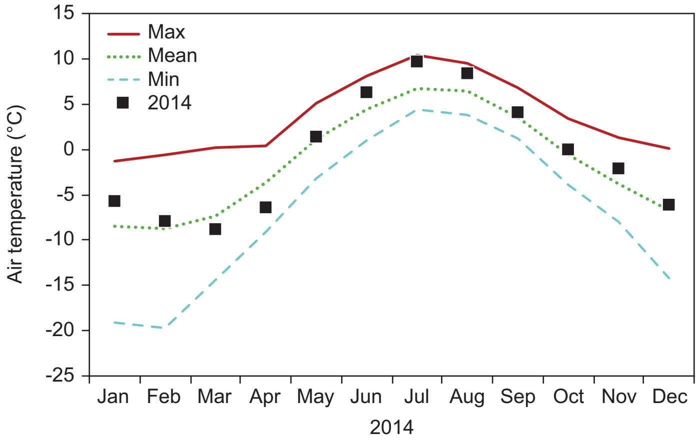

Figure 3.3 The monthly minimum, mean and maximum air temperature for the period 1866-2014 measured at Nuuk (solid and dashed lines) and monthly mean air temperature for 2014 (squares) (Cappelen 2014).

Data collected by the Danish Meteorological Institute (figure 3.3) shows that in 2014 the annual mean air temperature in Nuuk reached –0.6 °C, which is 0.8 °C warmer than normal (Cappelen 2014). The three summer months, June-August, were all warmer than normal. The warmest month was July with 9.7 °C, which was 3.0 °C warmer than normal but 0.7 °C colder than the previous July, which was the warmest July in the period 1866-2014. The coldest month in 2014 was March with –8.8 °C, which was 1.4 °C colder than normal, but 10.8 °C warmer than the record from February 1984.

3.1 Snow and ice

Snow cover extent

The first four automatic cameras were installed in 2007 at 300 and 500 m a.s.l. to monitor the snow cover extent in the central parts of the Kobbefjord drainage basin (Tamstorf *et al.* 2009). In September 2009 two snow-monitoring cameras K5 & K6 were installed. Both cameras were installed at position N64°9'06.25'' W51°20'46.47'' 770 m a.s.l. (figure 3.2). K5 is facing to the south monitoring the central parts of the drainage basin with Badesø and Langsø while K6 monitors Qassi-sø in the northern valley of the

Figure 3.4 First inspection of camera K3_500 (N64°7'21.46" W51°22'19.31") in the first week of June 2014. The background is showing the field of view for camera K3 which monitors Kobbefjord and the fen location.

drainage basin (figure 3.4). In 2011 a new camera was reinstalled at K1_300 (N64º7'26" W51º22'55") overlooking the Fen area. This automatic camera takes photos three times daily from March to November, and once daily during the winter months.

One of the main advantages of camera-based snow monitoring is that it is relatively insensitive to cloud cover (in contrast to satellite-based techniques). Only low clouds and foggy conditions can make the image data unsuitable for mapping purposes. A new updated and more user-friendly algorithm for snow-cover monitoring has been developed in MatLab, so it is now possible, for each melting season, to construct snow-cover depletion curves for user-specified regions of interest (ROI) on the basis of image data obtained at daily frequency. In the previous year's depletion curves for three regions of interest seen from K2_300 have been shown (Hansen *et al.* 2012), but due to technical problems it has not be possible to show any depletion curves from these ROI in 2012 and 2013.

Instead three new ROI are shown in figure 3.5. They cover the vegetation types copse (willow with a maximum height of 1 m), fen and dwarf shrub heath. Fen is very similar to the footprint for the CO_2-station in the fen. All ROI are covered by K1_300 and K3_500 so a future monitoring of the two ROI should be more stable. Figure 3.5 shows the snow depletion curves for all three ROI. The DOY (day of year) for the 50 % of the snow cover in the dwarf shrub

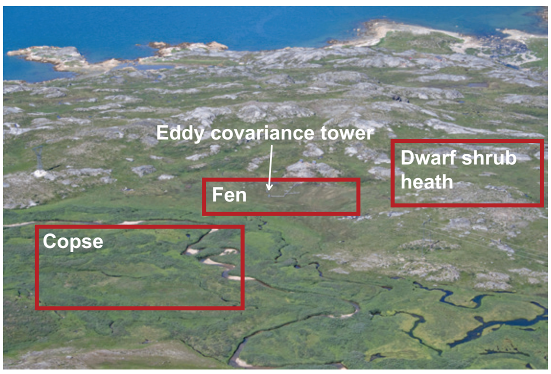

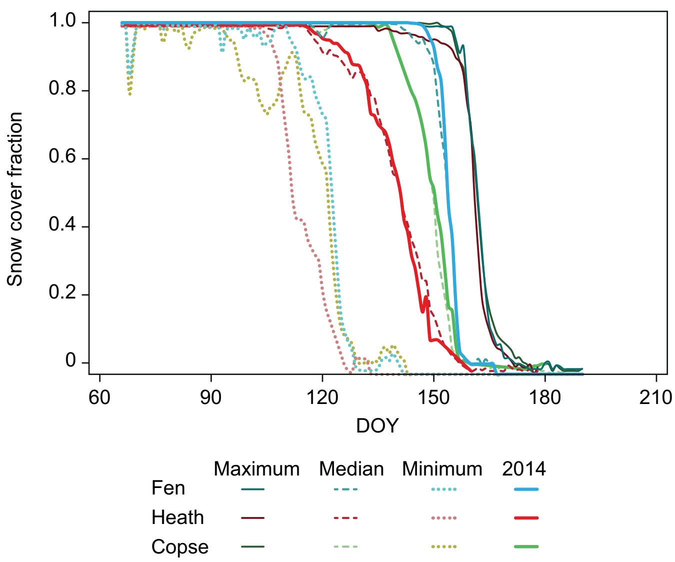

Figure 3.5 Snow cover depletion for three regions of interest: copse, fen and dwarf shrub heath at 50 m a.s.l. have been analysed using a new snow-cover algorithm. The regions are specified on the image to the left, and the depletion curves for each region in the period 2010-2014 are shown in the diagram to the right. DOY (day of year).

Table 3.1 Comparison of snow depth/densities (in brackets) at GeoBasis sites A-C, 2009-2014. No snow pit was dug at SoilEmpSa in 2010 (see figure 3.7).

Snow survey dates	Soil Fen (A) Average depth [m] Density (kg m³)	Soil Emp Salix (B) Average depth [m] Density (kg m³)	Soil Emp (C) Average depth [m] Density (kg m³)
15-16 April, 2009	0.91 (237)	0.90 (275)	1.02 (329)
15-16 April, 2010	0.20 (339)	0.19 (n.a.)	0.17 (366)
7-9 April, 2011	0.87 (364)	0.92 (297)	0.91 (383)
17-18 April, 2012	0.96 (373)	0.74 (353)	0.92 (320)
20-22 March, 2013	0.42 (316)	0.35 (311)	0.32 (282)
8-9 April, 2014	0.67 (283)	0.81 (329)	0.55 (302)

heath shows a minimum (earliest) of 112, a median of 141 and a maximum (latest) of 161. For the copse ROI, the same figures were 122, 150 and 162 and for the fen ROI they were 122, 153 and 162. For all three ROI, minimum depletion curves were equal to 2010 and the maximum curves were equal to 2011. Figure 3.5 also shows that the melting in 2014 was very close to the median curves for the period 2010-2014. The dwarf shrub heath in 2014 had the earliest DOY for the 50 % of the snow cover due to a much smaller amount of snow and the dwarf shrub heath was also 10 days earlier than the two other ROI. In the period 2010-2014, it also had the widest range of days in the 50 % snow cover, namely 49 days or nine days more the two other ROI. In 2014, the melting season for the dwarf shrub heath started on DOY 118, 20 days later on the copse ROI and 30 days later on the fen ROI. The great difference in the start of the melting season was due to great difference in the amount of snow cover, so all three ROI ended the melting season within four days (DOY 158-162).

Snow cover

To support the studies under the Nuuk Basic monitoring programme, a snow cover survey using ground penetrating radar (GPR) and taking manual stake measurements was carried out in the main parts of Kobbefjord drainage basin on 8-9 April 2014. A comparison of average snow depth for the three GeoBasis sites can be seen in table 3.1. A snow depth of 67 cm as an average for the three sites is only 1 cm above the average for the three sites in the period 2009-2014. However, an average of 305 kg/m³ in density is well below the average of 323 kg/m³ for the six-year period.

Even though the snow survey is carried out at nearly the same time every year, snow depth has large variations from year to year and the maximum snow cover date is also strongly variable from year to year, see figure 3.6. The snow cover in the winter 2013/2014 started on 27 October and over the following month it reached 25-30 cm where it settled for the next three months. During a heavy snowfall at the beginning of March, the snow depth suddenly increased to 55 cm, and until 20 April the snow depth steadily increased to this season's maximum of 105 cm. Over the next 38 days a steady snowmelt took place and it ended on 28 May. Figure 3.6 shows the maximum (2010/2011), minimum (2009/2010) and the median for the period 2009-2014 and it is seen that the winter 2013/2014 was very close to the median for the period.

Table 3.2 describes snow depths and densities at the three GeoBasis soil microclimate stations SoilFen, SoilEmpSa and SoilEmp using ground penetrating radar (GPR) and manual stake measurements (figure 3.7). The snow survey strategy used in Kobbefjord is outlined in the 3rd Annual Report, page 18 (Hansen *et al.* 2010). In order to document the properties

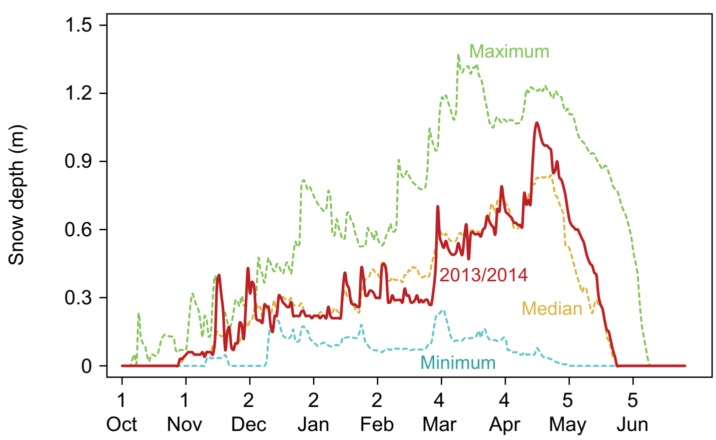

Figure 3.6 Snow depth measured at the ClimateBasis station and placement of snow surveys, 2009-2014.

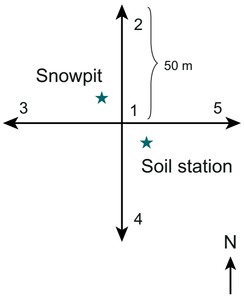

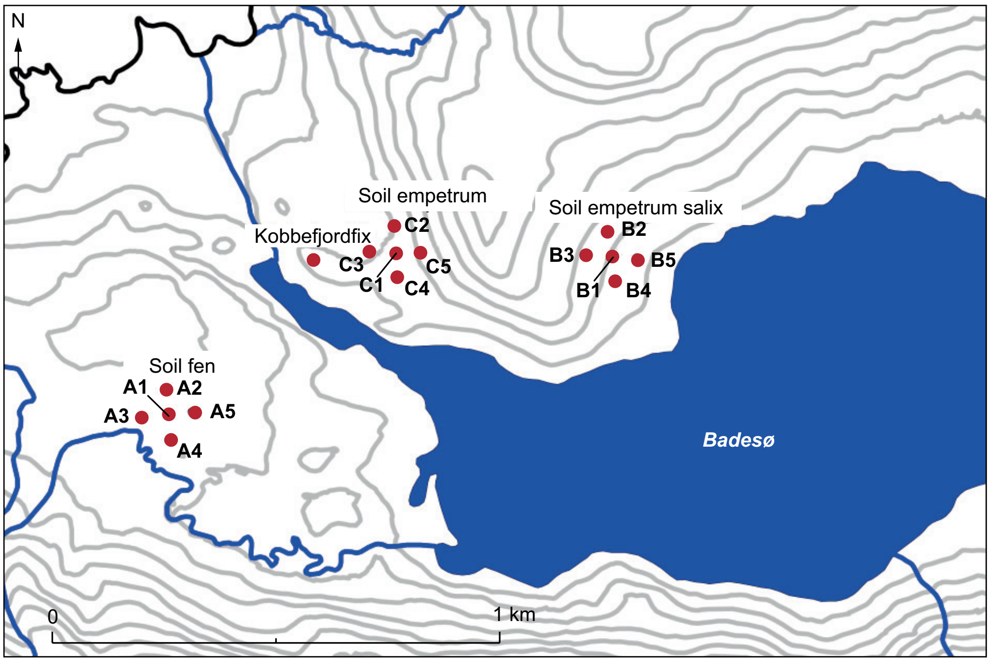

Figure 3.7 Map showing the three snow survey sites. The figure on the right outlines the strategy at each site.

of the snowpack, snow pits were dug at SoilFen in point A1, at SoilEmpSa in point B1 and at SoilEmp in point C1 (figure 3.7). The examination of the snowpack included temperature profiling, density measurements and texture description. Table 3.2 summarizes the snow depth, density and temperature results from the three stations. The texture of the snow profile at all three sites is characterized as homogenous coarse grained snow, with densities between 283-329 kg m^{-3}. The variation in densities are within the normal range for the period 2009-2014 (Hansen *et al.* 2013) and the normal huge variation in snow depths ranging from 33 cm to 119 cm causes again a huge variations in snow water equivalents ranging from 109 to 337 mm within few metres at SoilEmpSa.

Ice cover

Sea-ice cover in Kobbefjord developed as early as 24 October, which is the earliest registration in the seven years of monitoring in Kobbefjord (table 3.3). The fjord was ice-free on 1 June, which is nearly 17 days later than the normal for the six previous years.

In 2014 the ice cover was formed two days later on Qassi-sø (250 m a.s.l.) than on Badesø (30 m a.s.l.) while in the three previous years it has been formed 2-3 weeks earlier. As usual, the ice cover on Qassi-sø broke up ten days later than the ice cover on Badesø. The difference in the period of ice cover is due to the difference in elevation of the two lakes.

Micrometeorology

Table 3.4 reports the monthly mean air temperature, relative humidity, surface temperature and soil temperature measured at SoilFen 2011-2014 (monthly data for the period 2007-2010 can be found in previous annual reports). In 2014 March was the coldest month with –9.4 °C, while July with 10.7 °C was the warmest month and it was 0.5 °C warmer than the average for the period 2007-2014. These measurements are in line with the air temperature measured in Nuuk located 30 km away (figure 3.3).

Table 3.2 Snow pit depth, average density, snow depth, standard deviation of snow depth, average snow temperature and average water equivalent in three soil stations (SoilFen, SoilEmpSa and SoilEmp).

Site	Snow pit depth (cm)	Avg. density (kg m^{-3})	Snow depth (min-avg.-max) (cm)	Standard dev. of snow depth (cm)	Avg. snow temperature (°C)	Avg. water eq. (mm)
SoilFen (A1)	68	283	37-67-119	10	–4.7	192
SoilEmpSa (B1)	58	329	33-58-90	15	–4.0	191
SoilEmp (C1)	55	302	40-55-102	16	–5.4	166

Table 3.3 Visually estimated dates for perennial formation (50 %) of ice cover and date for break-up of ice cover on selected lakes within the Kobbefjord drainage basin and on Kobbefjord from 2007 to 2014. Dates are reported for perennial formation of ice cover in the fall and for the break-up of ice cover in the spring. Badesø is the main lake in the area and Qassi-sø is the lake at 250 m a.s.l. in the northern valley of the drainage basin. indicate no data in the period and the formation of ice cover took place within the period.*

	Badesø		Langsø		Qassi-sø		Kobbefjord	
Year	Break-up	Formation	Break-up	Formation	Break-up	Formation	Break-up	Formation
2007		23 Oct		22 Oct		22 Oct		27 Dec–12 Feb*
2008	2 Jun	5 Nov	13 May	5 Nov	9 Jun	4 Nov	17 May	no data
2009	13 Jun	1 Nov	11 Jun	6 Oct	22 Jun	10 Oct	4 Jun	12 Feb
2010	14 May	22 Nov	18 May	31 Oct	24 May	6-11 Nov	2 Jun	23 Nov
2011	18 Jun	22 Oct	no data	no data	28 Jun	20 Oct	23 May	16 Nov
2012	9 Jun	15 Nov	no data	10 Nov	18 Jun	11 Nov	22 May	24 Feb
2013	14 Jun	24 Oct	13 Jun	23 Oct	22 Jun	26 Oct	26 Apr	15 Oct
2014	10 Jun	no data	no data	no data	20 Jun	no data	1 Jun	no data

For the GeoBasis monitoring period 2007- 2014, the minimum monthly mean air temperature was –13.5 °C measured at SoilFen in February 2008 and the maximum monthly mean air temperature was 11.7 °C measured in July 2012.

The micrometeorological station M500 measures air temperature, relative humidity, surface temperature and shortwave irradiance and data are presented in table 3.5 (monthly data for the period 2007-2010 can be found in Hansen *et al*. 2014). M500 is placed approximately 500 m a.s.l. south of Badesø. These measurements are in line with the air temperature measured in Nuuk located 30 km away (figure 3.3) and at SoilFen 1 km away (figure 3.8). In 2008-2014 the mean air temperature in July at the M500 station was between 6.6 °C and 10.4 °C, in 2014 it was 9.5 °C, only +0.9 °C above the average for the period. The relative humidity measured at the M500 station in the period 2008-2014 shows an annual average of 76 % with maximum values of 90-91 % during the snowmelt in April and in the cold rainy autumn from September to November. The incoming shortwave irradiance in the period 2008-2014 was between 211-295 W m^{-2} in June

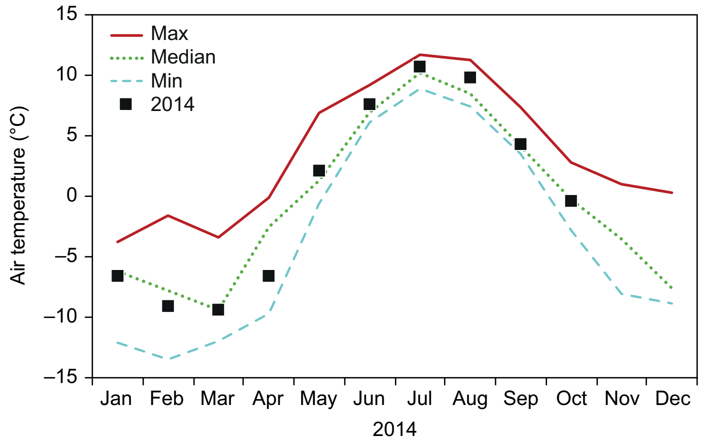

Figure 3.8 Monthly mean air temperatures in 2014 (square), maximum (red line), average (thin line) and minimum (dashed line) monthly mean air temperatures from 2007-2014. Measured at the SoilFen station 2.5 metre above ground.

Figure 3.9 In order to minimize the number of gaps in the time series from the climate station and the two flux stations at the Fen location, two 350W wind generators and four new 100Ah batteries were added to the existing power supply of six 110W solar panels and 8 100Ah batteries.

Table 3.4 Air temperature, relative humidity, surface temperature and soil temperature at five depths (1 cm, 10 cm, 30 cm, 50 cm and 75 cm) from the SoilFen station in the fen area from January 2011 to October 2014.

Month - year	Air temp. (°C)	Rel. hum. (%)	Surface temp. (°C)	Soil temp. (°C)	Soil temp. (°C)	Soil temp. (°C)	Soil temp. (°C)	Soil temp. (°C)	Soil temp. (°C)
	2.5 m	2.5 m	0 m	–1 cm	–5 cm	–10 cm	–30 cm	–50 cm	–75 cm
2011									
January	–5.6	70.6	–8.7	–0.7	–0.5	–0.2	0.7	1.0	1.4
February	–9.1	73.2	–12.0	–0.4	–0.4	–0.2	0.5	0.7	1.1
March	–9.5	73.6	–11.6	–0.2	–0.2	–0.2	0.5	0.7	1.0
April	–9.7	69.5	–12.6	0.0	0.0	0.0	0.5	0.7	1.0
May	0.5	71.5	–1.2	0.0	0.0	0.1	0.5	0.7	1.0
June	6.1	77.0	5.4	4.8	3.5	2.5	1.2	1.1	1.2
July	9.6	78.5	11.2	12.4	11.8	11.0	7.4	6.6	5.3
August	8.2	81.3	9.4	11.0	10.8	10.5	8.6	8.1	7.1
September	3.5	77.8	3.2	4.1	4.5	4.8	5.9	6.0	5.9
October	–2.4	70.5	–4.3	0.0	0.3	0.7	2.3	2.6	3.1
November	–6.2	65.8	–8.7	–2.3	–1.8	–1.1	0.8	1.1	1.7
December	–7.6	74.3	–9.5	–0.7	–0.7	–0.5	0.2	0.5	1.0
2012									
January	–8.8	70.6	–11.2	–0.7	–0.7	–0.6	0.1	0.4	0.8
February	–7.8	74.0	–9.8	–0.4	–0.4	–0.4	0.1	0.3	0.7
March	–11.1	73.2	–12.2	–1.2	–1.1	–0.9	0.0	0.2	0.6
April	–1.7	81.0	–2.7	–0.1	–0.1	–0.1	0.1	0.3	0.6
May	3.2	78.8	2.7	1.0	0.3	0.0	0.2	0.3	0.6
June	9.2	74.4	11.2	11.3	9.3	6.6	1.3	1.1	1.0
July	11.7	78.7	13.2	14.7	14.1	13.0	8.6	7.5	5.9
August	9.3	80.2	9.8	11.4	11.3	11.0	9.3	8.7	7.7
September	6.0	76.3	5.7	6.2	6.4	6.6	6.8	6.8	6.5
October	2.6	72.4	1.6	1.6	1.8	2.2	3.4	3.7	4.1
November	–3.3	71.2	–4.4	–0.4	–0.2	0.2	1.7	2.0	2.5
December	–6.2	68.8	–8.3	–0.4	–0.3	–0.1	0.9	1.2	1.6
2013									
January	–6.2	65.2	–7.7	–0.7	–0.6	–0.3	0.6	0.8	1.3
February	–7.4	69.7	–8.4	–0.9	–0.7	–0.5	0.4	0.6	1.0
March	–3.4	67.9	–4.3	–0.5	–0.4	–0.3	0.3	0.5	0.9
April	–1.3	63.8	–1.4	–0.2	–0.2	–0.1	0.4	0.5	0.8
May	–0.6	69.9	0.0	0.0	0.0	0.0	0.3	0.5	0.8
June	6.1	76.3	7.6	7.3	5.6	3.7	1.3	1.2	1.1
July	8.9	74.4	10.2	11.9	11.3	10.3	6.7	5.8	4.7
August	7.9	71.5	8.5	10.0	10.0	9.8	8.5	8.0	7.0
September	4.2	81.0	4.2	4.6	4.7	4.8	5.2	5.2	5.2
October	0.5	77.0	0.2	0.5	0.9	1.3	2.8	3.1	3.4
November	–4.1	72.8	–4.8	–0.6	–0.4	–0.1	1.1	1.4	1.9
December	–8.8	69.2	–9.7	–0.6	–0.5	–0.3	0.7	0.9	1.3
2014									
January	–6.6	64.7	–7.7	–0.6	–0.5	–0.4	0.5	0.7	1.0
February	–9.1	70.1	–9.7	–0.9	–0.8	–0.5	0.3	0.5	0.9
March	–9.4	70.2	–9.1	–0.7	–0.7	–0.5	0.2	0.4	0.7
April	–6.6	70.3	–6.0	–0.4	–0.3	–0.3	0.2	0.4	0.7
May	2.1	73.4	–	0.0	0.0	0.0	0.3	0.4	0.7
June	7.6	73.5	–	7.7	5.8	3.7	0.9	0.9	0.9
July	10.7	71.4	–	13.3	12.5	11.2	6.8	5.9	4.6
August	9.8	74.7	–	11.4	11.3	10.9	8.9	8.3	7.2
September	4.3	73.7	–	5.1	5.4	5.7	6.3	6.3	6.1
October	–0.4	70.9	–	1.0	1.2	1.5	2.8	3.1	3.5
November									
December									

Table 3.5 Air temperature, relative humidity, surface temperature and shortwave irradiance measured at the M500 station from January 2011 to August 2014. (Data from September to December are not yet retrieved).

Month - year	Air temp. (°C)	Rel. hum. (%)	Surface irradiance temp. (°C)	Shortwave irradiance (W m^{-2})
	2.5 m	2.5 m	0 m	2.5 m
2011				
January	–7.6	73.8	–11.0	6.8
February	–11.5	78.1	–13.9	27.8
March	–11.7	80.7	–13.9	76.8
April	–12.6	82.3	–14.5	187.5
May	–3.0	81.0	–3.5	239.2
June	4.6	77.9	7.2	238.7
July	7.6	79.2	8.6	165.8
August	6.8	77.0	7.3	149.8
September	0.7	80.2	–0.8	77.9
October	–4.8	73.1	–8.2	43.4
November	–8.8	70.7	–12.7	11.8
December	–10.8	84.1	–12.3	2.4
2012				
January	–11.3	74.8	–13.7	6.5
February	–10.2	81.7	–12.3	29.0
March	–13.1	78.3	–14.9	72.8
April	–4.0	90.0	–5.1	134.6
May	1.2	82.5	0.2	192.3
June	8.7	68.2	11.1	265.9
July	10.4	74.9	12.2	194.6
August	7.5	79.5	7.4	131.6
September	2.7	85.2	1.8	60.4
October	–0.4	78.5	–2.9	31.3
November	–6.1	77.2	–8.4	8.7
December	–7.3	68.7	–11.7	3.0
2013				
January	–8.4	66.9	–12.1	6.8
February	–10.3	77.8	–12.9	28.5
March	–4.7	64.5	–8.3	80.2
April	–4.0	68.5	–6.1	155.4
May	–4.3	82.3	–5.0	204.8
June	3.8	80.2	5.7	230.6
July	6.6	76.2	7.7	201.5
August	5.6	73.1	6.2	155.3
September	0.9	90.0	–0.6	58.6
October	–1.4	77.8	–4.4	34.5
November	–6.8	81.0	–9.4	9.7
December	–11.0	75.3	–13.9	2.8
2014				
January	–8.6	67.3	–12.6	5.7
February	–10.9	75.9	–13.4	24.6
March	–12.2	79.7	–14.1	79.8
April	–9.7	82.3	–11.6	157.7
May	–0.7	81.2	0.9	230.0
June	6.0	74.4	8.2	231.9
July	9.5	66.8	11.1	232.2
August	7.8	75.0	8.2	146.8
September				
October				
November				
December				

and in 2014 it was 232 W m^{-2} or 11 W m^{-2} below the average. The annual shortwave irradiance is 104 W m^{-2} as an average for the period 2008-2014. Unfortunately the micromet station, M1000, has been out of order since February 2012 although it has been repaired several times, frequent strong winds and icing have damaged all sensors shortly after each repair (figure 3.1.), so it has now has now been decided to close down the station during the field season 2015.

3.2 Soil

Physical soil properties

The results of selected parameters for the soil stations SoilFen, SoilEmp and SoilEmpSa are presented in table 3.4, 3.6 and 3.7 (monthly data for the period 2008-2010 can be found in Hansen *et al.* 2014). The differences in soil properties between the three locations, which were detected in previous years, are also seen in the data collected in 2014. Those being higher winter soil temperatures at SoilFen than at SoilEmp and SoilEmpSa, as the snow depth at SoilFen is significantly higher. During summer, the soil temperatures at SoilFen are significantly higher, as the site is more protected from cold winds from Kobbefjord and Badesø. The temperature in a depth of 30 cm is at SoilFen less affected by fluctuations in surface temperature than at SoilEmp and SoilEmpSa where the soil is well-drained. The results of the measured soil water content show markedly lower values for the well-drained soil at SoilEmp than at SoilEmpSa. The summer season (June-September) mean soil moisture is 20-24 % at SoilEmp and 34-36 % at SoilEmpSa in the period 2008-2014. At all three soil stations, the soil was 4 °C colder in June than most of the years in the period 2008-2014 due to a colder and more prolonged winter season in 2013/2014.

Throughout the season, soil water was collected from two depths at three characteristic soil profiles representing the dominating plant communities in the drainage basin. During the period 20 June to 1 October 2014, thirty soil water samples were collected from the soil water stations at SoilFen (10 and 80 cm) and SoilHeath (10 and 50 cm).

At the research house in Kobbefjord, measurements of pH, temperature and conductivity were carried out on each sample. In August 2011, laboratory equipment was installed in the research house, which enabled analyses of soil water alkalinity. After the field season, the soil water samples have been analysed for all major anions and cations as well as for dissolved organic carbon content, and all data can now be downloaded from the database.

3.3 River water

In 2014, 42 water samples were collected from end May to start October. Due to a very late snow-/icemelt the field season was one month shorter than previous years. *In situ* measurements of river water temperature, conductivity and pH were conducted and the measured values are presented in figure 3.10. The water temperature varied through the 2014 season as it did in field season 2009 and

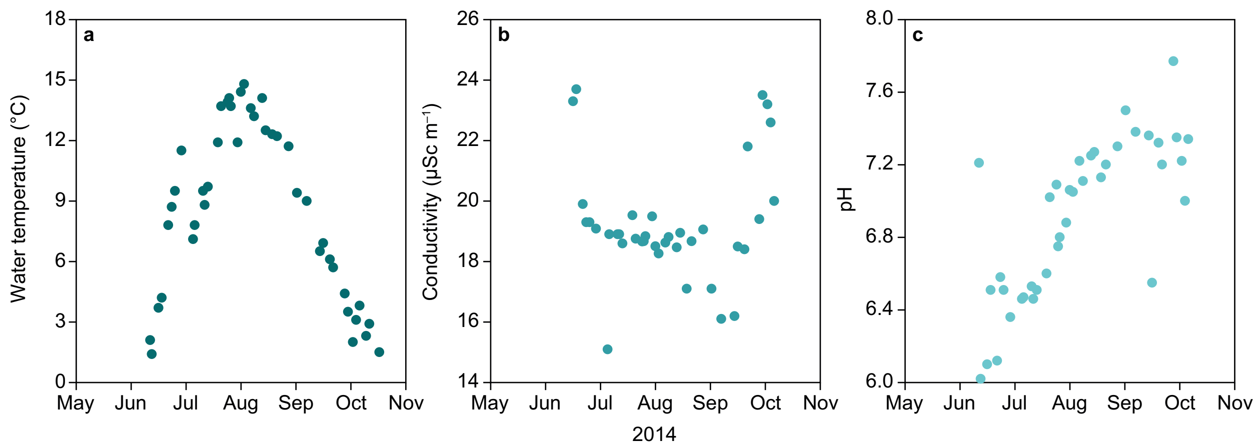

Figure 3.10 a) water temperatures, b) conductivity and c) pH measured in 2014 in the river flowing into Kobbefjord at the water sampling point near the research station.

Table 3.6 Soil temperature and soil moisture at four depths measured at SoilEmp from January 2011 to October 2014.

Month - year	Soil temp. (°C) –1 cm	Soil temp. (°C) –5 cm	Soil temp. (°C) –10 cm	Soil temp. (°C) –30 cm	Soil moist. (%) –5 cm	Soil moist. (%) –10 cm	Soil moist. (%) –30 cm	Soil moist. (%) –50 cm
2011								
January	–1.7	–1.5	–1.2	–0.4	3.2	13.6	5.2	4.4
February	–1.3	–1.1	–1.0	–0.6	2.4	9.9	3.6	3.5
March	–1.3	–1.2	–1.1	–0.8	2.4	9.7	3.4	3.4
April	–0.7	–0.6	–0.5	–0.3	2.5	10.0	3.4	3.4
May	0.0	0.0	0.1	0.1	11.1	17.9	14.1	15.5
June	5.3	4.7	4.3	3.2	27.1	38.6	26.0	31.8
July	10.9	10.5	10.2	9.1	7.9	37.5	8.9	6.2
August	10.1	10.0	9.8	9.3	7.3	36.3	8.3	6.7
September	3.8	4.2	4.4	4.9	12.6	39.8	22.8	20.0
October	–0.7	–0.3	–0.1	0.7	6.4	25.3	7.7	6.0
November	–4.7	–4.4	–4.0	–2.5	2.8	8.4	3.6	4.9
December	–2.6	–2.5	–2.4	–2.1	2.9	8.5	3.5	4.1
2012								
January	–2.5	–2.4	–2.3	–2.0	2.9	8.7	3.6	4.1
February	–1.7	–1.6	–1.6	–1.5	3.2	10.3	3.7	4.2
March	–3.8	–3.7	–3.5	–3.1	2.8	8.5	3.4	4.0
April	–0.1	–0.2	–0.2	–0.3	3.6	12.9	3.8	4.3
May	1.0	0.9	0.7	0.2	19.5	27.9	19.0	17.5
June	11.3	10.5	10.0	8.2	17.3	40.1	25.7	22.9
July	13.3	12.8	12.4	11.3	7.7	32.5	16.3	13.0
August	10.6	10.4	10.3	9.9	16.3	39.6	23.6	20.3
September	5.9	6.1	6.2	6.4	25.4	41.7	25.6	23.5
October	2.0	2.1	2.3	2.6	31.7	46.1	35.6	32.9
November	–1.2	–0.9	–0.7	0.0	11.9	20.5	21.4	19.0
December	–1.7	–1.5	–1.4	–0.8	4.6	10.8	7.5	5.8
2013								
January	–3.3	–3.2	–3.0	–2.5	4.1	9.1	6.5	4.4
February	–3.4	–3.3	–3.2	–2.8	4.0	9.0	6.4	4.2
March	–2.3	–2.3	–2.3	–2.2	4.1	9.6	6.3	4.1
April	–0.7	–0.6	–0.6	–0.5	4.4	11.5	7.7	6.0
May	0.5	0.3	0.1	0.0	22.9	30.5	10.4	13.7
June	8.9	8.0	7.5	5.8	18.5	39.8	28.7	24.8
July	10.8	10.2	9.9	8.9	7.1	31.7	9.5	6.9
August	9.3	9.2	9.2	8.8	8.9	22.1	12.0	10.0
September	4.3	4.3	4.4	4.4	38.8	48.1	40.9	37.2
October	0.0	0.4	0.6	1.2	20.4	33.3	28.5	22.8
November	–2.6	–2.3	–2.0	–1.0	6.6	13.2	12.6	9.2
December	–1.5	–1.3	–1.2	–0.8	5.0	12.6	9.7	6.5
2014								
January	–1.9	–1.8	–1.7	–1.4	4.3	10.7	6.7	4.7
February	–2.8	–2.6	–2.5	–2.1	4.1	10.2	6.4	4.5
March	–3.3	–3.2	–3.1	–2.9	4.0	9.7	6.2	4.2
April	–2.0	–2.0	–2.0	–1.9	4.1	10.3	6.2	4.2
May	0.6	0.3	0.2	0.0	9.9	19.2	11.4	10.7
June	8.5	7.6	6.9	5.1	20.9	40.8	31.5	25.1
July	12.1	11.3	10.8	9.5	8.4	27.7	18.1	14.6
August	10.6	10.4	10.2	9.7	5.3	18.4	9.3	6.8
September	4.6	4.8	5.0	5.3	16.5	36.0	26.5	21.8
October	0.8	1.1	1.3	1.7	13.9	35.0	20.5	15.9
November								
December								

Table 3.7 Soil temperature and soil moisture at four depths measured at SoilEmpSa from January 2011 to October 2014.

Month - year	Soil temp. (°C) –1 cm	Soil temp. (°C) –5 cm	Soil temp. (°C) –10 cm	Soil temp. (°C) –30 cm	Soil moist. (%) –5 cm	Soil moist. (%) –10 cm	Soil moist. (%) –30 cm	Soil moist. (%) –50 cm
2011								
January	–1.1	–0.2	–0.5	0.0	32.7	25.9	44.5	43.3
February	–0.6	–0.3	–0.5	–0.2	23.5	14.8	41.8	37.0
March	–0.6	–0.4	–0.5	–0.3	23.6	14.5	25.0	33.5
April	–0.7	–0.5	–0.6	–0.4	23.8	14.4	19.3	31.5
May	0.1	0.1	0.1	0.2	30.5	21.5	20.0	32.7
June	3.9	3.2	3.4	3.0	53.4	47.0	35.9	45.1
July	10.3	9.0	9.2	8.9	60.0	51.9	47.4	49.9
August	10.2	9.3	9.6	9.1	58.0	39.9	45.0	44.2
September	4.7	5.1	5.0	5.2	60.1	53.3	46.9	49.4
October	0.2	1.0	0.6	1.3	52.0	40.2	45.2	45.5
November	–1.9	–0.8	–1.4	–0.3	21.9	15.1	40.5	39.4
December	–0.9	–0.7	–0.8	–0.5	21.3	13.5	15.7	35.1
2012								
January	–0.9	–0.7	–0.9	–0.5	21.3	13.4	15.6	32.2
February	–0.6	–0.5	–0.6	–0.4	23.1	14.0	15.8	22.2
March	–1.6	–1.3	–1.5	–1.0	20.0	12.5	14.5	17.0
April	0.0	0.0	0.0	0.0	27.2	14.9	16.2	17.3
May	0.6	0.2	0.3	0.1	45.1	26.4	18.0	18.8
June	8.6	6.3	7.1	5.7	58.8	45.5	44.4	37.6
July	11.9	10.6	11.2	10.2	57.6	42.3	44.9	42.7
August	10.2	9.7	9.8	9.6	59.5	49.7	46.1	47.7
September	6.6	6.8	6.7	6.9	58.9	48.5	45.6	45.7
October	2.8	3.1	3.0	3.1	60.4	56.7	46.8	50.0
November	–0.1	0.4	0.3	0.5	52.8	50.9	46.4	49.2
December	–0.8	–0.2	–0.4	0.0	27.0	30.0	44.3	41.9
2013								
January	–1.4	–0.8	–1.2	–0.4	21.6	14.1	35.6	35.3
February	–2.2	–1.6	–2.0	–1.1	19.6	13.2	14.7	25.8
March	–1.3	–1.0	–1.1	–0.8	21.1	14.4	14.8	16.1
April	–0.1	–0.1	–0.1	–0.1	25.8	15.4	16.0	16.9
May	0.2	0.0	0.0	0.0	30.5	16.8	17.3	17.8
June	4.4	1.6	2.5	1.1	58.7	40.7	32.3	23.9
July	9.1	7.2	8.0	6.7	57.6	39.9	45.2	44.0
August	9.0	8.4	8.7	8.2	55.2	35.1	43.8	38.9
September	4.5	4.5	4.5	4.5	60.4	56.7	46.5	46.4
October	1.2	1.5	1.5	1.6	60.3	53.3	46.8	49.9
November	–1.1	–0.3	–0.5	–0.1	31.1	21.7	45.1	43.4
December	–1.2	–0.6	–0.8	–0.3	24.6	20.1	39.0	41.3
2014								
January	–1.7	–1.4	–1.6	–0.9	20.3	13.9	15.0	24.8
February	–2.5	–2.2	–2.5	–1.7	19.2	13.4	14.3	15.9
March	–2.3	–2.1	–2.3	–1.8	18.9	13.1	14.1	15.2
April	–1.1	–1.1	–1.1	–0.9	20.0	13.5	14.3	15.3
May	0.3	0.1	0.1	0.0	29.0	16.3	15.9	16.1
June	4.7	2.0	3.0	1.2	59.9	44.2	33.2	23.3
July	9.3	7.3	8.0	6.6	57.9	42.4	45.5	45.8
August	10.0	9.1	9.4	8.8	56.7	39.6	44.7	42.2
September	5.2	5.4	5.4	5.5	59.9	53.8	46.0	48.1
October	1.3	1.7	1.6	1.7	60.5	54.1	46.6	50.1
November								
December								

2011 (Hansen *et al.* 2014). The minimum river water temperature was 1-2 °C from end May which was 1.0 °C lower than the previous year and the water temperature peaked with a maximum temperature of 14.8 °C at the end of July which was 1.9 °C higher and 2 weeks earlier than 2013. The conductivity measurements showed a normal decrease in conductivity within the snow-melting period from 23-24 µSc m^{-1} to a level of 18 +/- 1.5 µSc m^{-1}. From the beginning of July and through the rest of the field season, the conductivity showed no significant trend which is normal for the period. pH showed a normal trend from 6.0 at the beginning of the field season to 7.6 at the beginning of August, followed by some variation due to rain events during the autumn.

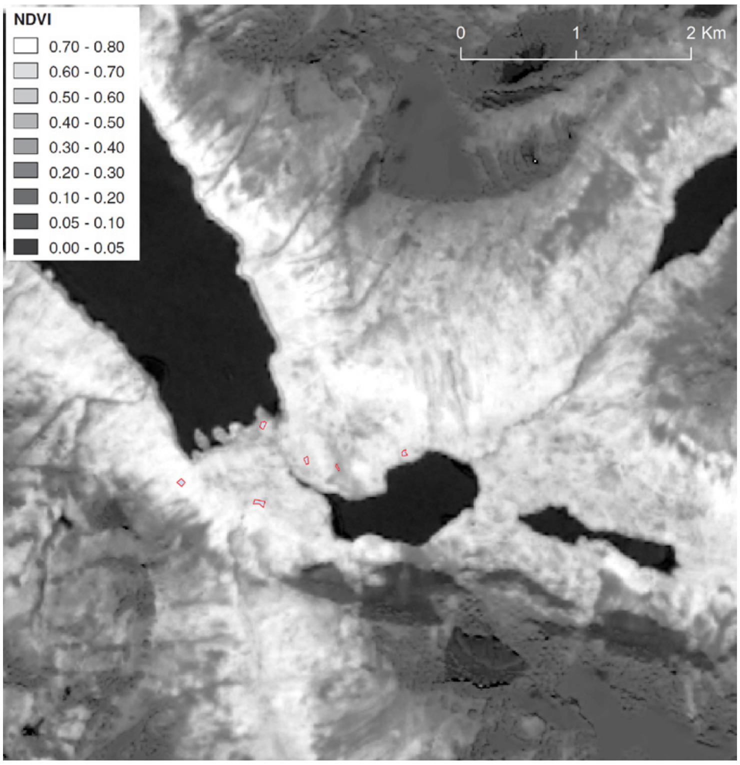

Figure 3.11 Normalised Difference Vegetation Index (NDVI) based on a Landsat8 scene from 14 July 2014. Data are dark subtracted as atmospheric correction and lack the topographic correction.

3.4 Vegetation

Vegetation in the Kobbefjord area is monitored both by the BioBasis and GeoBasis programmes. While BioBasis monitors individual plants and plant phenology using plot scale sites and transects, the GeoBasis programme monitors the phenology of the vegetation communities from satellite.

Satellite imagery

Unlike the previous years, it has not been possible to acquire QuickBird, WorldView or Aster image data, due to cloudy conditions in the requested period (optimum of growing season at the end of July). Instead, a Landsat8-scene was acquired from 14 July at around 14:30 GMT. The scene was geometrically corrected with RPC and known ground control points from former campaigns in Kobbefjord (30 GCP also used to correct previous QuickBird scenes). Moreover, it was orthorectified using the 10 m digital elevation model. Furthermore it was atmospherically corrected using a dark object subtraction approach and data were converted from digital numbers to top of atmosphere reflectance. Finally, NDVI was derived from the reflectance (see figure 3.11) and average NDVI was extracted from regions of interest covering a fell field, an open mixed heath, an

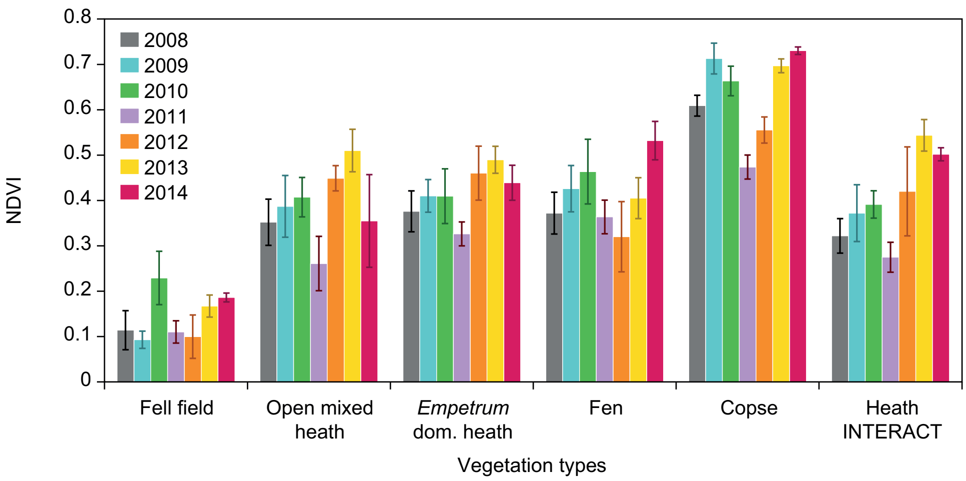

Figure 3.12 NDVI from 17 July 2008 and 2009, 10 July 2010, 14/30 July 2011, 25 July 2012, 28 July 2013 and 14 July 2014 for the six different vegetation types. NOTE that changes between greenness are due not only to phenology differences between years but also seasonal phenology as the images are acquired approx. 2 weeks around the maximum greenness dates.

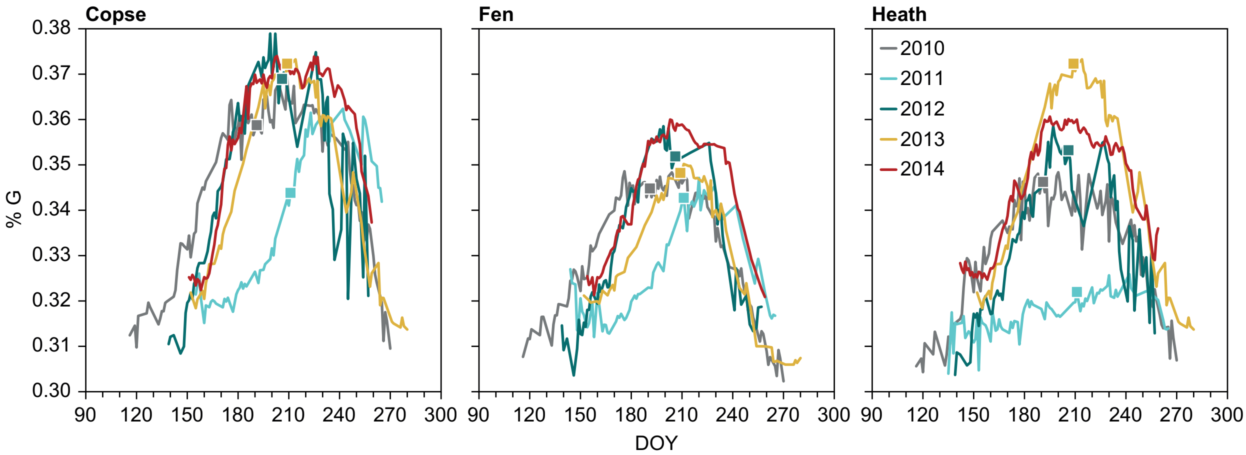

Figure 3.13 Greenness indices for three ecosystems copse, fen and heath at 50 m a.s.l. have been analysed using a new greenness index, %G. The regions are specified in figure 3.5 left and the fen area is very similar to the footprint for the CO_2-station in the fen. The %G for all three ecosystems in the period 2010-2014 is shown. The squares represent the days for the satellite measurements. DOY (day of year).

Empetrum nigrum dominated heath, a fen, a copse and the heath monitored by the INTERACT station (see figure 3.12). Over the seven years, the fell field had significant lower NDVI-values around 0.13±0.14, while copse had significant higher values around 0.60±0.13 all seven years. The four other vegetation classes had NDVI-values around 0.36-0.40 ± 0.05. As also noticed from ground truth measurements of NDVI (BioBasis 2013), higher NDVI values were observed in 2013 than 2011 and 2012, probably as a result of the shrubs recovering from the *Eurois occulta* larvae attack in 2011, combined with a more dominating understory resulting from the decreased competition from shrubs during the attack. The higher NDVI values were most prominent in heaths as expected.

Digital camera imagery

Phenology studies of Arctic ecosystems are still dependent on spatial scale and quality (e.g. percent cloud cover) of the image data. Furthermore, the sparse vegetation and heterogeneous surface can be difficult to trace with coarse spatial resolution NDVI. Greatly improved spatial and temporal scale can be achieved by monitoring the ecosystems with automated digital cameras. Better still, image data can thus be acquired under cloudy conditions, which is advantageous in Arctic ecosystems with short intense growing seasons where a high frequency of data is important. Major challenges when using digital cameras are to compensate for changes in incoming radiation, as well as having the limitation of low spectral resolution. Even so, indices based on visual bands available from unmodified digital cameras have been found to correlate with NDVI over numerous types of ecosystems. However, of the few existing studies, none investigates the performance in Arctic environments with high variability in species composition. The use of conventional RGB cameras as a tool to monitor landscape wide phenology has gained a lot of attention over the last few years. Mostly a measure of canopy greenness for a region of interest (ROI) is used to produce yearly time series, reflecting canopy phenology. The use of RGB prevents the use of established vegetation indices such as NDVI or RVI. However, since photosynthesis by vegetation is related to chlorophyll content and biomass in various vegetation types, we hypothesize that indices based on the excess of the green channel can describe seasonal growth patterns in vegetation. The most common is a greenness index, calculated as percent greenness, %G = DN(G) / (DN(R)+DN(G)+DN(B)), where DN is the digital value in each of the RGB channels. Figure 3.13 shows the significantly lower %G-values in 2011 due to the outbreaks of *Eurois occulta* larvae, but the figure also shows that all three ecosystems in 2013 seems to have recovered from the outbreak. Figure 3.13 also shows that copse has a fast and earlier greenness compared to fen and heath, but all three ecosystems reached the maximum within the same week at the end of July. In 2014, the %G-values for fen and copse were normal in the spring, but above normal in late summer and autumn, while heath

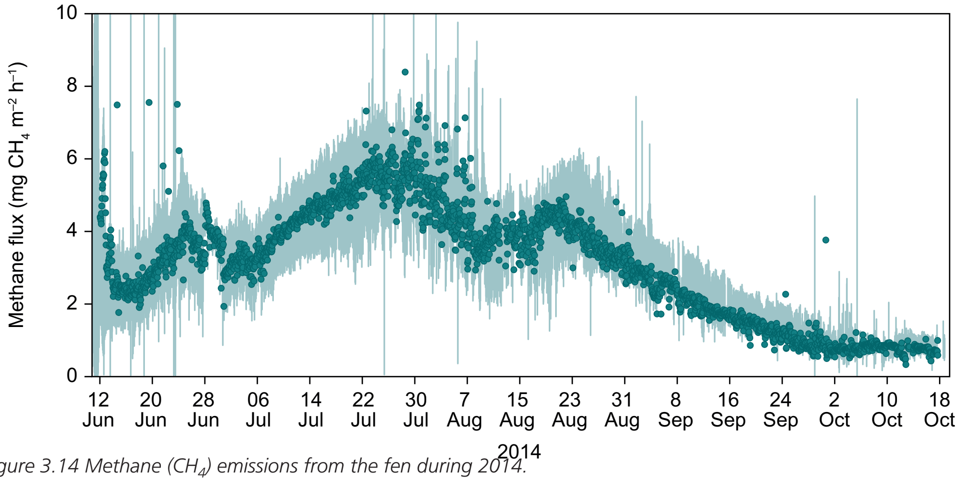

Figure 3.14 Methane (CH_4) emissions from the fen during 2014.

had high %G-values in the spring and close to normal values in late summer and autumn.

3.5 Carbon gas fluxes

Carbon gas fluxes are monitored on plot and landscape level in a fen area in Kobbefjord using two techniques:

- Automatic chamber measurements of CH_4 and CO_2 exchange on plot scale
- Eddy covariance measurements of CO_2 and H_2O exchange on landscape scale

Automatic chamber measurements

An automatic chamber system consisting of six flux chambers for monitoring the exchange of CH_4 and CO_2 was installed in the fen in August 2007 (Tamstorf *et al.* 2009). In 2014, measurements started on 12 June and lasted until 18 October, with only few interruptions in the data record (figure 3.14). During this period, approx. 16 % of the data were lost due to maintenance, calibration and preventive system close-downs (i.e. due to expected high winds that may break the auto-chamber lids).

The spatial and temporal variation in CH_4 emissions is primarily related to temperature, water table depth and primary production. The fen in Kobbefjord is a source of CH_4 due to the permanently wet conditions that promote anaerobic decomposition, by which CH_4 is an end product.

Mean CH_4 fluxes across chambers were initially relatively high, but decreased to below 3 mg CH_4 m^{-2} h^{-1} within a few days (figure 3.14). Interestingly, three distinct peaks appear in the measurement record: one in early season (25-27 June), one in mid-season (27-29 July) and one in late season (20-21 August). The early season and mid-season peaks have been observed in previous years and can possibly be explained by different sources of carbon for the methane production: i.e. old litter-derived carbon from previous growing season during first peak and recently assimilated carbon during second peak. The peak in late season has not been observed previously. The mid-season peak amounted to slightly above 6 mg CH_4 m^{-2} h^{-1}, a magnitude that is similar to the previous year. The variation between years is likely related to variations in timing of snowmelt, meteorological conditions, and primary production in the fen. After the late season peak, CH_4 fluxes decreased steadily and reached approximately 1 mg CH_4 m^{-2} h^{-1} in late September.

Eddy covariance measurements

In order to describe the interannual variation of the seasonal CO_2 budget, the land-atmosphere exchange of CO_2, H_2O and energy in the fen has been monitored using the eddy covariance technique since 2008. The eddy covariance system consists of a 3D sonic anemometer and closed path infrared CO_2 and H_2O gas analyser (Tamstorf *et al.* 2009). Raw data from the eddy covariance system was calculated using the software package EdiRe (Robert Clement, University of Edinburgh). For more details on the flux calculation procedures see Hansen *et al.* (2010).

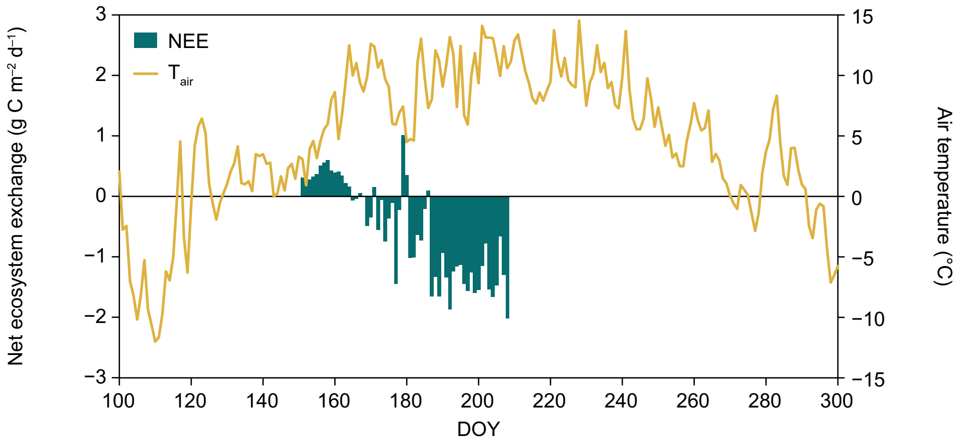

Figure 3.15 Diurnal net ecosystem exchange (NEE) and air temperature (Tair) measured in the fen in 2014.

Table 3.8 Summary of the eddy covariance measurement periods and CO_2 exchanges 2008-2014 at the fen site. Please note that the measurement period varies from year to year.

Year	2008	2009	2010	2011	2012*	2013	2014
Measurements start	5 Jun	15 May	4 May	15 May	6 Jun	29 May	30 May
Measurements end	29 Oct	31 Oct	9 Oct	14 Oct	31 Oct	22 Oct	28 Jul
Start of net uptake period	–	1 Jul	29 May	28 Jul	16 Jun	23 Jun	18 Jun
End of net uptake period	16 Aug	27 Aug	18 Aug	7 Sep	31 Aug	24 Aug	–
NEE for measuring period (g C m^{-2})	–45.5	–14.0	–20.9	42.6	–22.3	–24.2	–32.7
NEE for net uptake period (g C m^{-2})	–	–42.5	–65.4	–14.3	–61.3	–67.3	–
Max. daily accumulation (g C m^{-2} d^{-1})	–2.27	–1.48	–3.14	–1.58	–2.88	–2.74	–2.02

* = values for 2012 have been updated compared with previous reports

The temporal variation in mean daily net ecosystem exchange of CO_2 (NEE) and air temperature during 2014 for the fen site is shown in figure 3.15 and various variables summarized in table 3.8. NEE refers to the sum of all CO_2 exchange processes at the ecosystem scale; including photosynthetic CO_2 uptake by plants, plant respiration and microbial decomposition. The CO_2 exchange is controlled by climatic conditions, mainly temperature and photosynthetic active radiation (PAR), along with amount of biomass and soil moisture content. The sign convention used in figures and tables is the standard for micrometeorological measurements; fluxes directed from the surface to the atmosphere are positive whereas fluxes directed from the atmosphere to the surface are negative.

Eddy covariance measurements of the CO_2 and H_2O exchange in the fen were initiated on 30 May. At the end of July, a pump broke down and due to unexpected long delivery time from the supplier, it was unfortunately not possible to resume the measurements during 2014.

The fen was still snow-covered when measurements began. During the snowmelt period and pre-green season, CO_2 fluxes were generally small. Highest daily spring time emission (0.6 g C m^{-2} d^{-1}) was measured on 7 June (figure 3.15). As the vegetation developed, photosynthetic uptake of CO_2 started, and on 18 June the fen ecosystem switched from being a net source to a net sink of atmospheric CO_2 on a daily basis.

The measurements during 2014 did not cover the entire net uptake period. However, between 18 June and 28 July, the fen accumulated –36.6 g C m^{-2}. Maximum daily uptake (–2.0 g C m^{-2} d^{-1}) was recorded on the last day with complete measurements (27 July). During the entire measurement period, the fen constituted a sink for atmospheric CO_2, amounting to –32.7 g C m^{-2}.

4 Nuuk Basic

The BioBasis programme

Maia Olsen, Josephine Nymand, Katrine Raundrup, Peter Aastrup, Paul Henning Krogh, Torben L. Lauridsen, Magnus Lund and Marie Buchardt

This chapter presents the results of the eighth year of the BioBasis monitoring programme at Nuuk. The chapter gives an overview of the activities and presents examples of the results. The programme aims at providing long-term data series on biotic variables from the Kobbefjord area, approximately 20 km south-east of Nuuk. Methods and sampling procedures are described in detail in the manual 'Conceptual design and sampling procedures of the biological programme of Nuuk Basic' (Aastrup *et al.* 2009).

The programme was initiated in 2007 by the National Environmental Research Institute (now Department of Bioscience), Aarhus University in cooperation with the Greenland Institute of Natural Resources. BioBasis is funded by the Environmental Protection Agency as part of the environmental support programme DANCEA – Danish Cooperation for Environment in the Arctic. The authors are solely responsible for all results and conclusions presented in this chapter, which do not necessarily reflect the position of the Environmental Protection Agency.

4.1 Vegetation

Reproductive phenology

The reproductive phenology has been studied since 2008 on three vascular plant species: The evergreen dwarf shrub *Loiseleuria procumbens*, the herb *Silene acaulis*, and the shrub *Salix glauca*. For each species, four phenology plots cover an ecological amplitude with respect to snow cover, soil moisture, and altitude. In 2014, the recording of phenology started on 15 May (DOY 135) and ended on 14 October (DOY 287). Examples of the results from 2008-2014 are shown and commented in the following text.

The reproductive phenology of *L. procumbens* and *S. acaulis* in 2014 is comparable to that of 2013, with intermediate timing of budding, flowering and onset of senescence. However, there was a tendency to produce larger numbers of flowers in most plots. The timing of 50 % flowering was similar to previous years (figure 4.1).

The flower bud production, onset of flowering and peak flower production of *L. procumbens* occurred at roughly the same time as in 2013 and 2012 (figures 4.2a and 4.2b). In *L. procumbens* plot 1 (Loi1) snowmelt occurred at an earlier date this year than in 2013 (DOY 140 compared to DOY 148) which resulted in an earlier observation of bud production but not an earlier flower production or peak (figure 4.2b). All plots produced more flowers than the previous two seasons and two plots produced more than has previously been recorded. The first senescent flowers were recorded on the same day (18 June, DOY 169) as in 2013 (figure 4.2c).

S. acaulis also followed approximately the same pattern as last year (figure 4.3a-c), but all four plots produced more flowers than has been recorded so far. First bud-

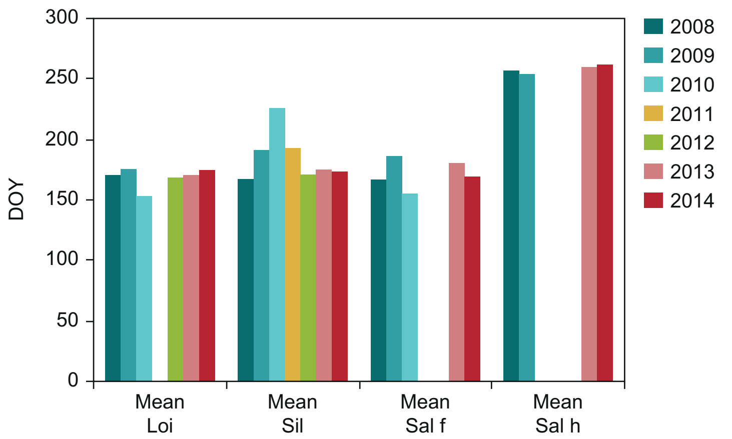

*Figure 4.1 Mean value for days of year (DOY) of 50 % flowers/catkins for each of the species (*Loiseleuria procumbens, Silene acaulis, *and* Salix glauca*) in the plant reproductive phenology plots for 2008-2014. Also included are the senescent catkins of* S. glauca *(Sal h). Erratum: Please note that the similar figures in annual reports from 2008-2011 are incorrect.*

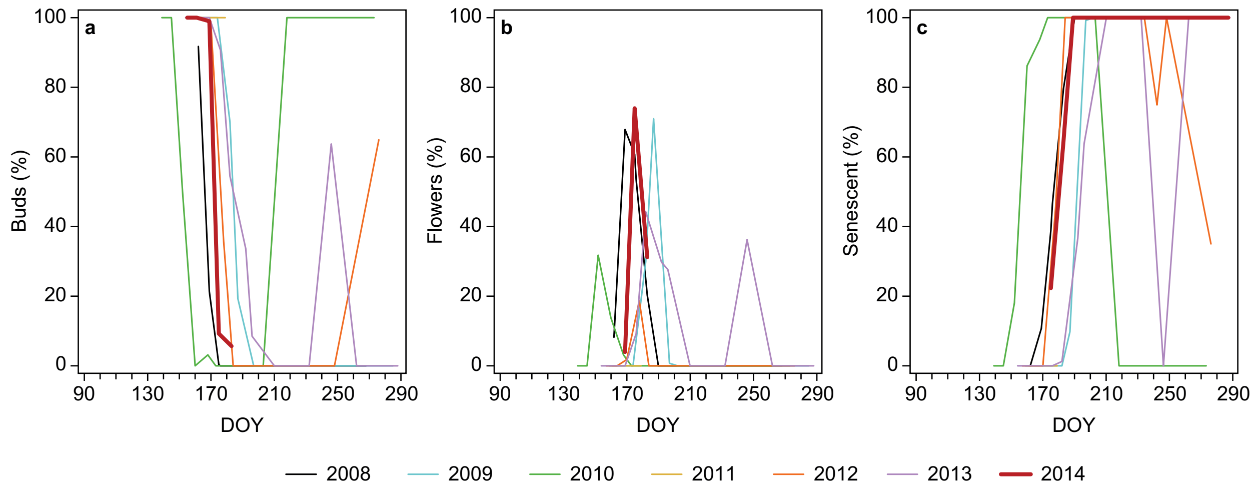

Figure 4.2 Percentage of Loiseleuria procumbens *a) buds, b) flowers, and c) senescent flowers in plot 1 during the growing seasons of 2008-2014.*

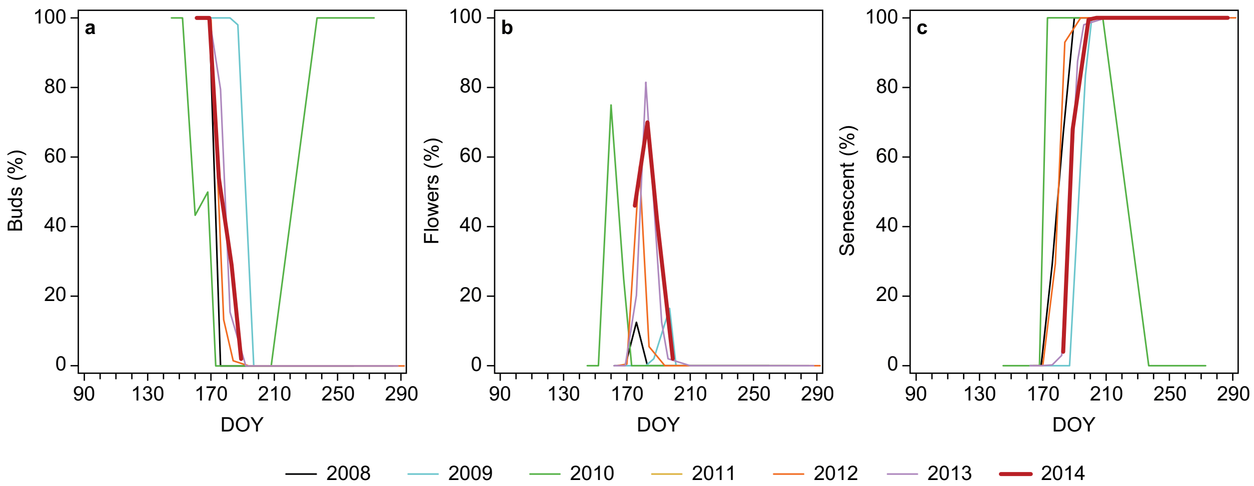

Figure 4.3 Percentage of Silene acaulis *a) buds, b) flowers and c) senescent flowers in plot 3 during the growing seasons of 2008-2014.*

ding was recorded on 10 June (DOY 161) while onset of flowering was recorded on 18 June (DOY 169), one week later than in 2013. In all plots but one, flowering also peaked at the same time as in 2013, but in Sil3 flowering peaked approx. two weeks later (figure 4.3b), the latest peak recorded so far except for 2011. Onset of senescence was recorded on 24 June (DOY 175), one day earlier than in 2013.

The first flower buds of *S. glauca* were observed on 4 June (DOY 155), just two days later than the earliest year 2010 (DOY 153) and two weeks earlier than in 2013 (DOY 170). First flowering male and female catkins were observed on 18 June (DOY 169). The first female flowers with hairs were observed on 28 July (DOY 209), 17 days later than in 2013 (DOY 192). Three plots produced more flowers than in 2013 and all together more flowers were produced in 2014 than in any other year. Plot 4 produced more than twice as many flowers in 2014 than in 2009, which was previously the year with the highest recorded number.

In the CO_2 flux plots *S. glauca* catkins were produced in more plots than any previous years (23 plots out of 30), but the number of catkins was lower compared to 2013.

Summing up reproductive plant phenology

The field season was drier than 2012 and 2013. A preliminary review of data related to flowering indicates that 2013 was characterised by:

- Large numbers of flowers in most plots
- Intermediate timing of budding, flowering and senescence; very similar to 2012 and 2013

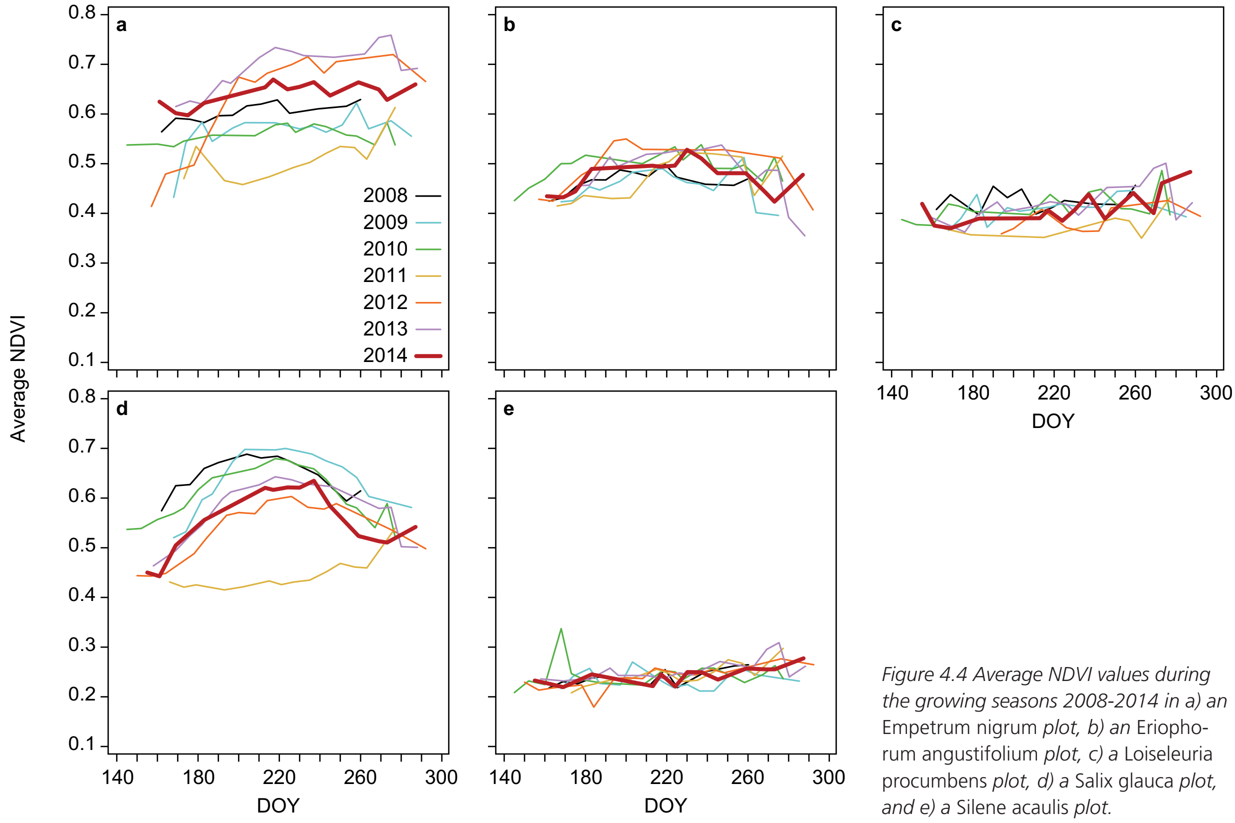

Figure 4.4 Average NDVI values during the growing seasons 2008-2014 in a) an Empetrum nigrum *plot, b) an* Eriophorum angustifolium *plot, c) a* Loiseleuria procumbens *plot, d) a* Salix glauca *plot, and e) a* Silene acaulis *plot.*

Vegetation greening, NDVI

The seasonal greening of the vegetation was monitored 1) in plots with *Empetrum nigrum ssp. hermaphroditum* and *Eriophorum angustifolium*, 2) in the plant phenology plots, 3) along the NERO line (Bay *et al.* 2008) and 4) in the CO_2 flux plots. We used a handheld Crop Circle TM ACS-210 Plant Canopy Reflectance Sensor, which calculates the greening index (Normalized Difference Vegetation Index – NDVI). Measurements were made weekly in the *Empetrum nigrum*-plots, *Eriophorum angustifolium*-plots, and the plant phenology plots, and monthly along the NERO line. This season there were some problems with the wiring in the Crop Circle, which led to a gap in the monitoring from DOY 183 to DOY 213. Furthermore, this season measurements of NDVI in the CO_2 flux plots were included using the SpectroSense 2+ handheld system with two mounted sensors.

NDVI – Plots

Empetrum nigrum consistently reached high NDVI values throughout the season (figure 4.4a). Although the values were lower than in 2012 and 2013, they were higher than the values recorded in the previous years. All *Empetrum* plots had high NDVI values, with little variation throughout the season.

Eriophorum angustifolium reached intermediate NDVI values compared to previous years (figure 4.4b). A peak was recorded on 18 August (DOY 230). Compared to the four other species *Eriophorum* reached intermediate to high NDVI levels.

The NDVI values for *L. procumbens* were low to intermediate in 2014 (figure 4.4c) with only small fluctuations throughout the season. All *L. procumbens* plots tend to have intermediate NDVI values, except for plot 4, which has lower density of vegetation leading to lower overall NDVI values. Plot 1 was the only *L. procumbens* plot with a defined peak (DOY 213).

Salix glauca (figure 4.4d) plots 3 and 4 both displayed a bell-shaped greening with values tending to be lower in 2014 than in most other years. Plot 3 was more inconsistent this season and started out with higher values than usual, which then dropped to an intermediate level. Plot 1 was consistently low, with no discernible peak.

Low NDVI values were recorded in all four *S. acaulis* plots with little variation over time (figure 4.4e). There seems to be

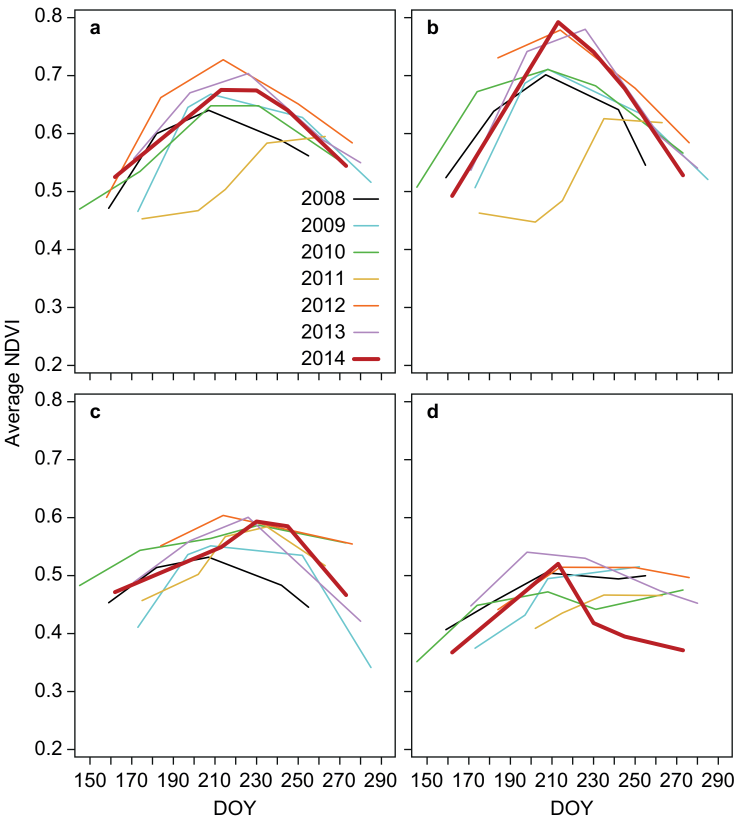

Figure 4.5 Average NDVI values along the NERO line during the growing season from the vegetation types a) dwarf shrub heath, b) copse, c) fen, and d) snow patch.

Figure 4.6 Landslide in the uppermost snow patch on the north-facing slope of the NERO line.

a tendency to a slight increase, with some fluctuation in the values indicating an increase in greenness from the beginning to the end of the season.

NDVI – NERO line

Overall the NDVI values were lower than in 2012 and 2013 but higher than the previous years (figures 4.5a-d). Maximum NDVI occurred at an intermediate time around 1 August (DOY 213) for all vegetation types but fen (figure 4.5c), which peaked later in the season around 18 August (DOY 230) close to the peak recorded in 2013. Copse reached maximum values at roughly the same time as in 2012 but the peak was the highest recorded so far (figure 4.5b). A landslide (figure 4.6) had occurred in the snow patch between 1 August (DOY 213) and 18 August (DOY 230), explaining the sudden drop in NDVI values (figure 4.5d) observed after 1 August (DOY 213).

NDVI – CO_2 flux plots

The CO_2 flux plots are dominated by *Empetrum nigrum* and *Salix glauca*, but in different fractions. Because the different species have a different greening pattern, the plots have been divided into *E. nigrum* and *S. glauca* plots (figure 4.7a-b). NDVI values were measured from 12 June (DOY 163) to 14 October (DOY 287). The plots dominated by *E. nigrum* have little change in the NDVI values. There is a slight increase at the beginning of the season, in most cases followed by a slow decrease. In the two plots dominated by *S. glauca* a bell shaped greening curve is observed, with a steep increase at the beginning of the growing season followed by a distinct drop towards the end of the season.

Summing up the vegetation greening

NDVI values measured were intermediate, with *S. glauca* and *E. angustifolium* showing bel-l shaped greening curves whereas the remaining plots showed mostly uniform values with some fluctuations throughout the season.

Carbon dioxide exchange

In 2008, a manipulation experiment was initiated with five treatments, each with six replicates. The experiment is located in a mesic dwarf shrub heath dominated by *Empetrum nigrum* with *Salix glauca* as a subdominant species. Treatments include control (C), shortened growing season (SG: addition of snow in spring), prolonged growing season (LG: removal of snow in spring), shading (S: hessian tents) and increased temperature (T: ITEX plexiglas hexagons). We have conducted measurements of land-atmosphere exchange of CO_2, using the closed chamber technique, soil temperature, soil moisture and phenology of *Salix glauca* approximately weekly during June-September each year. The net ecosystem exchange (NEE) was measured with transparent chambers while the ecosystem respiration (R_{eco}) was measured with darkened chambers. Gross primary production (GPP) was calculated as the difference between NEE and R_{eco}. The SG and LG treatments have not been applied in 2008-2014, therefore results from these plots can be considered as controls.

The first CO_2 flux measurement day in 2014 was 3 June (DOY 154). Until the last measurement day, 20 October (DOY 293), CO_2 fluxes were measured on 18 occasions (figure 4.8). Generally, all plots functioned as sinks for atmospheric CO_2 at the time of the measurement (midday). In October, NEE was generally close to zero. Similar to earlier years, NEE was generally more negative (i.e. higher CO_2 uptake) in C plots compared with T and S plots.

In previous years, T plots have generally had highest R_{eco} rates, which can be explained by warmer and drier conditions resulting in increased respiration rates. However, in 2014, R_{eco} rates from T plots were not consistently higher than those from C plots. Highest rates of GPP were generally observed in C plots, while especially S plots had lower GPP rates compared with other treatments. As photosynthesis is driven by solar radiation, shading decreases GPP and build-up of biomass.

Since the extensive outbreak of the larvae *Eurois occulta* in 2011, which defoliated large parts of the heath vegetation in the area, CO_2 flux magnitudes have been high in the following years. This trend was continued and further accentuated in 2014.

UV-B exclosure plots

Measurements of chlorophyll fluorescence as a measure of plant stress were carried out in the Kobbefjord area in 2014. The impact of ambient UV-B radiation on the vegetation was studied in a mesic dwarf shrub heath dominated by *Empetrum nigrum* and with *Betula nana* and *Vaccinium*

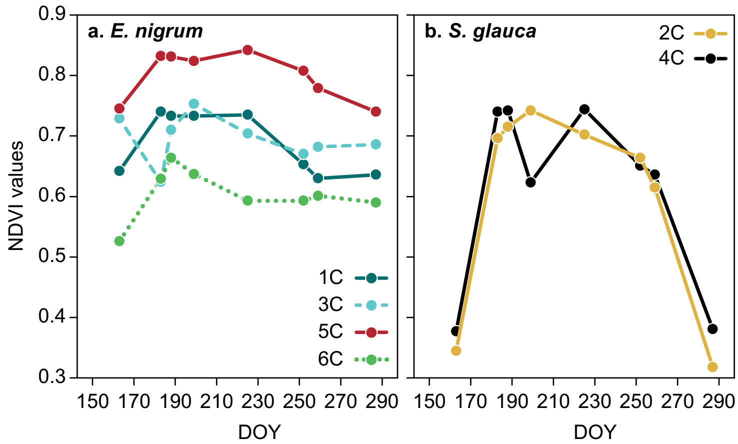

Figure 4.7 NDVI values during the growing season in six control CO_2 flux plots dominated by a) Empetrum nigrum *and b)* Salix glauca.

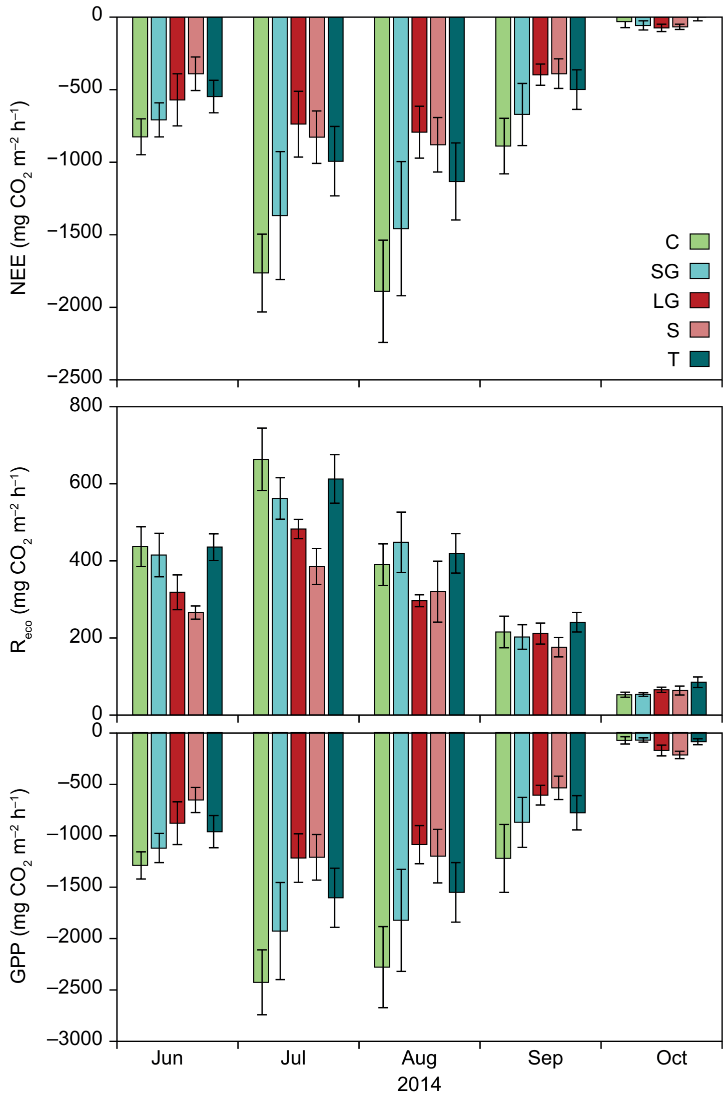

Figure 4.8 Monthly means of net ecosystem exchange (NEE: upper panel), ecosystem respiration (Reco: middle panel) and gross primary production (GPP: lower panel) in 2014 in the manipulation experiment. Error bars refer to standard error in spatial variability (six replicates). For explanation of treatment abbreviations, see text.

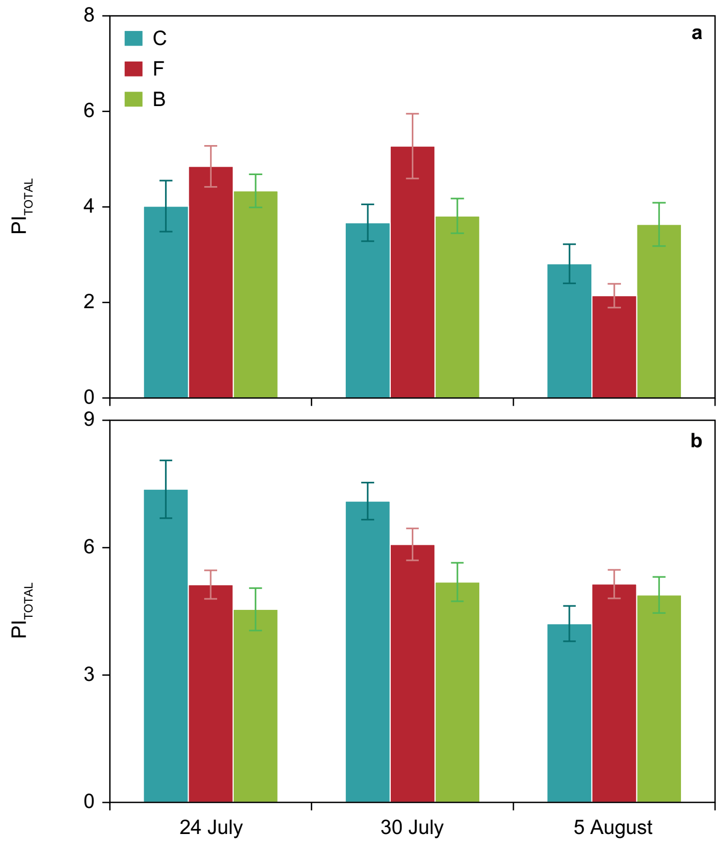

Figure 4.9 Seasonal variations in total performance index for a) Betula nana *and b)* Vaccinium uliginosum*. Treatments are C – Open control (no filter), F – filter control (transparent filter) and B – UV-B reduction (UB-B absorbing filter, Mylar).*

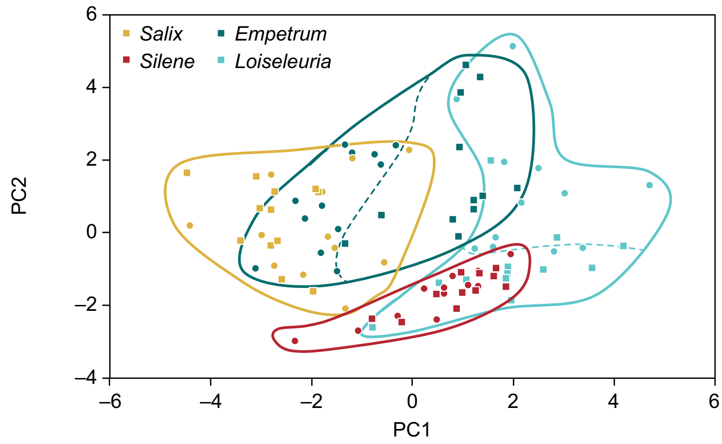

Figure 4.10. PCA plot of the correlation matrix of log-transformed microarthropod community samples showing the first and second principal components accounting for 32 % of the sample variation across the four monitoring habitats. Each soil core sample is represented by a symbol. Lines are drawn around clusters comprising the microarthropod samples belonging to a particular plant community. The broken line through the Empetrum and Loiseleuria clusters divides the clusters into the two replicate sampling plots. The two replicate sampling plots are indicated by a square and a circle.

uliginosum as subdominant species. The plots were set up between 4 June and 10 June (DOY 155 and DOY 161). In general, the frames were very resistant towards strong winds because they were reinforced with rope; the set-up was affected by the strong winds on only two occasions in mid-August and September until the frames were removed on 30 September (DOY 273) The frames were re-established shortly after disruption at each occasion.

The ambient UV-B radiation on fluorescence parameters was monitored on *V. uliginosum* and *B. nana*. The total performance index (PI_{total}), integrating responses of antenna, reaction centre, electron transport and end acceptor-dependent parameters is an indicator of the viability of a sample. The exclusion of UV-B is expected to have a positive effect on the total performance index. The measurements of 2014 are not showing significant positive responses. There seem to be similar patterns through the season for the two species although the magnitude is different (figure 4.9). This lacking of positive response is somehow unexpected; previous years have reported a positive effect on UV-B exclusion. The results may be due to other parameters influencing the performance for the plants (e.g. precipitation, cloud cover) thus inter-annual variation in light and UV-B dose.

4.2 Arthropods

In Kobbefjord, all four pitfall trap stations (each with eight traps) established in 2007 and the two window trap stations (each with two traps) established in 2010 were open during the 2014 season. Parts of the samples are being sorted by the Department of Bioscience, Aarhus University, Denmark. The material sampled during the 2013 and the 2014 season is stored in 70 % ethanol at Greenland Institute of Natural Resources.

Pitfall traps were established from 20 May (DOY 140) through 10 June (DOY 161) and they all worked continuously until 30 September (DOY 273) when the liquid began to freeze. In 2014, arthropods were caught during 4301 trap days (including 3839 pitfall trap days and 462 window trap days).

Microarthropods

Three sampling sessions for microarthropods in Kobbefjord took place at the end of June, August and September, respectively. Each sampling session consisted of three to four sampling occasions within approximately one week. The soil cores were placed in a high gradient extrac-

Table 4.1 Mean abundances ×1000 individuals m^{-2} of mites, at order level, and collembolans, at species level. Species are in order of decreasing abundance. Microarthropods are the sum of mites and collembolans. S: Collembolan species richness; Mean per sample Shannon diversity: H' = –∑ pi log2 pi, where pi is the proportion of species in a sample to total collembolans; Mean equitability: E: H'/log2 n, where n is number of collembolan species. Shaded areas: habitat characterising species.

	Salix glauca	***Empetrum nigrum***	***Silene acaulis***	***Loiseleuria procumbens***
α S	15	13	10	13
Mean S per sample	4.9	5.8	2.3	3.9
H'	1.6	1.4	0.83	1.1
E	0.41	0.38	0.25	0.30
Total microarthropods	54.9	129	119	218
Acari	35.9	62.3	114	160
Collembola	19.0	66.3	5.1	57.7
Tetracanthella arctica	0.33	37.0	1.2	35.9
Tullbergiinae	4.7	7.5	2.1	11.5
Folsomia quadrioculata	1.8	8.8	0.02	6.3
Isotomiella minor	6.0	4.3	0.05	1.1
Folsomia sensibilis	1.4	4.6	0.39	0.05
Desoria olivacea	3.04	1.7	0.02	0.17
Micranurida pygmaea	0.03	1.1	0.42	1.7
Willemia sp.	0.69	0.84	0.69	0.71
Oligaphorura ursi	0.46	0.05		
Heterosminthurus claviger	0.05	0.18	0.02	0.10
Desoria tolya	0.05	0.27		
Megalothorax minimus			0.19	
Lepidocyrtus violaceus	0.09			0.02
Pseudanurophorus binoculatus				0.10
Isotoma anglicana	0.03	0.02		0.02
Symphypleona[1]	0.05			
Arrhopalites principalis	0.03			
Neanura muscorum				0.02
Oribatida	24.7	29.7	78.8	78.3
Actinedida	8.2	28.5	34.6	79.0
Gamasida	3.0	4.2	0.29	2.9

[1]Unidentified species of the Symphypleona order assumed to contain at least one species

tor at the Greenland Institute of Natural Resources (Aastrup *et al.* 2009) after sampling, and the extracted microarthropods were stored in 70 % ethanol until shipment to Aarhus University. Figure 4.10 shows the population data structure as revealed by principal component analysis (PCA) of the correlation matrix of log(x+1) transformed population abundances.

The collembolan communities of the four plant communities have retained their basic characteristics (table 4.1). The otherwise ubiquitous *Parisotoma notabilis* was not found during the 2014 season, in contrast to being encountered in previous sampling years particularly in *Salix*. *Tetracanthella arctica* attained the highest abundance observed since our first monitoring year in 2007. The *Silene* and *Loiseleuria* habitats continue to support the smallest collembolan diversity, although the total microarthropod abundance was high due to favourable conditions for opportunistic species, typically contributed by *Actinedida* and primitive oribatids. Inspection of climatic conditions during the snow-free season expectedly would explain the abundance in the *Loiseleuria* habitat. Silene was still extreme by having only 4 % collembolans and 96 % mites and forms a small cluster overlapping only with the *Loiseleuria* MArt8 plot (figure

Table 4.2 Total number of passerines counted and the number of censuses per year. Also shown is the number of passerines per census. For explanation of bird abbreviations, see text.

Year/birds	LB	SB	NW	RP	No of census's	LB/census	SB/census	NW/census	RP/census
2008	57	61	44	7	9	6.3	6.8	4.9	0.8
2009	39	40	33	37	5	7.8	8.0	6.6	7.4
2010	182	152	110	49	17	10.7	8.9	6.5	2.9
2011	166	131	146	7	14	11.9	9.4	10.4	0.5
2012	102	69	109	37	13	7.8	5.3	8.4	2.8
2013	104	70	156	7	18	5.8	3.9	8.7	0.4
2014	79	86	52	36	15	4.4	4.8	2.9	2.0

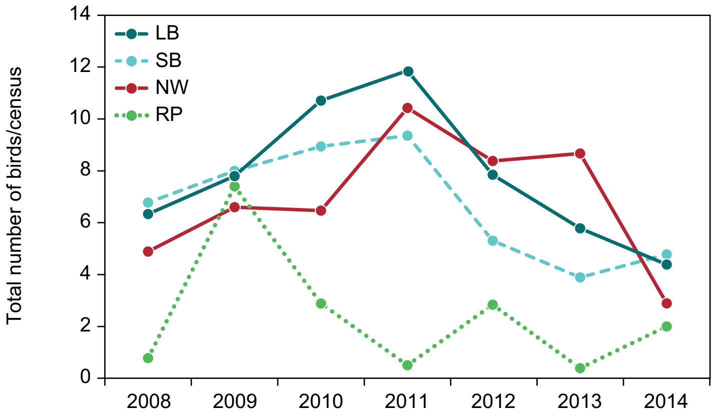

Figure 4.11 Total number of birds counted per census in 2008-2014. For explanation of the bird abbreviations, see text. The lines connecting the dots are only used for illustrative purposes.

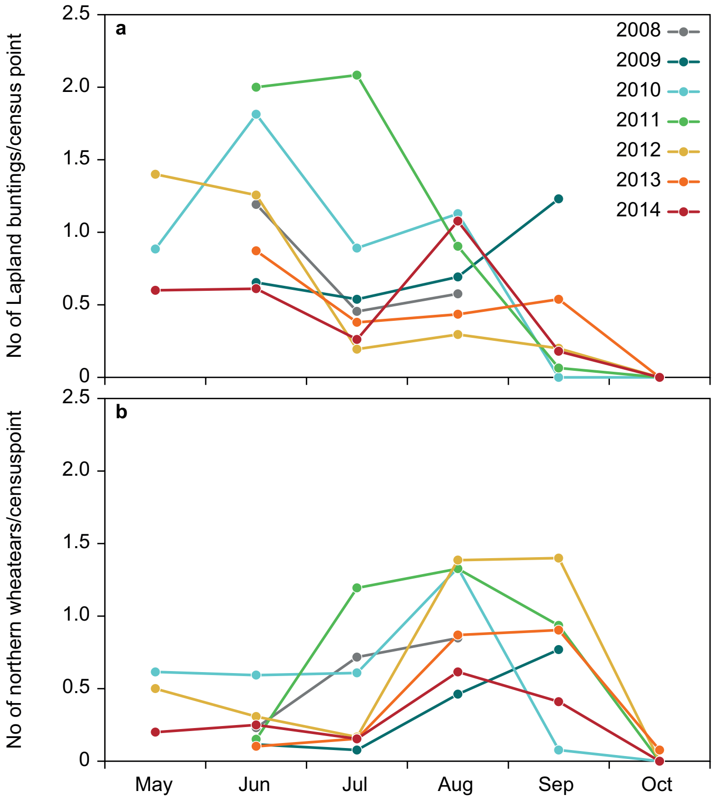

Figure 4.12 Numbers per census during the season in 2008-2014 of a) Lapland bunting and b) northern wheatear. The lines connecting the dots are only used for illustrative purposes.

4.10), indicating that the replicate plots turn out to have unique environmental characteristics creating particular communities. The *Loiseleuria* Mart7 plot is unique with only some resemblance to the *Empetrum* Mart2 plot.

4.3 Birds

Survey for breeding passerines

No formal survey was carried out in 2014.

Bird census points

Four passerine species, Lapland bunting (*Calcarius lapponicus*), snow bunting (*Plectrophenax nivalis*), northern wheatears (*Oenanthe oenanthe*) and common redpoll (*Carduelis flammea*), were counted at 13 census points within the 32 km^2 Kobbefjord catchment area. A total of 16 censuses were carried out from 30 May (DOY 150) to 14 October (DOY 287) 2014. All four species of passerines were already present at the time of the first census, and the survey was carried out until no more observations were made at any census point.

The total number of Lapland buntings (LB), snow buntings (SB), northern wheatears (NW), and redpolls (RP) has varied between the years (table 4.2). In 2014, the overall number of observations were low for all species (figure 4.11), with fewer observations of both LB and NW than in any previous year. SB's were also observed in lower numbers than any other year except for 2013. The number of observations of both LB and NW peaked in august (figure 4.12), which for LB is later than in previous years where observations peaked in June/July. SB's were observed only on the southern side of the river (census points

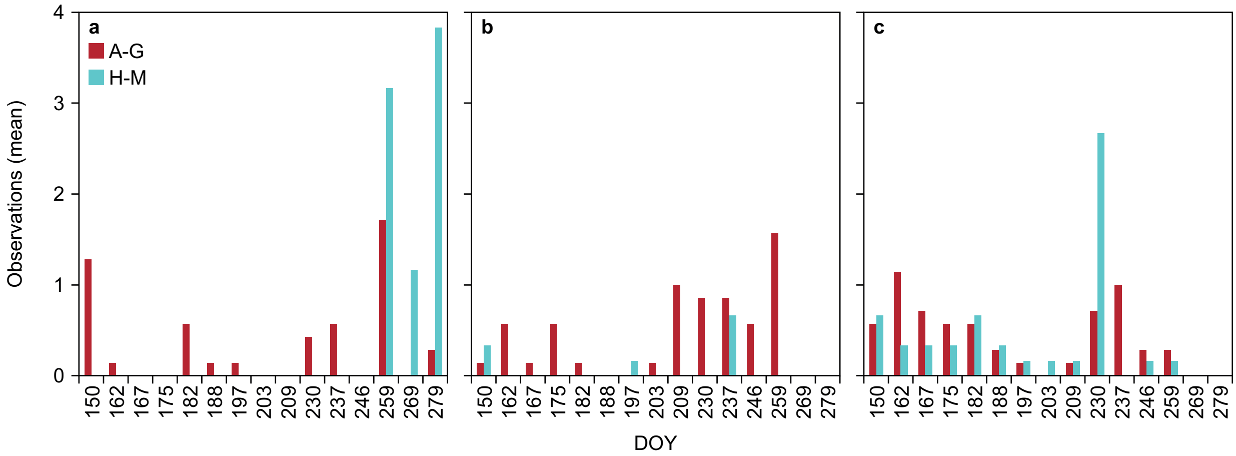

Figure 4.13 Mean number of bird observations on the southern side (Point A-G) and the northern side (Point H-M) of a) snow bunting, b) northern wheatear and c) Lapland bunting.

A-G) most of the season, until mid-September, when a shift to the northern side (census points H-M) was observed (figure 4.13a). NW also favoured the southern side, with only three days of observations on the northern side (figure 4.13b). LB's were evenly distributed on both sides throughout the season (figure 4.13c).

SB, LB and NW all had the highest number of observations in 2011, possibly due to the outbreak of noctuid larvae in 2010 and 2011, resulting in higher reproductive success in those years. The numbers of observations in the following years have steadily decreased.

4.4 Mammals

The Kobbefjord catchment area is only sparsely populated with mammals. During the field season two sightings of caribou (possibly the same animal) and one sighting of arctic hare were recorded. There were several sightings of tracks and faeces from arctic fox, though no actual sightings were made this season.

4.5 Lakes

The Kobbefjord catchment includes three lakes, of which two lakes have been monitored since 2008. They are both deep lakes with maximum depths of 35 and 27 metres, respectively. Badesø, which is the deepest, is situated downstream at 50 m a.s.l. and Qassi-sø upstream at 235 m a.s.l. Qassi-sø is the most wind exposed of the two lakes, and a small glacier drains into the lake resulting in silt input to the system. Due to the higher altitude, Qassi-sø generally has a longer ice-covered period than Badesø. In 2014, a flushing event occurred in mid-August into Langesø (upstream of Badesø) affecting Badesø too. Whether the flushing event was due to drainage of a glacial lake or another reason is not currently known.

Climate

Regarding precipitation, 2014 was an average year with 801 mm (table 4.3a). The summer months were a little drier than an average year of 289 mm precipitation, whereas precipitation days of 2014 were almost identical to the average 114 days (table 4.3a. Please notice that the annual precipitation days are only available from the DMI station in Nuuk). Also summer temperature 2014 was close to the norm, both when looking at the pre-summer period (May-June) and the entire summer/growing season (May-Aug, table 4.3a).

Water chemistry and ice cover

The ice out date was 7 June in Badesø and 13 days later, 20 June in Qassi-sø. (table 4.4). The date for ice formation on the two lakes was unknown at the time of report production. Both lakes are nutrient poor, although the relative variation can be large. In 2014, the average total nitrogen concentration in both lakes was close to average for the monitored period, 0.073 and 0.077 mg TN l^{-1} in Badesø and Qassi-sø, respectively (table 4.4, and figure 4.14). Average total phosphorus was 0.005 and 0.003 mg l^{-1} in Badesø and Qassi-sø, respectively.

*Table 4.3 a) Meteorological data from the official DMI station in Nuuk, which is the closest official station to the Kobbefjord catchment. A precipitation day is defined as a day with > 1 mm precipitation. b) Meteorological data from the Kobbefjord catchment based on data collected by the Climate Basis programme. A precipitation day is defined as a day with > 1 mm precipitation. *5 data points missing on 14 June and all data are missing on 15 and 16 June.*

a) Climate data from Nuuk	**2008**	**2009**	**2010**	**2011**	**2012**	**2013**	**2014**
Annual precipitation (mm)	1041	537	733	748	1201	962	801
Precipitation May-Aug (mm)	214	122	400	220	411	270	226
Annual precipitation days	134	82	102	123	129	124	115
Average temp May-Aug	6.5	4.9	7.3	5.2	7.5	4.7	6.5
Average temp May-Jun	4.7	2.3	5.9	2.8	5.5	2	3.9
b) Climate data from Kobbefjord	**2008**	**2009**	**2010**	**2011**	**2012**	**2013**	**2014**
Annual precipitation (mm)	1127	838	905	-	-	1046	709
Precipitation May-Aug (mm)	195	190	409	201	325.7	331	235
Annual precipitation days	–	-	-	-	-	-	95
Average temp May-Aug	7.1	5.9	9.6	6.3	8.7	6.2	8.4*
Average temp May-Jun	5.2	2.5	7.9	3.3	6.3	3.1	5.4*

Table 4.4 Morphometric data, time-weighted average of water chemistry (min-max values) and physical data measured in Badesø and Qassi-sø during the ice-free periods from 2008-2014. Date for ice covering of both lakes have not yet been retrieved.

				Badesø			
Area (ha)				80			
Maximum depth (m)				35			
Mean depth (m)				9.2			
	2008	**2009**	**2010**	**2011**	**2012**	**2013**	**2014**
Total phosphorus (mg l^{-1})	0.005 (0.001-0.012)	0.004 (0.003-0.005)	0.004 (0.003-0.004)	0.004 (0.003-0.005)	0.006 (0.002-0.008)	0.003 (0.001-0.004)	0.005 (0.002-0.016)
Total nitrogen (mg l^{-1})	0.084 (0.040-0.140)	0.027 (0.020-0.033)	0.08 (0.04-0.11)	0.17 (0.14-0.23)	0.06 (0.03-0.15)	0.037 (0.02-0.06)	0.073 (0.05-0.1)
pH	6.92 (6.59-7.13)	6.85 (6.46-7.14)	6.62 (6.09-7.3)	7.1 (6.51-7.85)	n.a.	n.a.	7.27 (6.83-7.6)
Conductivity (µS cm^{-1})	20 (19-22)	22 (21-23)	21 (18-26)	21 (15-27)	18 (14-19)	25 (20-42)	21 (17-24)
Ice-free, date	3 Jun	15 Jun	20 May	23 Jun	9 Jun	14 Jun	7 Jun
Ice-covered, date	24 Oct	30 Oct	13 Dec	25 Oct	14 Nov	24 Oct	
Ice-free period, days	143	137	207	124	158	132	
				Qassi-sø			
Area (ha)				52			
Maximum depth (m)				27			
Mean depth (m)				7.8			
	2008	**2009**	**2010**	**2011**	**2012**	**2013**	**2014**
Total phosphorus (mg l^{-1})	0.015 (0.005-0.029)	0.002 (0.001-0.005)	0.005 (0.003-0.009)	0.005 (0.003-0.006)	0.006 (0.004-0.008)	0.003 (0.001-0.004)	0.003 (0.002-0.004)
Total nitrogen (mg l^{-1})	0.09 (0.30-0.150)	0.022 (0.019-0.029)	0.084 (0.050-0.14)	0.138 (0.09-0.23)	0.03 (0.02-0.06)	0.026 (0.01-0.04)	0.077 (0.06-0.09)
pH	6.72 (6.44-6.96)	6.87 (6.79-6.93)	6.84 (6.37-7.31)	7.59 (6.79-7.97)	n.a.	n.a.	7.51 (6.95-8.38)
Conductivity (µS cm^{-1})	20 (15-24)	16 (16-17)	17 (15-18)	18 (15-20)	15 (10-20)	20 (17-26)	18 (16-19)
Ice-free, date	12 Jun	28 Jun	31 May	1 Jul	18 Jun	22 Jun	20 Jun
Ice-covered, date	18 Oct	17 Oct	10 Nov	20 Oct	1 Nov	24 Oct	
Ice-free period, days	128	111	163	112	136	124	

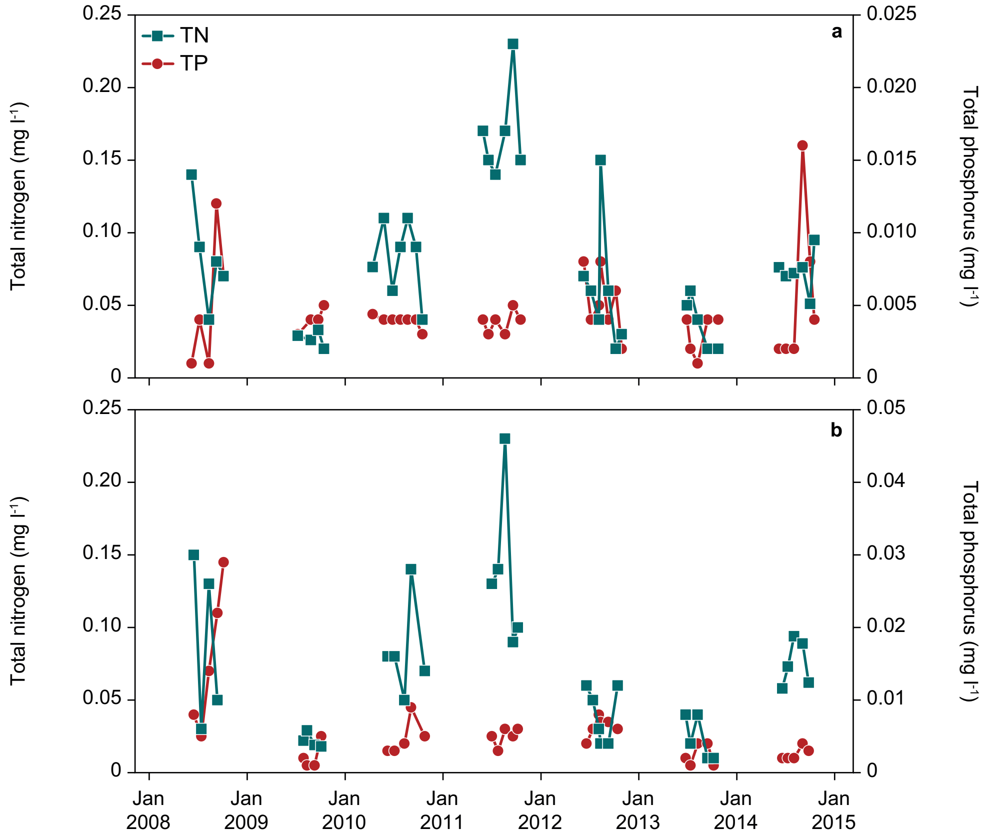

Figure 4.14 Total nitrogen (TN) and total phosphorus (TP) during 2008-2014 in a) Badesø and b) Qassi-sø

Chlorophyll and Secchi depth

Chlorophyll *a* (Chl *a*) is correlated to nutrient levels and the Chl *a* levels of the two lakes are therefore low (figure 4.15a). Chl *a* varied notably between the years, but compared to more nutrient-rich lakes, the variation remains within a very narrow range due to the low nutrient levels. During the monitored period, Chl *a* exhibited an increasing trend in both Badesø and Qassi-sø (figure 4.15a). In general, there is a slightly higher Chl *a* level in Badesø compared to Qassi-sø, which can be explained by the slightly higher temperature in combination with less silt in Badesø and consequently better transparency (Secchi depth) (figure 4.15b).

In Badesø the Secchi depth was 4.5 m on average and much lower compared to 2013 (8.06 m). The low average Secchi depth is explained by a flushing event into Langesø, which is upstream of Badesø. The flush occurred between 14 August and 15 August and resulted in a large input of soil/silt, reducing the Secchi depth from 10 m to 0.8 m overnight (figure 4.15b). The large input of soil/silt may have had an impact on the total phosphorus level too, which increased atypically between the third sampling in July and the fourth sam-

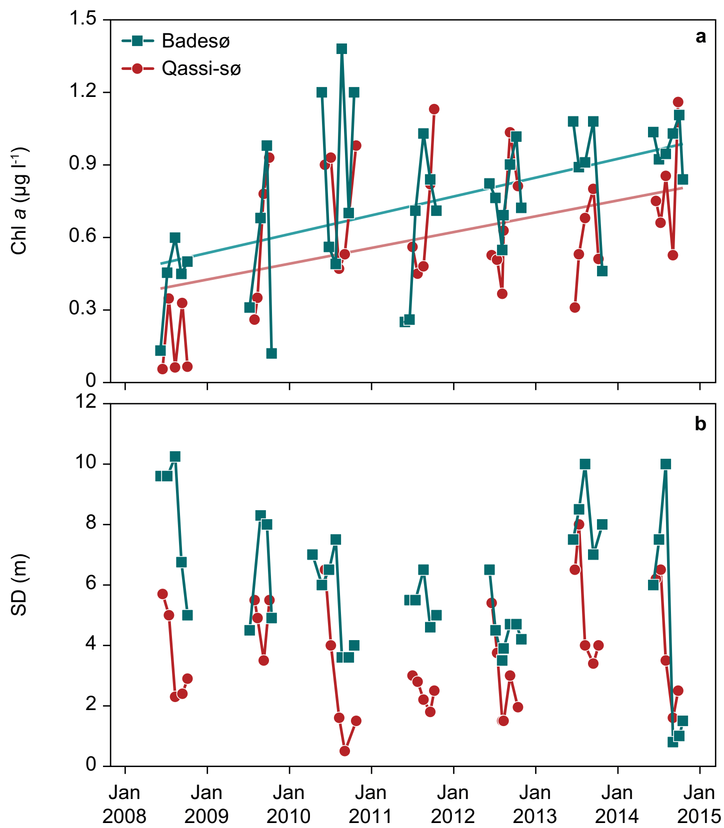

Figure 4.15 Chlorophyll a levels (a) and Secchi depth (b) in Badesø and Qassi-sø during 2008-2014.

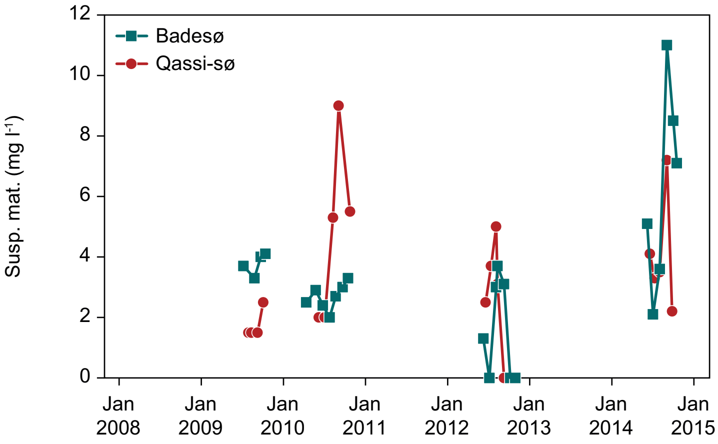

Figure 4.16 Suspended matter (solids) in Badesø and Qassi-sø during 2009-2014.

pling in August, followed by a decrease due to wash-out and settlement of the silt (figure 4.14a). In Qassi-sø, a reduction in Secchi depth was also found during the sampling period 2014. However, this was between the second and third sampling, and not larger than previous years (figure 4.15b). Thus, the dramatic change in Badesø was due to the flushing event into Langesø, which is also illustrated by the results from suspended solids (figure 4.16), increasing from less than 4 mg l^{-1} to more than 10 mg l^{-1} between the third and fourth sampling, which is a much larger change than observed in previous years.

Zooplankton

In Badesø, zooplankton biomass has slightly increased during 2011-2013 (figure 4.17), however, in 2014 it declined to the level before 2011 (figure 4.17a). Badesø is dominated by calanoid copepods (*Leptodiaptomus minutus*) together with either rotifers and/or cladocerans (figure 4.17a). When rotifers occur in high biomasses in Badesø, they consist of the large *Asplanchna* sp., but smaller rotifers (like *Keratella* spp. and *Polyarthra* spp.) were also found in large numbers, particularly in the last part of 2014. In Badesø, the cladocerans contributed with a relatively large percentage of the zooplankton community during certain periods of the ice-free periods in 2011 to 2014. The cladocerans consist of the small *Bosmina sp.* together with *Holopedium* sp. Overall the zooplankton composition in Badesø – fewer and smaller cyclopoid copepods, smaller cladocerans, and a relatively large contribution of rotifers – reflects the presence of zooplankton-eating fish.

In August, the large input of soil/silt into Badesø may have caused the dra-

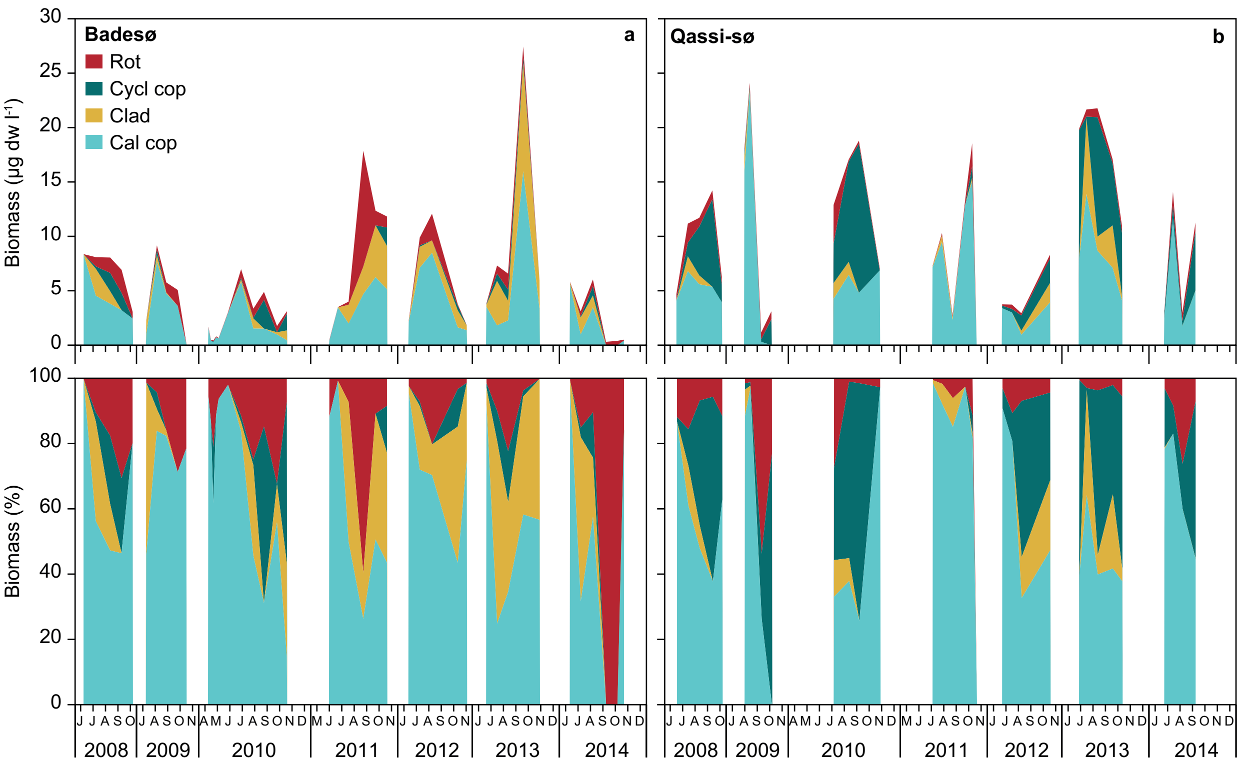

Figure 4.17a). a) Zooplankton biomass (top) and biomass, % (bottom) in Badesø during 2008-2014. b) Zooplankton biomass (top) and biomass, % (bottom) in Qassi-sø during 2008-2014. Zooplankton is divided into four groups: Cladocerans (Clad), cyclopoid copepods (Cycl cop), calanoid copepods (Cal cop) and rotifers (Rot).

matic effects observed in the zooplankton pattern, as all the large zooplankton disappeared from the system leaving the rotifers, contributing with 100 % of the zooplankton biomass during the last part of the sampling period (figure 4.17). However, the calanoid copepods reappeared in the lake in late October.

The overall inter-annual changes in zooplankton biomass may indicate changes in the predation pressure from fish to the zooplankton, as fish are size-selective in their choice of prey, preferring the large-sized and easy catchable individuals, leaving a reduced biomass and smaller-sized individuals in the system.

In Qassi-sø, the zooplankton community is slightly different from Badesø. Qassi-sø has a complete dominance of calanoid (*Leptodiaptomus minutus*) and cyclopoid copepods. The cladocerans are dominated by *Holopedium* sp. together with the large *Daphnia pulex*, which is in contrast to the presence of *Bosmina* in Badesø. Furthermore, the rotifers contribute with a much smaller proportion of the zooplankton biomass, compared to the situation in Badesø (figure 4.16). Another interesting phenomenon in Qassi-sø is the absence or almost absence of cladocereans in certain years (2009, 2011 and 2014). Preliminary results indicate that short ice-free periods (short summers) may reduce the success of the cladocerans (*Daphnia*).

Overall, the zooplankton communities reflect the presence and absence of fish in Badesø and Qassi-sø, respectively.

Phytoplankton

Phytoplankton has been collected during the last two years, but due to reductions in the budget, samples have not yet been analysed.

Vegetation

Callitriche hamulata dominated the submerged vegetation in both lakes throughout the monitoring period. Coverage varied in the different depth intervals, but overall the maximum coverage was at intermediate depths: between two and three metres in Qassi-sø and between two and four metre in Badesø (figure 4.18). The low coverage at the lowest depths was due to wind and wave-induced physical stress (disturbance). At the given nutrient levels, the macrophyte growth in Arctic lakes responds stronger to temperature and the length of the growing season, than to chlorophyll level (Mønster 2013). Conse-

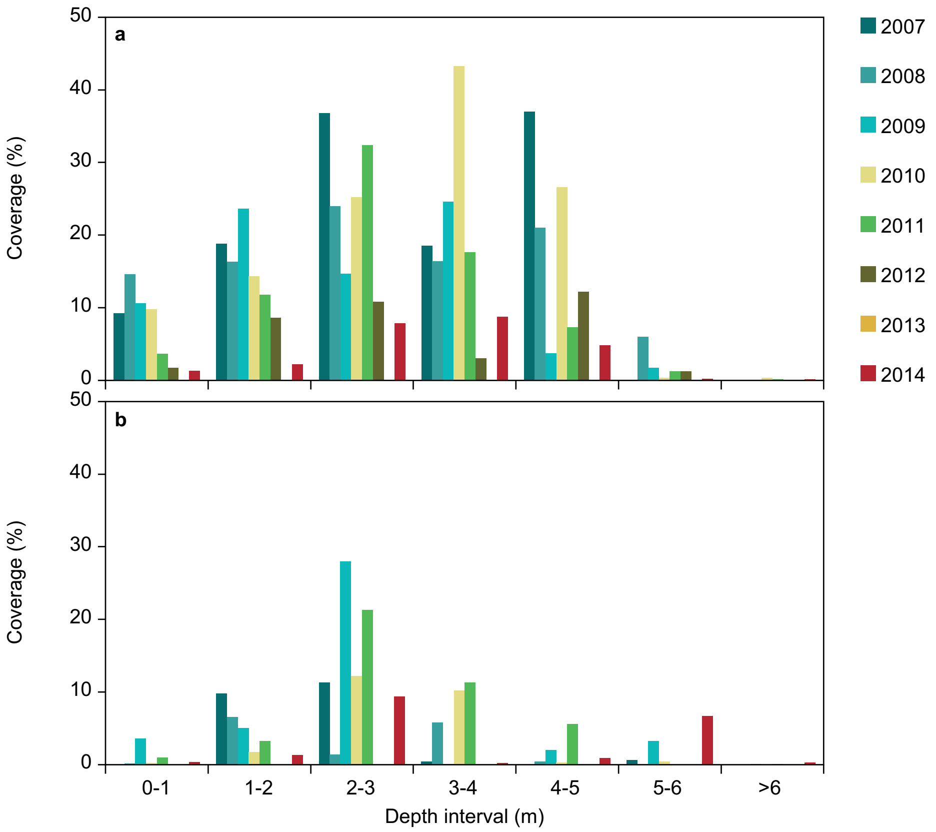

*Figure 4.18 Coverage (%) of total submerged vegetation (*Callitriche hamulata*) in a) Badesø and b) Qassi-sø.*

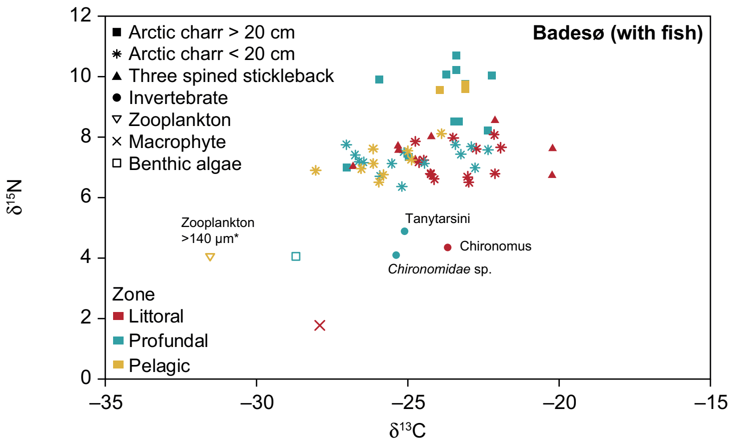

Figure 4.19. $\delta^{13}C$ and $\delta^{15}N$ values of the different organisms in Badesø in the littoral (near shore), profundal (bottom) and pelagic (open water) zones.

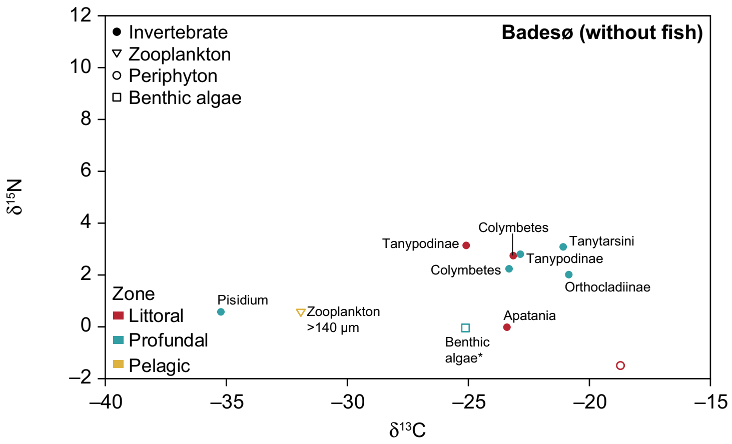

Figure 4.20. $\delta^{13}C$ and $\delta^{15}N$ values of the different organisms in the fishless Qassi-sø in the littoral (near shore), profundal (bottom) and pelagic (open water).

quently, we also find large inter-annual variability in the coverage. The 2014-coverage was among the lowest measured in both lakes during 2008-2014. This may reflect the relative cold and short ice-free period in 2013, and for Badesø also be a response to low coverage since 2012.

Food chains and stable isotopes

Large char can be piscivores and the smaller specimens can be omnivores or planktivores. Isotope results from the biological components in the trophic web can help verifying this since the $^{15}N/^{14}N$ ratio ($\delta^{15}N$) increases for every increase in trophic level or step in the food chain. Furthermore, $^{13}C/^{12}C$ ratio ($\delta^{15}C$) changes from very negative values for phytoplankton to less negative values for benthic algae.

The plot for Badesø (figure 4.19) does not include more than two basal resources (primary producers: macrophytes and benthic algae). For the small char (< 20 cm), there was a gradient with increasing $\delta^{13}C$-values from the pelagic, over the profundal to the littoral zone. The large char (>20 cm) are only found in the profundal zone and a few in the pelagic zone, however, these are placed similar for both $\delta^{13}C$ and $\delta^{15}N$-values. Three-spined sticklebacks are mainly found in the littoral zone. The invertebrates of both the profundal and littoral zones are placed lower than the fish. The total food chain covers a relatively narrow $\delta^{13}C$ range (figure 4.19).

The plot for Qassi-sø shows a large width of the food web ($\delta^{13}C$) and fewer trophic levels ($\delta^{15}N$) compared to Badesø (figure 4.20). The differentiation in $\delta^{13}C$ of the zones is not as clear here as for Badesø (figure 4.19), simply because zooplankton is the last trophic level of the pelagic food web. Generally, there is a lack of basal resources as only periphyton is included here and e.g. the bivalve *Pisidium* is placed at much lower $\delta^{13}C$ levels than the periphyton, illustrating that *Pisidium* probably feed primarily on phytoplankton or another food source. The invertebrates of the profundal and littoral zone (excluding *Apatania*) are placed at the highest trophic level for these zones; again because fish are not present in this system.

Summing up

The year 2014 was a normal year with respect to climate. Water chemistry was also at average levels compared to the previous monitored years. Chlorophyll levels are slightly increasing and were close to 1.0 µg Chl *a* l^{-1} in Badesø and slightly lower in Qassi-sø. The best explanation for the increasing trend in Chl *a* is predation from fish on zooplankton causing cascading effects to phytoplankton. Zooplankton communities are generally different in Qassi-sø compared to Badesø, which is consistent with the lack of fish in Qassi-sø. Overall, the vegetation coverage had its maximum at intermediate depths due to less physical disturbance and preferable light conditions. Coverage in 2014 was lower than most of the previous years, which can be a response to cold conditions in 2013. Isotope results from Badesø and Qassi-sø illustrated the differences between the food chain/food webs of the two lakes, where Badesø is holding an extra trophic level (the fish) compared to Qassi-sø. The presence of this extra trophic level forces the invertebrates to feed on a more narrow food range ($\delta^{13}C$ range).

5 Nuuk Basic

The MarineBasis programme

Thomas Juul-Pedersen, Kristine E. Arendt, John Mortensen, Diana Krawczyk, Anja Retzel, Rasmus Nygaard, AnnDorte Burmeister, Dorte Krause-Jensen, Núria Marbà, Birgit Olesen, Mikael K. Sejr, Martin E. Blicher, Lorenz Meire, Søren Rysgaard, Maia Olsen, Ole Geertz-Hansen, Tenna Boye and Malene Simon

The main objective of the MarineBasis programme is to collect and study long-term trends in key physical, chemical and biological oceanographic parameters of the Godthåbsfjord region. This sub-Arctic programme operates in parallel with the MarineBasis-Zackenberg programme in NE Greenland. This chapter describes the ninth full year of monitoring since the programme was initiated in late 2005. The collected data and findings from the monitoring programme contribute to a better understanding of this sub-Arctic marine ecosystem and identify and describe effects of climate change. The sampling programme is comprised of monthly pelagic samplings, seasonal sampling of sediment-water exchange, annual pelagic length and cross section studies of Godthåbsfjord and the adjacent coastal area, annual studies of macroalgae and macrobenthos, annual counting of seabirds, photo identification of marine mammals and collection of daily satellite and camera images of sea-ice conditions in the Godthåbsfjord and Baffin Bay. The collected data describe the seasonal, annual and inter-annual patterns and variation in key elements of the marine ecosystem. The time series facilitate identification and quantification of effects of climatic changes. The monthly pelagic sampling is conducted at a permanent sampling station (Main Station (GF3)); 64°07'N, 51°53'W; bottom depth approx. 350 m) located close to the fjord entrance, while the other parameters are sampled in and around the Godthåbsfjord system (figure 5.1). The methods used are described below, but more details can be obtained from the MarineBasis-Nuuk manual (www.nuuk-basic.dk).

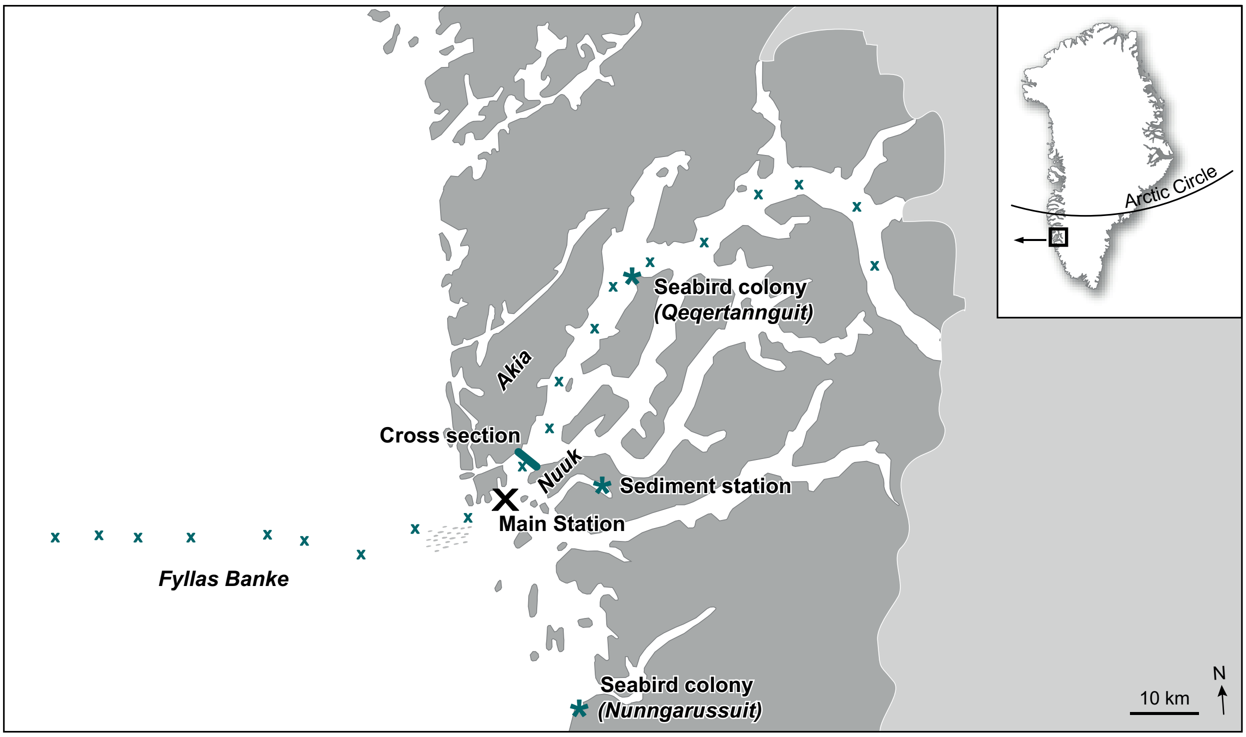

Figure 5.1 Map of sampling stations in and around the Godthåbsfjord system. X represents sampling stations along the hydrographical length section.

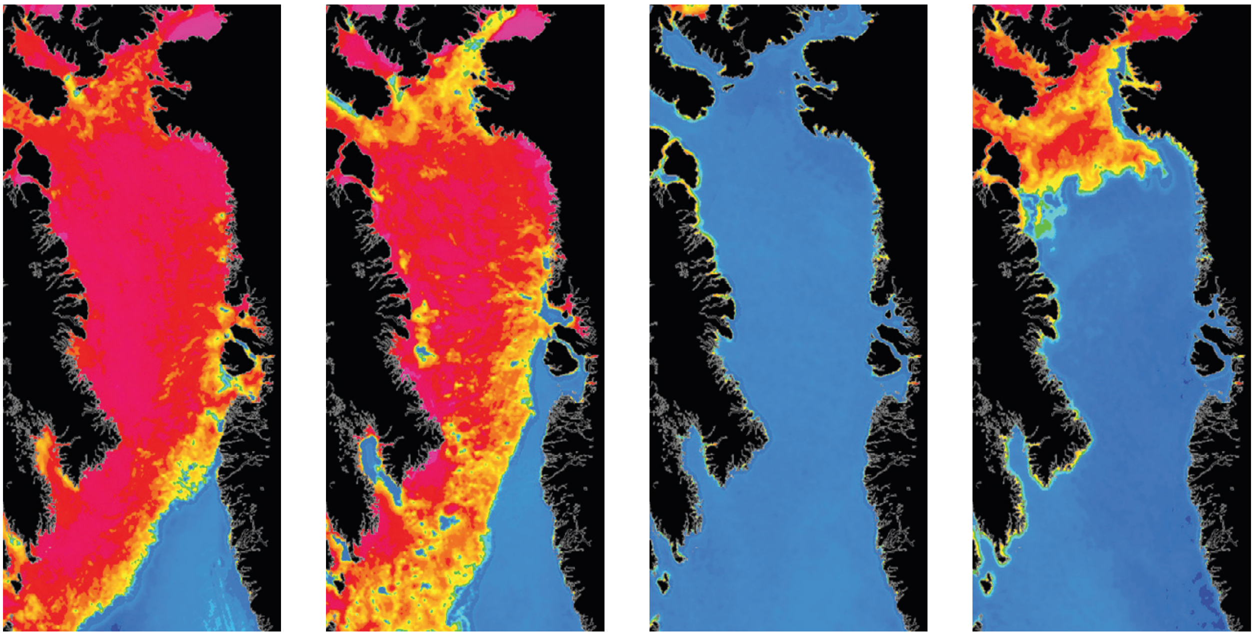

Figure 5.2 Satellite images (AMSR) showing sea-ice conditions in Baffin Bay during February, May, August and October 2014.

5.1 Sea ice

Sea-ice conditions in Godthåbsfjord and Baffin Bay were monitored using satellite images. Microwave-radiometer (AMSR, 3-6 km resolution) satellite images were collected for Baffin Bay, while MODIS (250 m resolution) satellite images were collected for Godthåbsfjord. Camera images of the sea-ice discharge covering a cross

Figure 5.3 Satellite images (AQUA-MODIS) showing sea-ice conditions in Godthåbsfjord during February, May, August and October 2014.

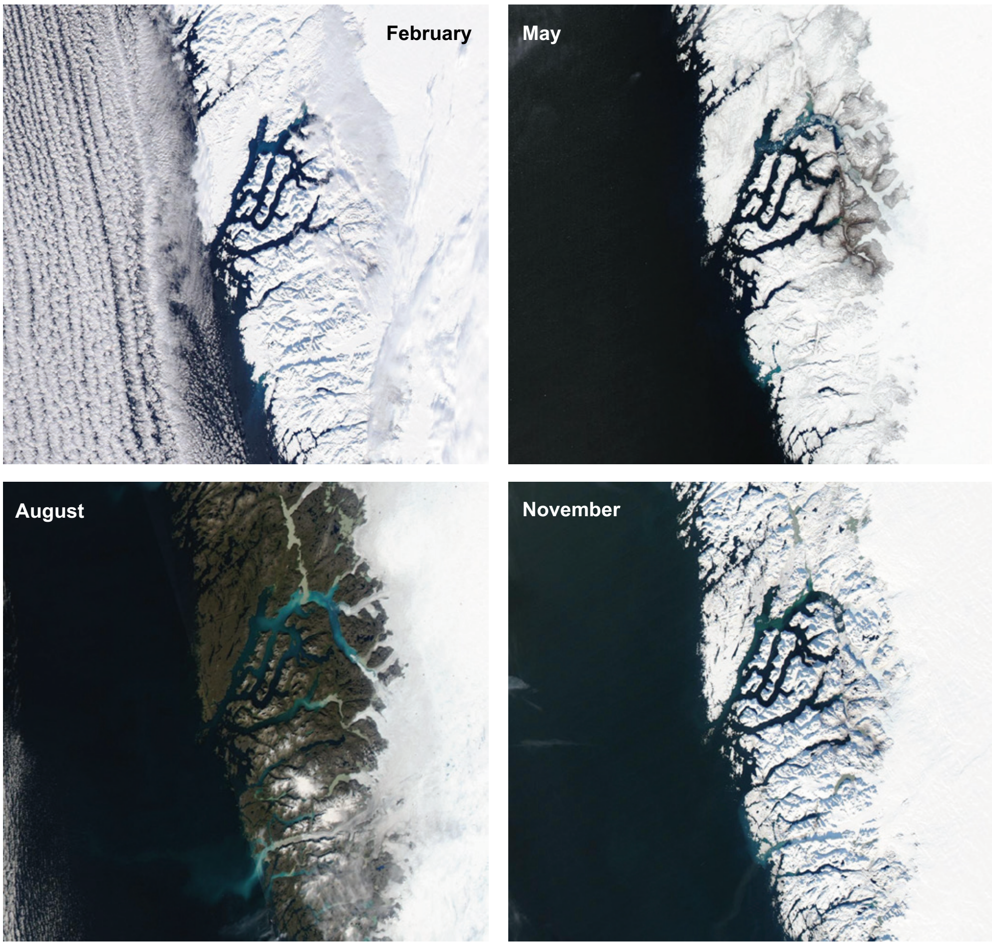

section of the fjord around Nuuk was unfortunately not collected in 2014, but the camera system has been re-established and was operational again from start-2015.

Sea-ice cover in Baffin Bay ('West Ice') began to retreat in spring with much ice still remaining in the north-western part of Baffin Bay in May (figure 5.2). During summer the ice dissipates almost completely from Baffin Bay, leaving only small localized pockets of land-fast ice. The sea ice started to form again from the north in October and typically covered much of Baffin Bay by December.

Only limited sea ice can be found throughout the year in the sub-Arctic Godthåbsfjord system (figure 5.3). Local land-fast ice during winter was observed mainly at the inner parts of the fjord and in smaller sheltered fjord branches. Camera images from previous years covering a cross section of the fjord have shown that sea ice and glacial ice are being exported out of the fjord in seasonal burst events. Much of the sea ice and glacial ice have, however, been shown to melt within the fjord. Collection of camera images covering a cross section near the fjord entrance (Nuuk) has been re-established in 2015.

Collection and analyses of satellite data on sea-ice coverage are currently conducted as a collaboration between Greenland Institute of Natural Resources, the Danish Meteorological Institute and Greenland Climate Research Centre (www.natur.gl). Daily satellite images covering Greenland are available at http://www.dmi.dk/groenland/maalinger/satellit/.

5.2 Length and cross sections

The marine monitoring programme includes an annual length section from Fyllas Banke to the ice edge at the innermost part of the fjord (approximately 200 km long, figure 5.1). The length section was conducted on board the research vessel R/V Sanna from 9-16 May 2014. Hydrographic measurements showed a weak stratification of the upper water column likely due to the early ice and snowmelt (figure 5.4). The surface layer showed a spring phytoplankton biomass (i.e. fluorescence). The weak pycnocline was not strong enough in spring to withstand tidal mixing at the outer sill region and the phytoplankton biomass was vertically mixed throughout the water column. Conditions on Fyllas Banke with the West Greenland Current on the outside flowing northward, cold water on top and frontal mixing along the edge sustained a high phytoplankton biomass on the bank. These patterns along the length section have also been identified in previous years.

A cross section of Godthåbsfjord was sampled towards the end of May (figure 5.5). Hydrographical profiles along the section at a narrow point of the fjord near Nuuk showed a pycnocline formed by fresher, warmer water. This pycnocline, which was strongest towards Akia, was formed by surface water flowing out of the fjord. The highest phytoplankton biomass (i.e. fluorescence) was also recorded in these surface waters.

5.3 Pelagic sampling

Seasonal and annual trends in key physical, chemical and biological parameters are monitored near the fjord entrance at the Main Station (GF3, approx. 360 m; figure 5.1). Monthly sampling included vertical profiles of salinity, temperature, density, turbidity, irradiance (PAR) and fluorescence was measured using a SBE19+ CTD profiler. Water samples were collected for chemical analyses of concentrations of nutrients (NO_x, PO_4^{3-}, SiO_4 and NH_4^+) at standard depths 1, 5, 10, 15, 20, 30, 40, 50, 100, 150, 250 and 300 m. Additional samples were taken for measurements of dissolved inorganic carbon (DIC) and total alkalinity (TA) at 1, 5, 10, 20, 30 and 40 m, representing the euphotic zone. Analysis of TA and DIC samples and the calculation of $p\mathrm{CO_2}$ have been delayed and cannot be completed in time for this report. The monitored biological parameters in the water column included chlorophyll *a* and phaeopigments concentrations at 1, 5, 10, 15, 20, 30, 40, 50, 100, 150, 250 and 300 m, which is a measure of the phytoplankton biomass. Phytoplankton primary production was also measured monthly using the *in situ* C^{14} incubation method, corrected for *in situ* light conditions, at 5, 10, 20, 30 and 40 m during an approx. two-hour deployment of a free-drifting mooring array. Triplicate plankton net tows were also taken for zooplankton (45 µm WP2 net from 0-100 m) and phytoplankton (20 µm net from

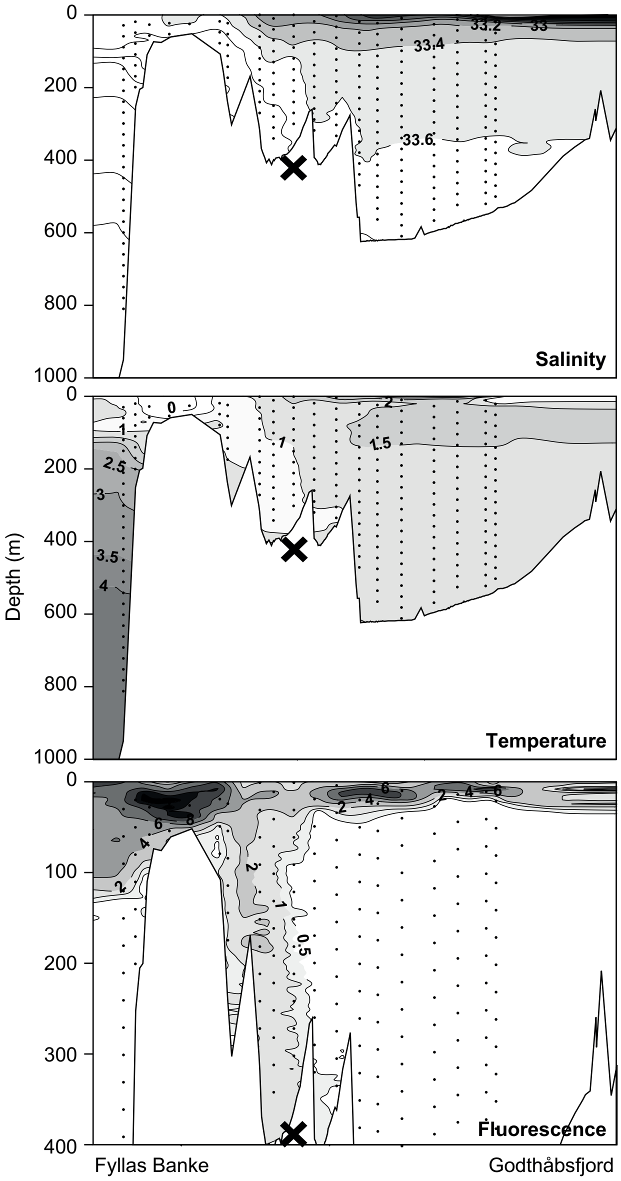

Figure 5.4 Salinity, temperature (°C) and fluorescence along the length section from Fyllas Banke to the inner part of Godthåbsfjord in May 2014. Vertical dotted lines represent sampling stations and depths in increments. X marks the location of the Main Station.

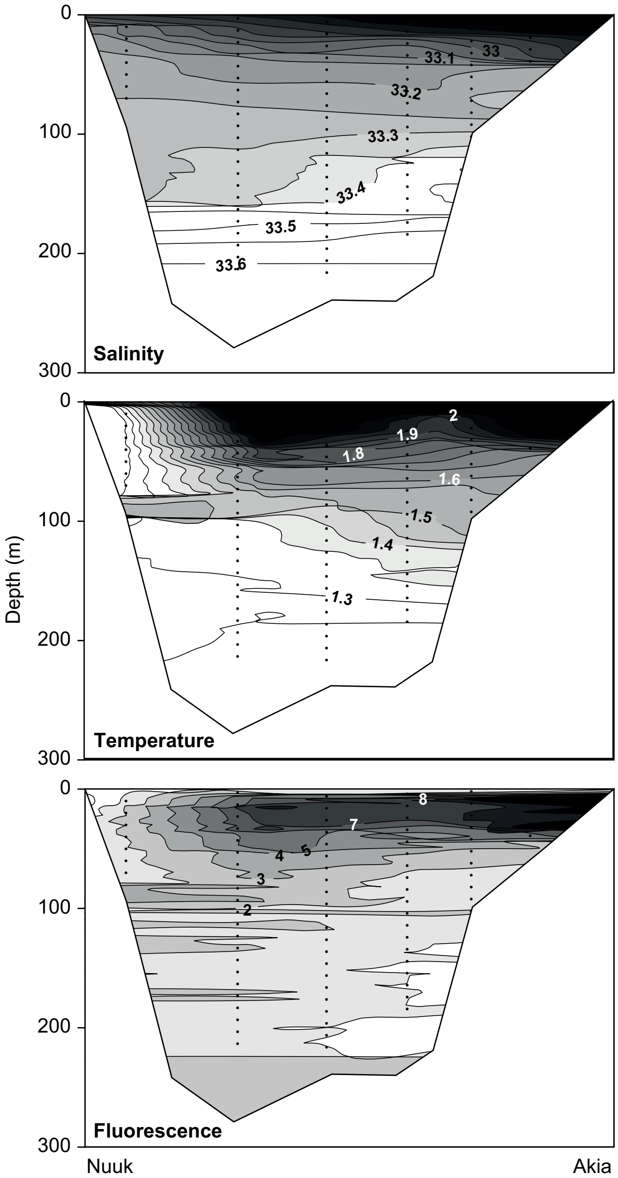

Figure 5.5 Salinity, temperature (°C) and fluorescence along the cross section from Nuuk to Akia in May 2014. Vertical dotted lines represent sampling stations and depths in increments.

0-60 m). To assess shellfish as well as fish larvae at the Main Station (GF3), single oblique sampling with a bongo net (335 µm) was used each month during 2008-2014. However, sampling was omitted in April and December 2014. Additional samplings with a double oblique bongo net (335 and 500 µm) were carried out along a length section from offshore Fyllas Banke to the inner part of the fjord from 2006 to 2014. Number of collected stations along the length section vary among years, but typically are sampling of stations FB3.5, FB2.5, GF3, GF7, GF7 and GF10 attempted each year. In 2013 collections also included FB 2.5, FB 1.5 and a new station "ice edge" close to the ice edge in the inner part of the fjord. Vertical sinking flux of particulate material was measured using four particle interceptor traps also deployed on a free-drifting mooring array at 60 and 65 m (considered the same depth) for approx. two hours. The collected material was analysed for chlorophyll *a*, phaeopigments, total particulate carbon and nitrogen, while a sample was saved for identification.

Abiotic parameters

Winter conditions showed largely homogenous salinities and temperatures throughout the water column (figure 5.6).

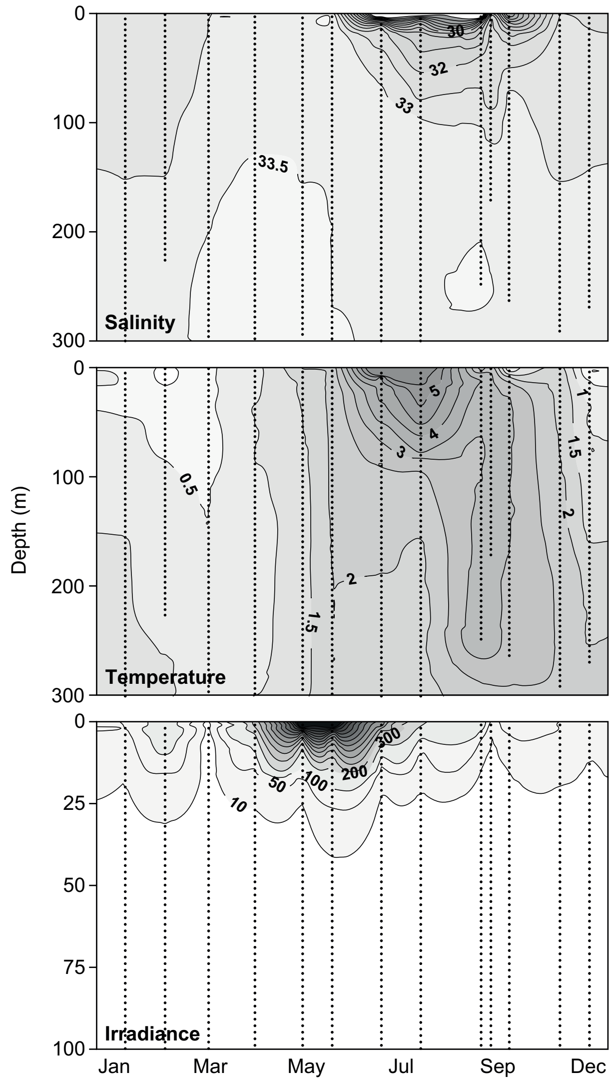

Figure 5.6 Annual variation in salinity, temperature (°C) and irradiance (PAR) at the Main Station in 2014. Vertical dotted lines represent sampling days and depths in increments.

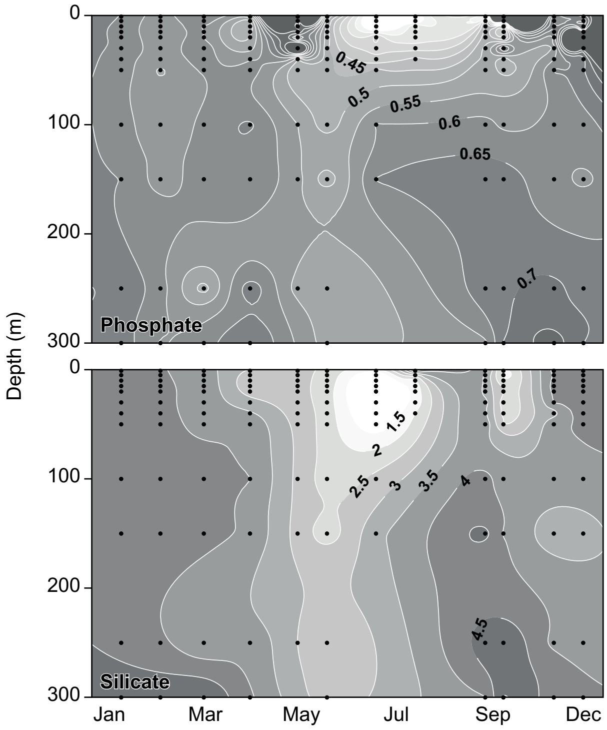

Figure 5.7 Annual variation in phosphate (µM) and silicate (µM) concentrations at the Main Station in 2014. Vertical dotted lines represent sampling days and depths.

In contrast to most of the previous years, no apparent deep warm costal inflow was recorded during winter. The largely homogenous vertical conditions persisted in spring. In summer, decreasing surface salinities depicted the onset of the glacial melt season, which peaked in August. Air-sea heat exchange, solar heating of the surface layer and freshwater runoff strengthened the pycnocline during summer. This stratification started to weaken in autumn, mainly due to a reduction in freshwater runoff. Seasonal light conditions in the water column, i.e. irradiance, generally follow the level of incoming solar radiation during the year. Particles in the water column, e.g. phytoplankton cells and silt particles, do, however, also influence irradiance distribution in spring and summer.

Phosphate and silicate showed high concentrations during winter and spring; while production in spring and summer reduced nutrients levels particularly in the surface layer (figure 5.7). The decreases in primary production in autumn combined with weakening of the surface stratification promoted the replenishing of nutrients from below. Due to the implementation of new analysis techniques for nitrogen and ammonia (NO_x and NH_4^+), data were not ready in time for this report.

Biotic parameters

Phytoplankton biomass and primary production were also measured as part of the monthly sampling programme (figure 5.8). Low phytoplankton biomass was observed during the dark winter months. The increased light conditions

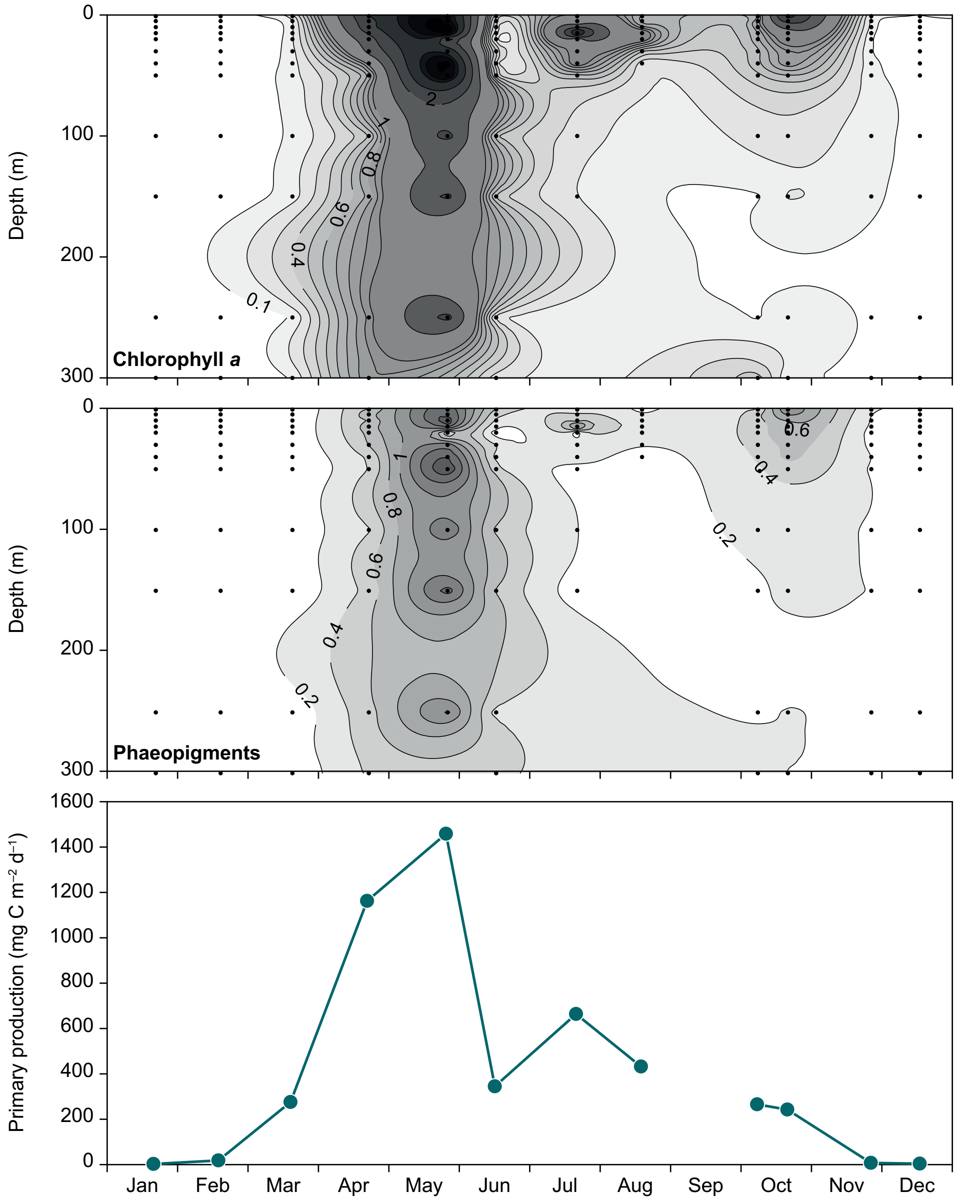

Figure 5.8 Annual variation in chlorophyll a concentration (μg l^{-1}), phaeopigments concentration (μg l^{-1}) and primary production (mg C m^{-2} d^{-1}) at the Main Station in 2014. Vertical dotted lines on chlorophyll a and phaeopigments plots represent sampling days and depths.

along with amble nutrient concentrations in spring lead to an immense increase in phytoplankton production and biomass. High production values in both April and May (> 1100 mg C m^{-2} d^{-1}) suggests a long spring bloom, while in most years the high spring production is confined to one month. An abrupt decrease in phytoplankton biomass and production in June signifies post-bloom conditions. A strong pycnocline in summer withstanding the tidal mixing maintains phytoplankton in suspension, but the pycnocline also reduces the supply of nutrients to the algae in the photic zone. The onset of glacial melt and runoff, particularly as sub-glacial discharge, introduces nutrients to the surface waters from deeper fjord waters, which induce a summer phytoplankton bloom. A long-lasting summer bloom was observed with significant production values lasting into October. The combined long-lasting and intense spring and summer blooms resulted in the highest integrated annual primary production estimate (187 g C m^{-2} y^{-1}) recorded since 2006 (from 84.6-139.1 g C m^{-2} y^{-1} from 2006 to 2013; data not shown).

The plankton community

Samples for phytoplankton analysis were collected at the Main Station using vertical net hauls (20 μm) from the approximate photic zone (0-60 m). Phytoplankton analysis included autotrophic algae and mixotrophic/heterotrophic dinoflagellates with ciliates. Diatoms dominated the phytoplankton assemblage throughout the year with total average of 83 % (figure 5.9). Haptophytes represented by *Phaeocystis* sp. showed high relative abundances in March-April and maximum in June (90.2 %). *Phaeocystis* sp. usually represents spring blooms in Godthåbsfjord. Haptophytes together with diatoms are common components of spring blooms in the sub-Arctic and Arctic regions. Diatoms, however, contributed most from July to October (average of 98 %) during summer bloom when the major freshwater runoff from Greenland Ice Sheet took place. Dinoflagellates and ciliates were mostly observed in winter, prior to the spring bloom. In addition, low relative abundances of silicoflagellates were recorded in winter. This phytoplankton group usually has a minor contribution to the phytoplankton in the Godthåbsfjord, as well as other sub-Arctic and Arctic regions. Chrysophytes showed only low relative abundances in summer (2.2 % in June). Chrysophytes are known to occur in low-salinity summer waters in the Arctic fjords. Throughout the year, two diatom genera, i.e. *Chaetoceros* spp. and *Thalassiosira* spp., contributed to more than half of the phytoplankton counts (table 5.1), and were complemented by *Phaeocystis* sp. Diatom species *Striatella unipunctata* was observed for the first time in Godthåbsfjord during winter 2014. This species was identified as a large colony, probably originating from sea-ice melt. Unlike the previous years, species belonging to other phytoplankton groups, such as dinoflagellates (*Protoperidinium* spp.) and silicoflagellates (*Dictyocha speculum*) were among dominants this year.

Vertical zooplankton net hauls (45 μm WP2 net) were conducted from 0-100 m. In 2014, abundances of copepod nauplii increased in May with *Calanus* spp. nauplii peaking in July whereas *Microsetella norvegica* nauplii dominated in July with high abundances > 74.000 ind m^{-3} (figure 5.10). However, abundance of copepods was low during the mid-summer months compared with previous years.

The copepod community was dominated by *Microsetella norvegica, Oithona spp. and Microcalanus sp.* through the winter months. *Calanus* spp. showed rising abundances in April and May, whereas the rise in copepod abundances in July was due to *Microsetella norvegica*. However, *M. norvegica* did not emerge in extreme numbers compared to previous years. Therefore,

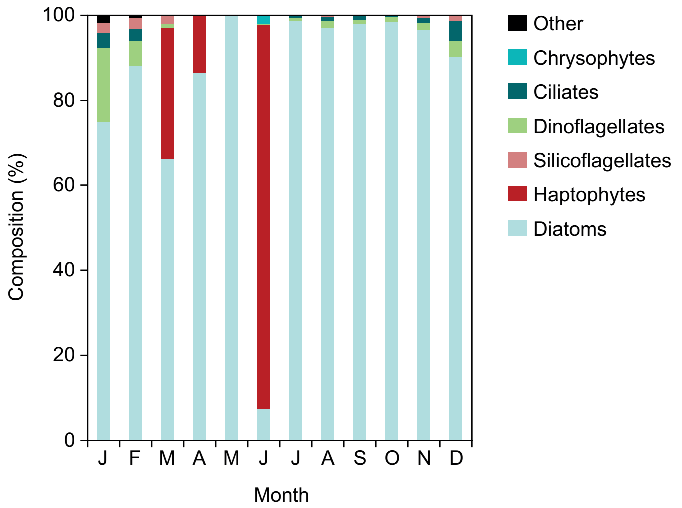

Figure 5.9 Seasonal variations in phytoplankton assemblage (%) at the Main Station during 2014.

Table 5.1 Ten most dominant phyoplankton species presented as their relative accumulated proportion of total cell counts (%) at the 'Main Station' in 2014.

2014	
Chaetoceros spp.	49.2
Thalassiosira spp.	69.9
Phaeocystis sp.	81.1
Striatella unipunctata	84.4
Navicula spp.	87.2
Protoperidinium spp.	89
Thalassionema nitzschioides	90.7
Fragilariopsis spp.	91.9
Cylindrotheca closterium	92.8
Dictyocha speculum	93.6

Oithona spp. comprises a relative high percentage of the total abundance (figure 5.10B) from August and throughout the autumn.

Abundances of other zooplankton groups increased in April (figure 5.10) due to Cirripedia nauplii. Hereafter two distinct peaks occurred in bivalvia larvae in May and two months later in July. The portion of rotifers was high in both July and August (6600 and 4465 ind m^{-3}, respectively).

Since the beginning of the annual sampling at the Main Station (GF3) in 2008, the abundance of fish larvae has varied over the years with a temporal shift in species composition during summer (figure 5.11). In general, sandeel (*Ammodytes* sp.) larvae dominates the abundance in late winter/early spring (February/March),

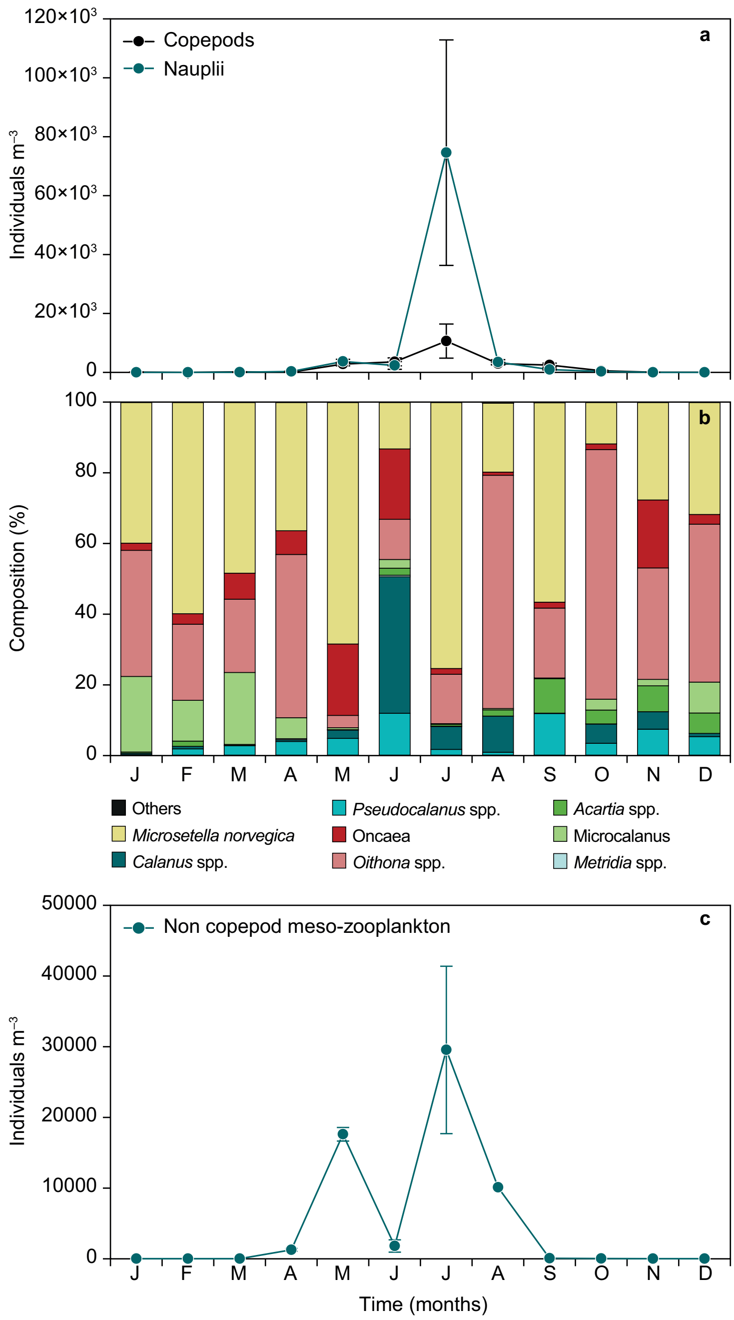

Figure 5.10 Annual variations in abundance (individuals m^{-3}) of copepod nauplii and copepods (i.e. copepodites and adult stages) (a), copepod community composition (%) (b) and abundance of other zooplankton groups (individuals m^{-3}) (c) at the Main Station in 2014. Error bars represent standard deviation.

Arctic shanny (*Stichaeus punctatus*) larvae dominates the abundance in spring (April/May) followed by capelin (*Mallotus villosus*) larvae dominating the abundance in summer/autumn (July-September). The abundance of sandeel larvae varies in general greatly between years. In 2013 the abundance of sandeel larvae in February was record high with 50 individuals per 100 m^3. In 2014, however, abundance was very low with only 0.58 individuals per 100m^3, which is the lowest observed since 2011. Sandeel larvae had a second peak in abundance in summer (June). The abundance of Arctic shanny larvae in May was also the lowest recorded since 2011. The abundance of capelin larvae was in 2014 on the same level as in 2012 and 2013.

American Plaice (*Hippoglossoides platessoides*) larvae peak in abundance in June and highest numbers were observed in 2011. Atlantic cod (*Gadus morhua*) larvae seem to peak in different months between years from May to June and highest numbers were observed in June 2011. Overall the abundance of fish larvae varies greatly between years and especially 2010 was a year with very low abundance of fish larvae in all month. Since 2010, the abundance of fish larvae has increased and 2013 was a year with the highest abundance of fish larvae in the time series caused mainly by an increase in sandeel, capelin and Arctic shanny larvae in the samples. In 2014, the total abundance of fish larvae was lower than in 2013 caused by the absence of sandeel larvae in the samples, but the total abundance was still second highest in the time series caused by the presence of capelin larvae in summer.

In 2014, at the Main Station, no samples were taken in April and December and no fish larvae were found in the samples from March, October and November. The highest concentration of fish larvae was found in July (figure 5.12a), where capelin larvae accounted for 92 % of the total abundance (figure 5.12b). Sandeel larvae were caught from January to June and dominated the abundance in January and February, however, in low numbers. Arctic shanny larvae were caught in May and June and dominated the abundance in May. Atlantic cod larvae were caught in May, June and July and had the highest abundance in June accounting for 37 % of the total abundance in that month. Capelin larvae were caught from June to September and dominated the abundance in the same months. The majority of species were caught in May as seen in previous years. Greenlandic halibut (*Reinhardtius hippoglossoides*) larvae were for the first time in the time series caught on the Main Station in July.

The length section in the fjord in May 2014 showed a similar pattern in fish larvae abundance and species composition as in the years 2006, 2007 and 2011 with highest abundances found on Fyllas Banke (FB2.5) due to high numbers of sandeel larvae (figure 5.13). Especially in 2006 the

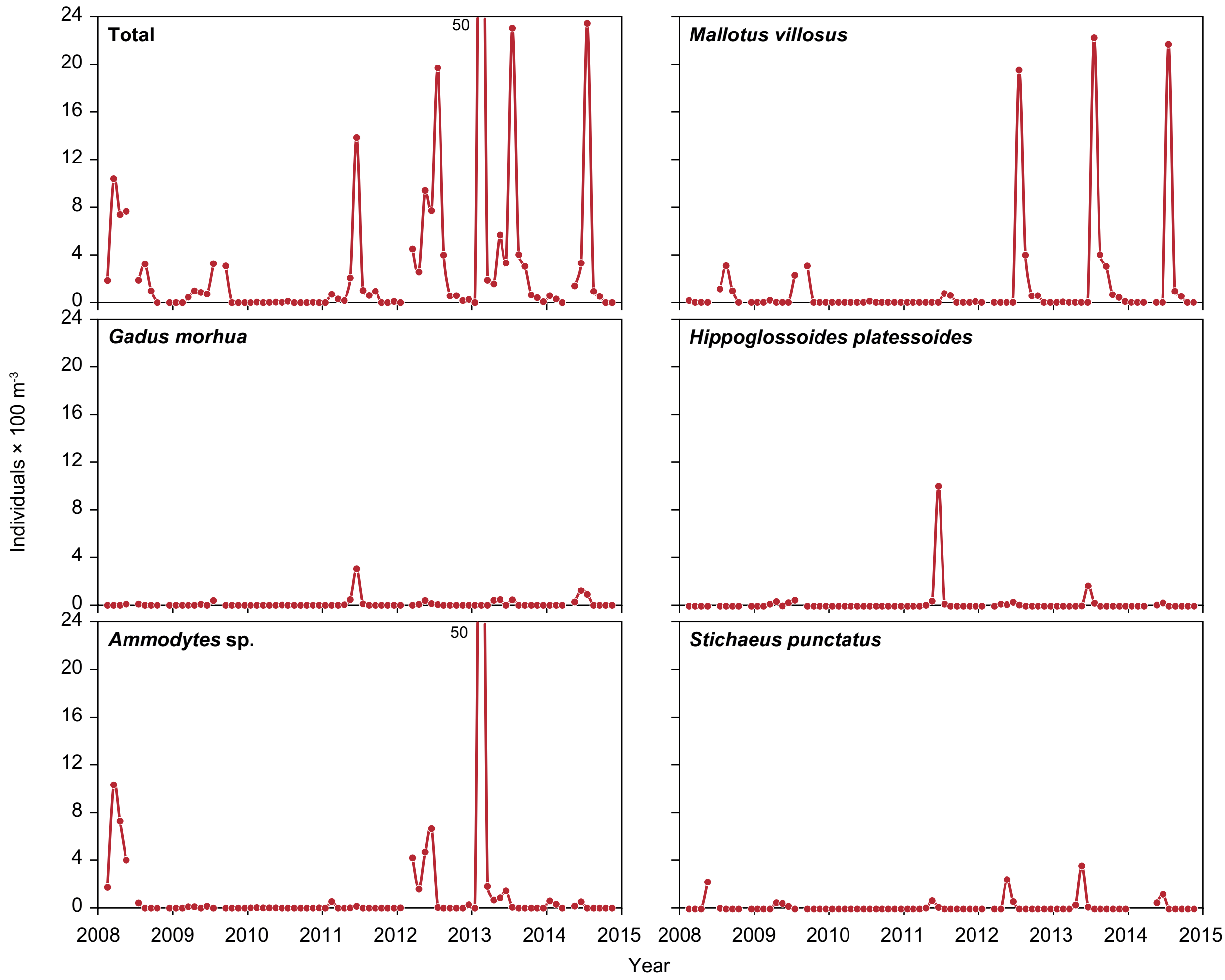

*Figure 5.11 Annual variation in abundance of fish larvae in total, capelin (*Mallotus villosus*), Atlantic cod (*Gadus morhua*), American plaice (*Hippoglossoides platessoides*), sandeel (*Ammodytes sp.*) and arctic shanny (*Stichaeus punctatus*) from 2008 to 2014 at the Main Station (GF3). Samples were collected each month except January, June and November 2008, August 2009, February 2012, April and December 2014.*

abundance was record high with 112 individuals per 100 m^3. In 2014, abundance of sandeel larvae was the same as in 2007 with 33 individuals per 100 m^3.

In 2008, 2009, 2010, 2012 and 2013 highest abundances were found closer to the inlet of the fjord at the Main Station mainly due to the absence of sandeel larvae in the samples from Fyllas Banke. In 2014, sandeel larvae dominated the samples from the outer slope of Fyllas Banke (FB3.5), on the top (FB2.5) to the inner slope towards the fjord (FB1.5). Redfish larvae (*Sebastes* sp.) were only found on the slopes of the bank (FB3.5 and FB1.5). For the first time in the time series, Atlantic cod was found on Fyllas Banke and on all stations. Inside the fjord, Atlantic cod was found on all stations with highest concentration at the Main Station (GF3). Arctic shanny dominated the abundance on all stations inside the fjord, except the station deepest inside the fjord (GF10) where abundance was lowest. Overall species composition varied on the length section with fewer species in the samples from Fyllas Banke and from deeper inside the fjord.

Fish larvae species composition seems to vary between years with most species found in 2014 (table 5.2). The increase in species found from 2008 was due to the implementation of monthly samples from the Main Station (GF3). In 2006 and 2007 only the length section in May was conducted.

The shellfish larvae community at the Main Station (GF3) showed the characteristic pattern with peak abundance of *Pandalus* sp. in May, whereas *Chionoecetes opilio* and *Hyas* spp. peaked one month later in June. Peak density of *Pandalus* sp. increased slightly to a level almost comparable with observations from 2012.

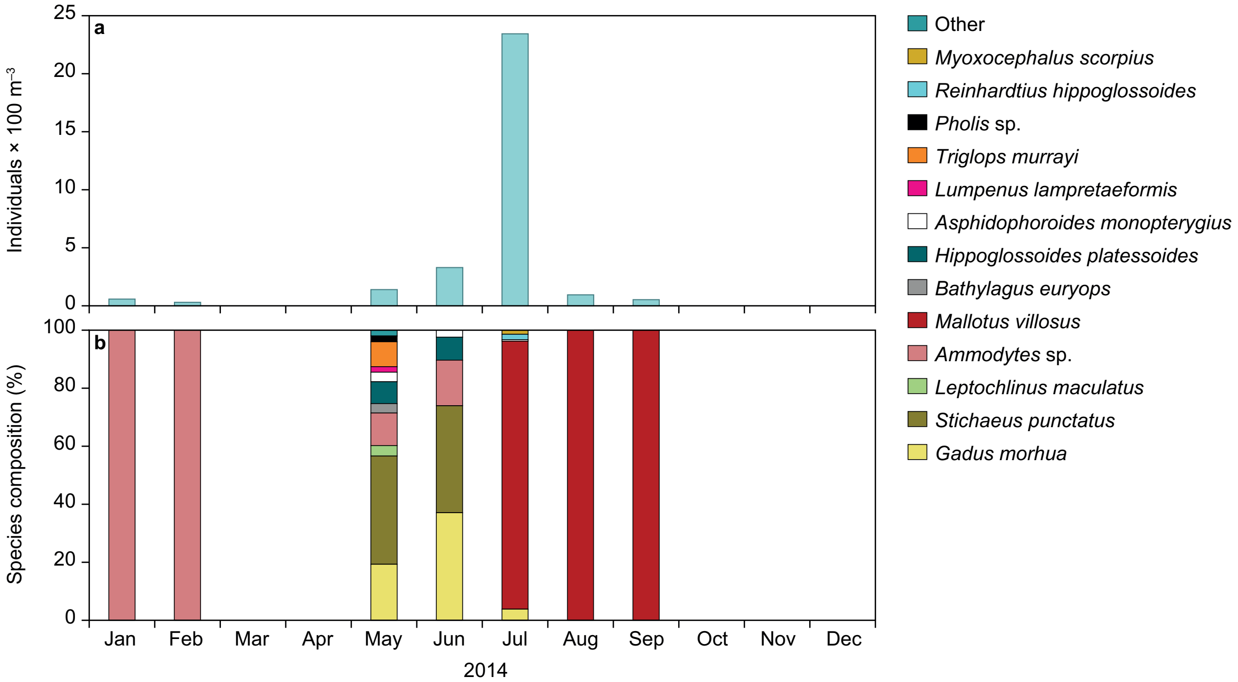

Figure 5.12 Annual variation in abundance (individuals per 100 m3) (a) and community composition (%) (b) of fish larvae at the Main Station (GF3) in 2014. No samples were taken in April and December.

Table 5.2 Species list of fish larvae 2006-2014.

Species list	**2006**	**2007**	**2008**	**2009**	**2010**	**2011**	**2012**	**2013**	**2014**
Gadus morhua	X	X	X	X	X	X	X	X	X
Stichaeus punctatus	X	X	X	X	X	X	X	X	X
Leptochlinus maculatus	X	X	X	X	X	X	X	X	X
Ammodytes sp.	X	X	X	X	X	X	X	X	X
Mallotus villosus		X	X	X	X	X	X	X	X
Aspidophoroides monopterygius	X	X	X			X			X
Bathylagus euryops		X	X	X	X	X	X	X	X
Cyclothone sp.		X							
Liparis sp.		X				X		X	X
Liparis gibbus					X		X		
Pholis sp.	X	X	X					X	X
Pholis fasciatus					X	X	X	X	
Pholis gunellus							X		
Reinhardtius hippoglossoides	X		X			X	X	X	X
Myoxocephalus scorpius			X		X		X	X	X
Hippoglossoides platessoides			X	X	X	X	X	X	X
Sebastes sp.			X			X	X	X	X
Gadus ogac			X	X	X				
Leptagonus decagonus				X	X	X	X	X	
Agonidae				X					
Lumpenus lampretaeformis				X	X		X	X	X
Triglops murrayi						X	X		X
Cottidae						X			X
Anarchias minor									X
Anarchias sp.						X			
Total	**7**	**10**	**13**	**11**	**13**	**16**	**16**	**15**	**17**

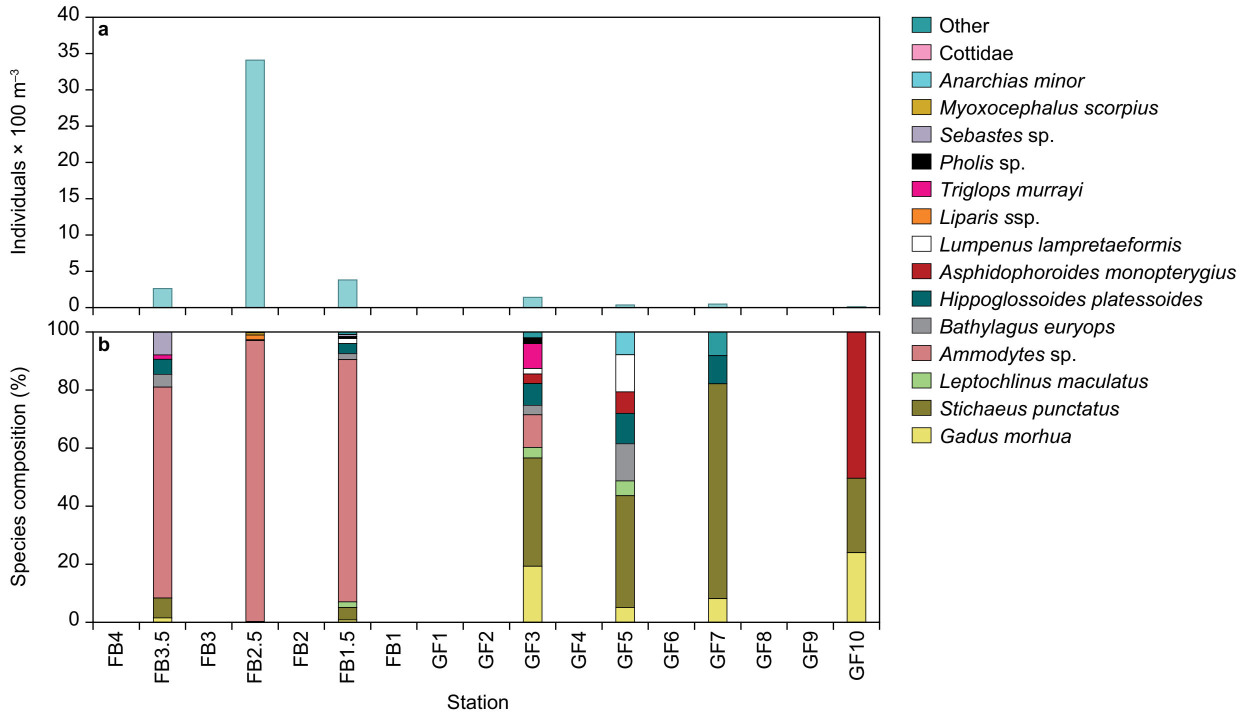

Figure 5.13 Variation in abundance (individuals per 100 m^3) (a), and community composition (%) (b) of fish larvae on the length section in May 2014.

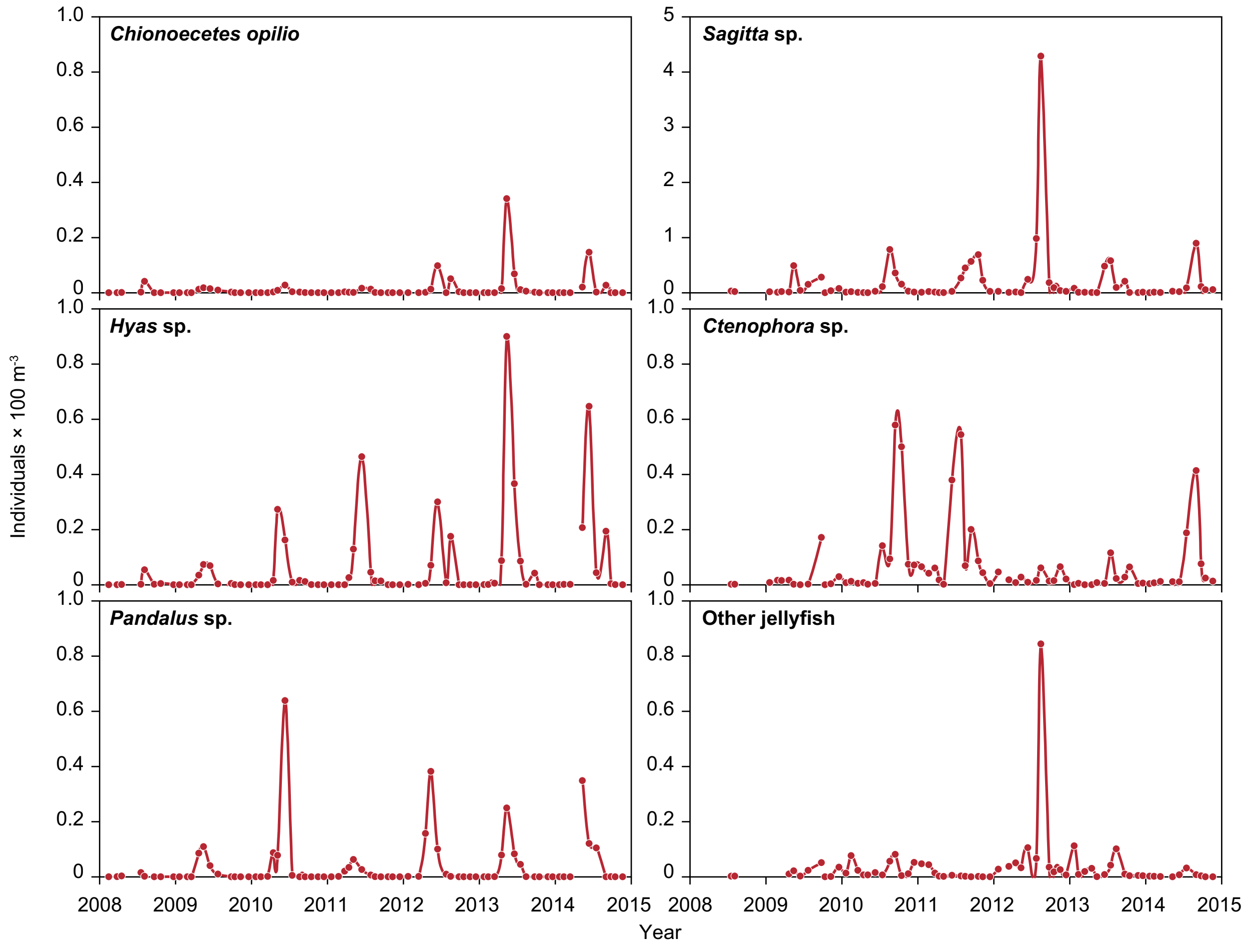

Figure 5.14 Annual variation in abundance (individuals m^{-3}) of Chionoecetes opilio, Hyas *sp.,* Pandalus *sp.* Sagitta *sp.,* Ctenophora *sp. and other jelly fish at the Main Station (GF3) from 2008 to 2014. Samples were collected each month except November 2008, August 2009, and April and December 2014.*

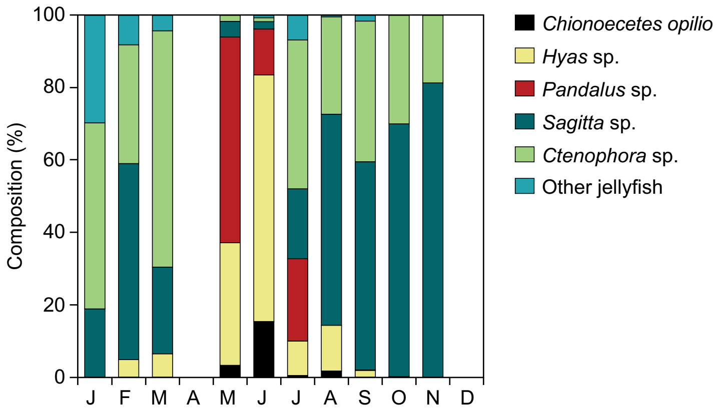

Figure 5.15 Annual variation in community composition (%) at the Main Station (GF3) in 2014. Samples were collected each month except April and December.

Density of *Chionoecetes opilio* declined over 2013, but the number of individuals m^{-3} in June 2014 was still higher compared to estimates from 2009 to 2012. The continued increasing trend from 0.05 individuals (m^{-3}) in 2008 to 0.9 individuals (m^{-3}) in 2013 of *Hyas* spp. turned out to a 29 % drop from 2013 to 2014 (figure 5.14). Larvae stage zoae I of *C. opilio* and *Hyas* spp. dominated samples in April to June where as larvae stage zoae II was more prevalent in July. Low concentrations of megalope stage of *C. opilio* and moderate concentrations of *Hyas* spp megalop stages were observed in October. Throughout the entire years of sampling, abundance of *C. opilio* has been low compared to the other crab species *Hyas* spp.

At the Main Station (GF3), the community was mainly dominated by *Ctenophora* and *Sagitta* spp., in all the months of sampling, except in the period from May to June where *Pandalus* spp., *Chionoecetes opilio* and *Hyas* spp. became more abundant. As a contrast to 2013, *Sagitta* spp. became the most dominating species from August to December (figure 5.15), but unlike the previous years of sampling, *Sagitta* spp. were less abundant in June and July. Number of individuals (m^{-3}) of *Sagitta* spp. was recorded in considerably high number and peaked at four individuals (m^{-3}) in August 2012, followed by a significant decline in 2013 and remains at a comparable level in 2014 (figure 5.16). *Ctenophora* showed high concentrations in March (65 %) and in the months from July to November (30 to 41 %). Throughout 2014, other jellyfish were observed in unusually low relative abundance and comprised only a minor part of the community except for January (figure 5.14 and 5.15).

Along the length transect from Fyllas Banke (offshore) to the inner part of the fjord (GF10), concentrations of crab larvae (*Hyas* spp.) and *Chionoecetes opilio* were significantly lower in 2014 compared to the preceding years (figure 5.16), but with comparable high abundance of *Hyas* spp. at the offshore station FB2.5. The commercial species *Chionoecetes opilio* was mainly observed at the offshore station FB2.5, in minor abundance at the Main Station GF3, but was absent at the more inner stations along the fjord transect. *Pandalus* spp. were found at almost all stations along the fjord transect, with variations in density between stations and with lower abundance compared to 2013, except for the Main Station (GF3) where abundance was unchanged from previous years (figure 5.16). The community composition differed not only between stations but also between years (figure 5.17). In 2014, larvae of *Chionoecetes opilio* were less abundant at all stations, compared to previous years. *Sagitta* spp. conquered the community at the inner stations GF7 and GF10, except

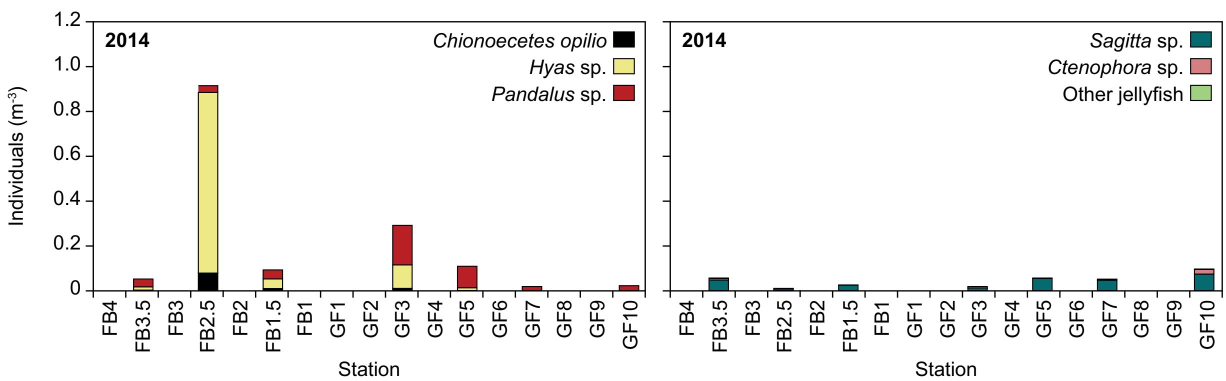

Figure 5.16 Annual variation in abundance (individuals m^{-3}) of Chionoecetes opilio, Hyas *sp.,* Pandalus *sp.* Sagitta *sp.,* Ctenophora *sp. and other jelly fish along the length section from Fyllas Banke (offshore) to the inner part of Godthåbsfjord conducted in May 2014.*

with occurrence of few individuals of *Hyas* spp., *Pandalus* spp. and *Ctenophora*. The latter species were most abundant at the most inner station GF10, whereas it was almost insignificant at the offshore stations FB2.5 and FB1.5 (figure 5.17).

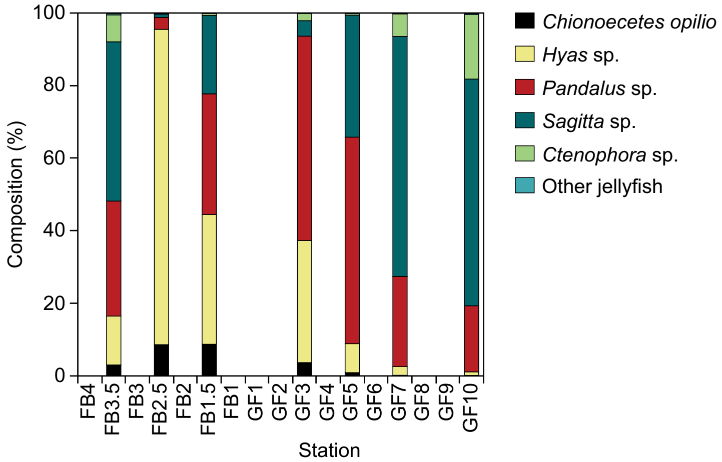

Figure 5.17 Community composition (%) along the length section from Fyllas Banke (offshore) to the inner part of Godthåbsfjord conducted in May 2014.

Vertical sinking flux

A part of the particulate material produced in the photic zone sinks through the water column towards the ocean sediment. This vertical transport of organic material provides the main source of energy for the benthic communities. Sediment traps moored on free-drift traps arrays for approx. two hours are used to measure the sinking flux of particulate material. The collected particulate material is analysed for chlorophyll *a*, particulate organic carbon and nitrogen, and isotopic composition. The sinking flux of phytoplankton material (i.e. chlorophyll *a*) showed a single abrupt peak during the spring bloom, while only moderately elevated values were observed during summer (figure 5.18). The spring also resulted in a high sinking flux of particulate organic carbon and nitrogen, which continued in summer. The organic material sinking during spring was largely comprised of fresh algae material, as seen by the high $\delta^{13}C$ (i.e. less negative) values and low $\delta^{15}N$ values. Lower $\delta^{13}C$ values and higher $\delta^{15}N$ in summer could indicate a higher proportion of degraded organic material, perhaps due to a higher contribution of faecal material from zooplankton grazing. The POC sinking fluxes recorded in 2014 (up to 1610 mg C m^{-2} d^{-1}) were in the high end of values observed during the entire monitoring programme (up to 2369 mg C m^{-2} d^{-1}). The integrated annual POC sinking flux estimate was 312 g C m^{-2} y^{-1} in 2014 (data not shown).

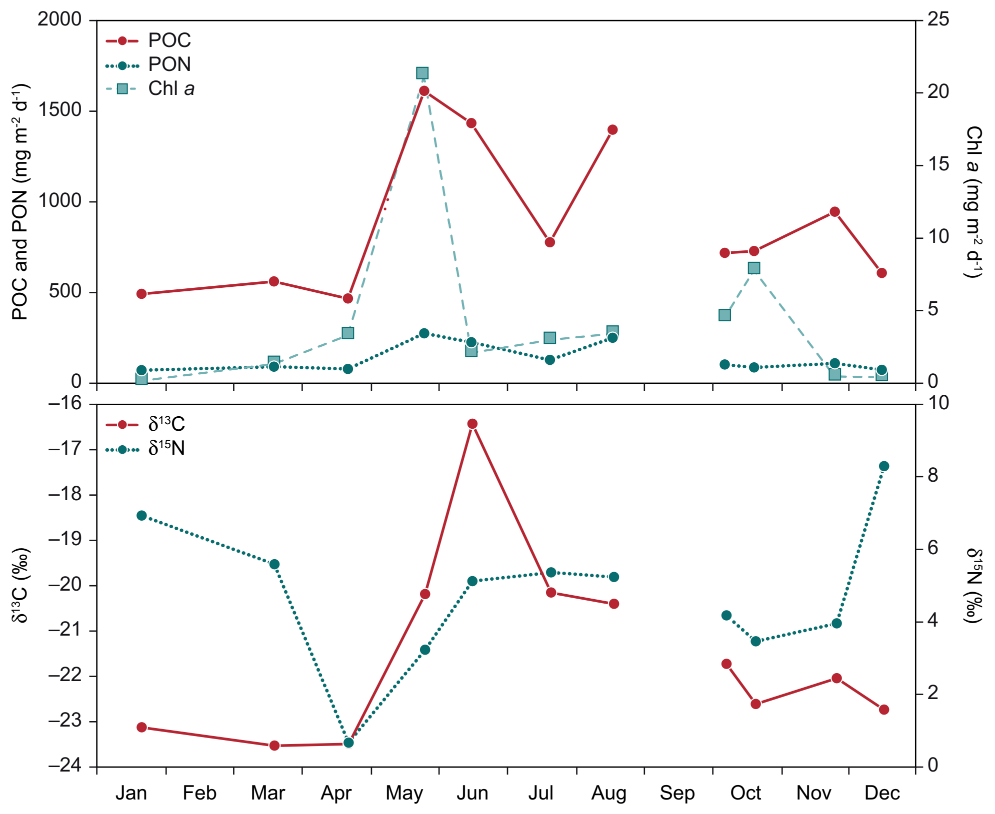

Figure 5.18 Annual variations in vertical sinking flux of particulate organic carbon and nitrogen (POC and PON; mg m^{-2} d^{-1}), chlorophyll a (Chl a; mg m^{-2} d^{-1}) and isotopic composition ($\delta^{13}C$ and $\delta^{15}N$; ‰) of the sinking particulate material collected at the Main Station in 2014.

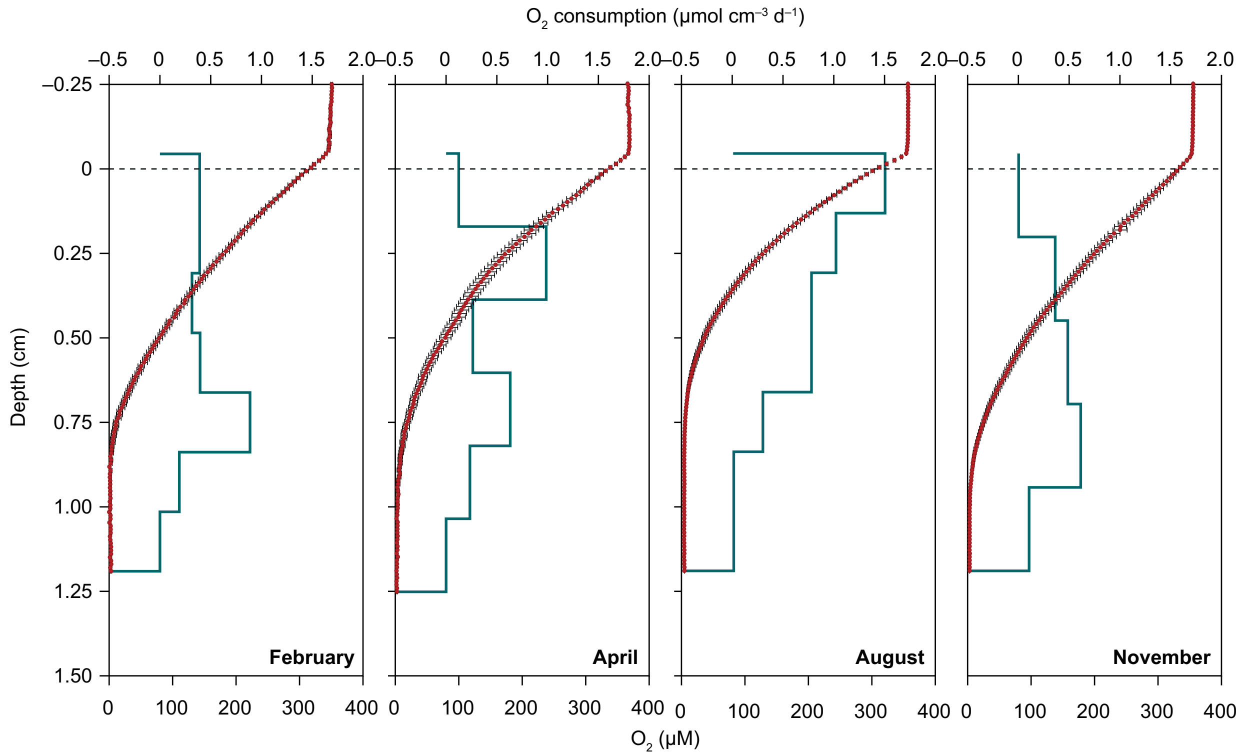

Figure 5.19 Vertical concentration profiles of oxygen (closed dots) and modelled consumption rates (solid line) from micro electrode profiles with sediment depth for each of the three sampling periods. Error bars represent standard error of the mean.

5.4 Sediments

The benthic communities are largely fuelled by organic material sinking from the photic zone. The organic material reaching the benthos is being mineralized by benthic organisms or buried in the sediment. Oxygen is primary oxygen receptor in the upper oxic zone of the sediment, while sulphate is the main receptor in the anoxic zone below. Both processes use oxygen either directly or indirectly, and oxygen uptake into the sediment is, therefore, used to measure the rate of remineralization.

Sediment cores are collected for laboratory experiments and analysis four times during the year at a permanent sediment sampling station in Kobbefjord ('Sediment station', depth approx. 120 m; figure 5.1). Microprofiling is used for measuring the diffusive oxygen uptake (DOU) into the sediments. The oxygen profiles showed that the oxic zone ranged between 0.7 and 0.9 cm and that DOU ranged between 3.7 and 7.5 mmol m^{-2} d^{-1} during the four seasonal samplings (figure 5.19 and 5.20, respectively). The total oxygen uptake (TOU) ranged from 5.3 to 8.0 mmol m^{-2} d^{-1}. The highest oxygen uptake rates are

Figure 5.20 Variation in total oxygen uptake (TOU) and diffusive oxygen uptake (DOU) (mmol m^{-2} d^{-1}) and in the TOU/DOU ratio from 2005-14.

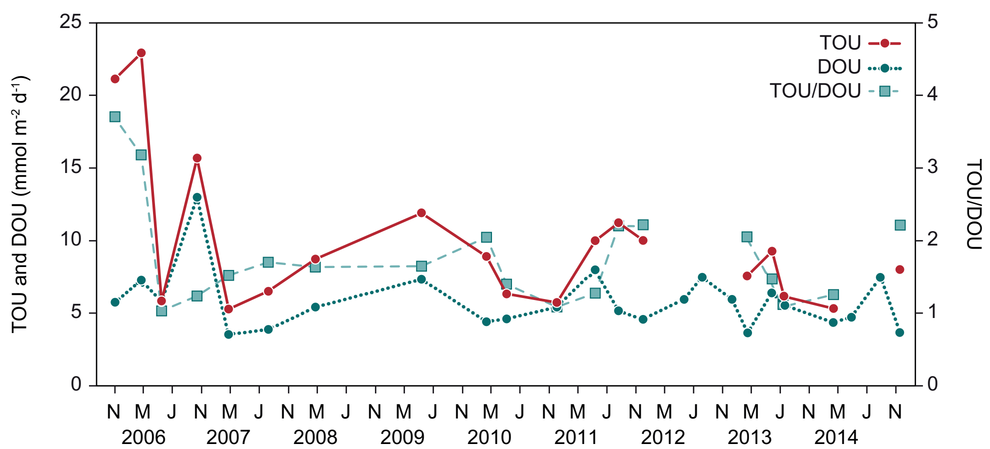

*Figure 5.21 Left: Sampling in the tidal zone in inner Kobbefjord, Nuuk, where knotted wrack (*Ascophyllum nodosum*) dominates the algal community and bladder wrack (*Fucus vesiculosus*) and *Fucus evanescence* are also abundant (Photo: Peter Bondo Christensen). Upper right: Tips of* A. nodosum *with knots/bladders (Photo: Núria Marbà). Lower right: Blue mussels (*Mytilus edulis*) (Photo: Peter Bondo Christensen).*

generally observed during spring and summer, when primary production and sedimentation of organic material are highest (figure 5.20).

5.5 Benthic fauna and flora

The monitoring of benthic flora and fauna (since 2012) focuses on population dynamics of key species of the intertidal zone – the brown macroalgae 'knotted wrack' (*Ascophyllum nodosum*) and 'blue mussel' (*Mytilus edulis*), in relation to temperature, ice cover/light availability and tidal level. Knotted wrack and blue mussel are expected to respond positively to increases in water temperature as both species are north-temperate with temperature optima (15-20 °C for *A. nodosum*, Fortes and Lüning 1980) considerably higher than current temperatures in the Godthåbsfjord system. These species have the additional advantages as indicator organisms that 1) their growth is reflected in their morphology (see details below) and 2) their presence in the tidal zone facilitates monitoring.

The coastal waters around Nuuk have a tidal range of 3-5 m offering a large potential habitat for intertidal communities (figure 5.21). The composition of the tidal community varies markedly with exposure to ice and waves (Høgslund *et al.* 2014), with *Ascophyllum* being a dominant keystone species of protected inner fjords such as represented by the monitoring site in inner Kobbefjord.

Permanent monitoring plots were established in late August/early September 2012 in the mid intertidal zone as well as in the upper (MWL + 0.5 m) and lower intertidal (MWL –0.5 m) and are revisited annually at the same time of year.

Tip growth of *Ascophyllum*

Knotted wrack grows from the tip and forms a bladder/knot every year allowing an assessment of annual growth by simply measuring the distance between consecutive bladders to obtain elongation rates and weighing them to assess tip growth in biomass units. Actively growing tips were sampled randomly in the population outside the permanent plots in each of the tidal zones (upper, mid, lower) and the length of the three youngest segments was measured and weighed (i.e. segment 0 = tip to base of 1st bladder, segment 1 = base of 1st to base of 2nd bladder and segment 2 = base of 2nd to base of 3rd bladder).

The size of the tip segments increased markedly from segment 0 (initiated the year of sampling) to segment 1 (initiated the previous year), and levelled off towards segment 2 (initiated 2 years before) (figure 5.22). This pattern suggests that the most sensitive tip growth indicator is the size of segment 1 and its annual

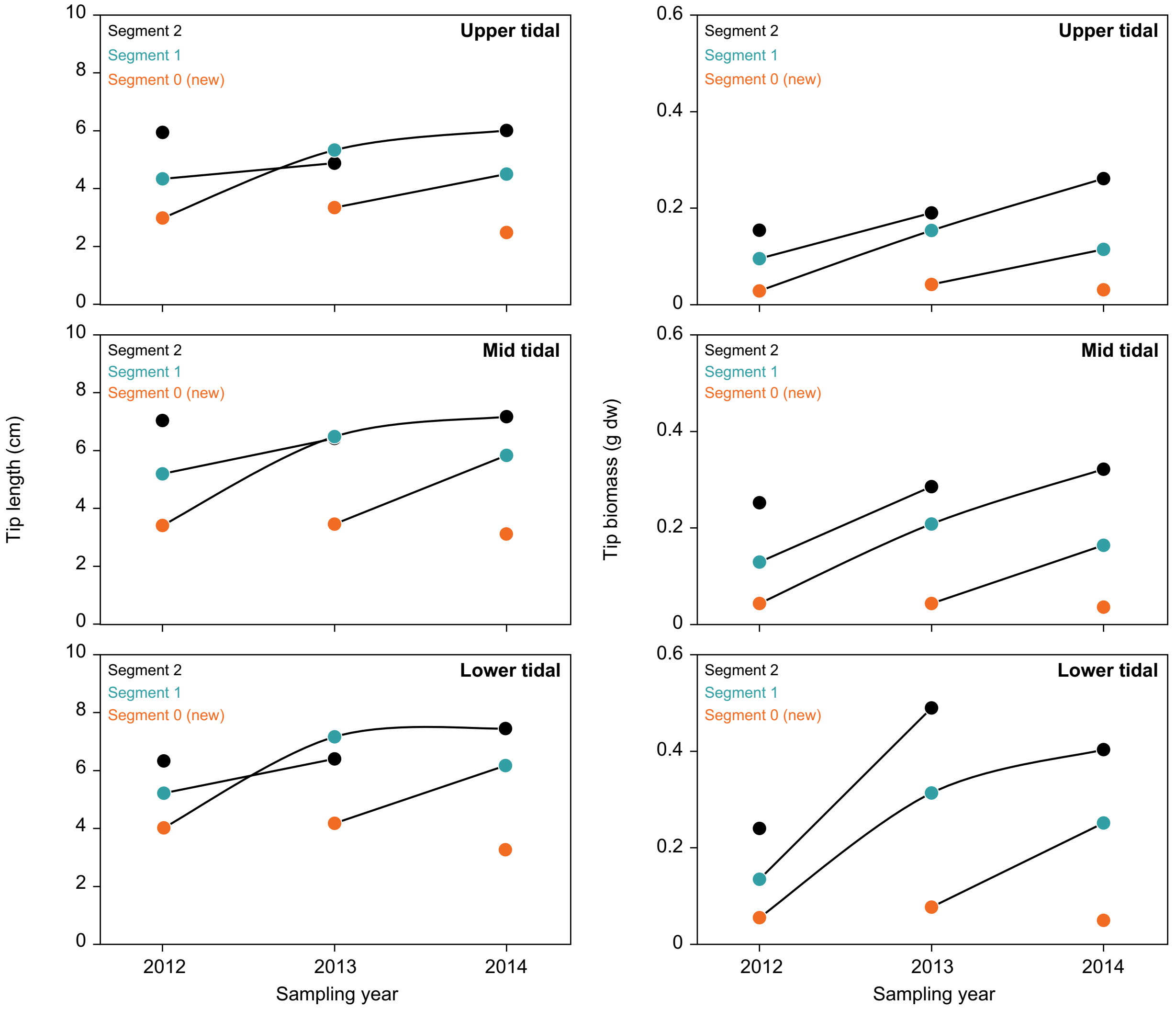

Figure 5.22 Growth of Ascophyllum tips in the upper, mid and lower tidal zone in 2012-2014. Data represent tip segment 0 (newest, initiated the year of sampling, tip-base of 1st bladder), segment 1 (initiated the year previous to sampling, base of 1st-base of 2nd bladder) and segment 2 (initiated 2 years previous to sampling, base of 2nd-base of 3rd bladder). Data represent averages of about 20 tips (with 1-3 branches) in each tidal zone each year.

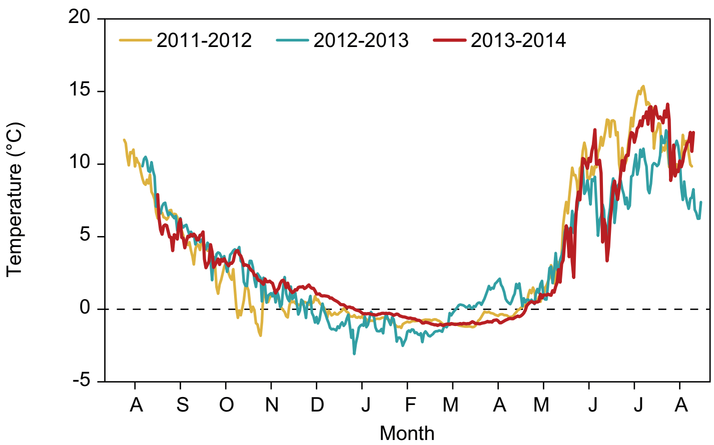

Figure 5.23 Temperature loggings at the monitoring site in inner Kobbefjord in the lower part of the tidal zone from August 2011 to August 2014.

growth as quantified by the increase in size since the previous year (when it was segment 0). Tip size varied interannually with segments 0 and 1 tending to be largest in 2013 and the annual growth of segment 1 also being larger in 2012-2013 (length increase 58 ± 2 % y^{-1}, biomass increase 161 ± 5 % y^{-1}) than 2013-2014 (length increase 41 ± 7 % y^{-1}, biomass increase 120 ± 10% y^{-1}) (figure 5.22). This pattern likely reflects the mild winter 2012-2013 with very limited sea-ice-cover leaving the inner part of Kobbefjord merely ice-free and the algae hence exposed to full incident irradiance. Temperature loggings in the lower tidal zone confirmed that the winter 2012-2013 was characterized by much higher temperature variability, reflecting lack of ice cover, than the winters 2011-2012 and 2013-14

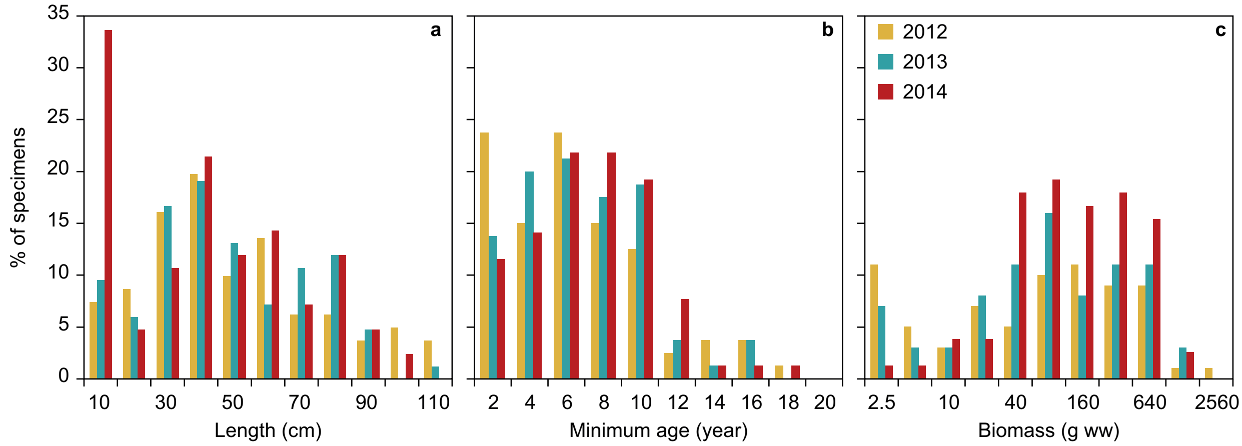

*Figure 5.24 Population structure of knotted wrack (*Ascophyllum nodosum*) in 10 permanent plots located in the mid-tidal zone in inner Kobbefjord. Length distribution (upper panel), age distribution (central panel) and biomass distribution (lower panel) of individuals are are shown. The many new individuals < 2 cm length appearing in 2014 are included in the upper panel, but do not appear in the central and lower panels as they were < 1 year and their biomass was negligible.*

when an insulating layer of ice covered the shore (figure 5.23).

The size of tip segments also increased from the upper tidal level towards the mid and lower tidal levels (e.g. segment 1 in 2014 upper tidal: 4.51 ± 0.15 cm/0.11 ± 0.004 g dw, mid tidal: 5.84 ± 0.18 cm/0.16 ± 0.005 g dw, lower tidal: 6.17 ± 0.17 cm/0.25 ± 0.007 g dw) where exposure to wind, dessication and ice is reduced (figure 5.22).

Population dynamics of *Ascophyllum*

Population structure of knotted wrack was quantified non-destructively in 10 permanent plots (0.25 m × 0.25 m) in the mid-tidal zone. Each individual (representing 1-several 'shoots' arising from a common basal disk) with bladders and exceeding a minimum length of 5-10 cm, was tagged and numbered in 2012 and length (L), minimum age (= number of bladders of the longest shoot) and circumference (C) at the base was quantified each year. New shoots arising over the monitoring period were similarly tagged and measured. Based on this information, population density, biomass (B) and age structure of individuals were estimated ($B = 0.1057 \times LC^2$, Merzouk *et al.* unpublished).

The habitat-forming role of *Ascophyllum* was underlined by the huge population biomass (estimated at 13.9 ± 2.2, 15.7 ± 3.1, 19.2 ± 2.8 kg Fresh weight (FW) m^{-2} in 2012, 2013 and 2014, respectively) and density (130 ± 13, 134 ± 13 and 126 ± 14 individuals m^{-2} in 2012, 2013 and 2014, respectively) completely covering the rocky shore. The bulk of the biomass was composed of 4-10 year old shoots extending 30-80 cm above the surface of the rocks when lifted by the tide while the longest shoots exceeded 1 m, highlighting the three-dimensionality of the habitat (figure 5.24).

Population dynamics in terms of growth, mortality and recruitment was assessed on the basis of changes in size of previously marked individuals in combination with observations of appearance and disappearance of individuals between years. From 2012 to 2013 the population was very stable with a net population growth rate of only 3 ± 4 % yr^{-1}, a slow recruitment rate of 6.2 ± 5.0 individuals m^2 (5 %) per year and a mortality rate of 1.6 ± 1.6 individuals m^2 (1 %) per year and no major change in biomass (1761 ± 1367 g FW m^{-2} yr^{-1}), reflecting that losses of old shoots/branches were balanced by tip growth. By contrast, the population was highly dynamic from 2013 to 2014 with high net population growth rate (29 ± 10 %) driven by a high recruitment rate (32 %) of tiny recruits by far exceeding mortality rates of existing shoots (8 ± 6 %). Despite higher mortality than in 2012/2013, it is still in the lowest range of mortality rates reported for *Ascophyllum* (8-77 % yr^{-1}; Åberg 1992ab). In 2013/2014 the population experienced an overall biomass increase of 26 % reflecting that biomass gain through tip growth and new individuals/shoots by far outweighed biomass loss. Ice cover was more pronounced in 2013/2014 than in 2012/2013 (3 of 10 "ice screws" mounted at the monitoring site were bent in 2013/2014 as opposed to only one in 2012/2013 and temperature loggings also indicated ice cover during the winter 2013/2014, Figure 5.23 and probably the ice foot protects *Ascophyllum* against biomass losses during winter storms even though the ice foot also shades the algae.

Survival and growth of intertidal *Mytilus*

On 4 September 2013, 225 individuals with an average (± S.D.) shell length of 30.84 mm (± 2.80) were collected, marked individually using commercial shell fish tags, and their shell length recorded. 15 individuals were then placed in each of 15 cages along with a temperature logger recording temperature every 15 minutes. Five cages were then mounted at the different elevations in the intertidal zone; the upper, mid and lower intertidal zone (MWL + 0.5 m, MWL and MWL –0.5 m.). The site was the same as for the *Ascophyllum* study. On 23 August 2014 the cages were collected again. 14 of 15 cages were retrieved. One of the cages was ripped open with no experimental animals within. This resulted in bivalve data from 13 out of 15 cages. Five, five and three cages from the upper, mid and lower intertidal zone, respectively. Eleven of the 15 temperature loggers were still functional. In the 13 available cages, a total of 76 animals was still alive at retrieval. Survival was lowest in the upper intertidal zone (average 0,4 %(± SD)), whereas 48 % (± SD) survived in the mid intertidal and 87 (± SD) in the low intertidal zone (figure 5.25) . Survival was significantly lower in the top of the intertidal zone compared to the lowest (Kruskal-Wallis ranked test). The increase in shell length of the 76 animals retrieved allowed calculation of the annual shell growth rates. Average annual shell growth was 1.66 (± SD), 1.33 (± SD) and 1.04 mm (± SD) in the upper, mid and lower intertidal zone, respectively. However, rates were not significantly different (Kruskal-Wallis ranked test).

Data from the temperature loggers (figure 5.26) showed a similar seasonal trend across the intertidal elevations, but with larger fluctuation in the high intertidal zone. Table 5.3 shows that the median temperature varied very little between cages from different tidal elevations. In fact, even the 5 % and 95 % percentiles were remarkably similar. When compar-

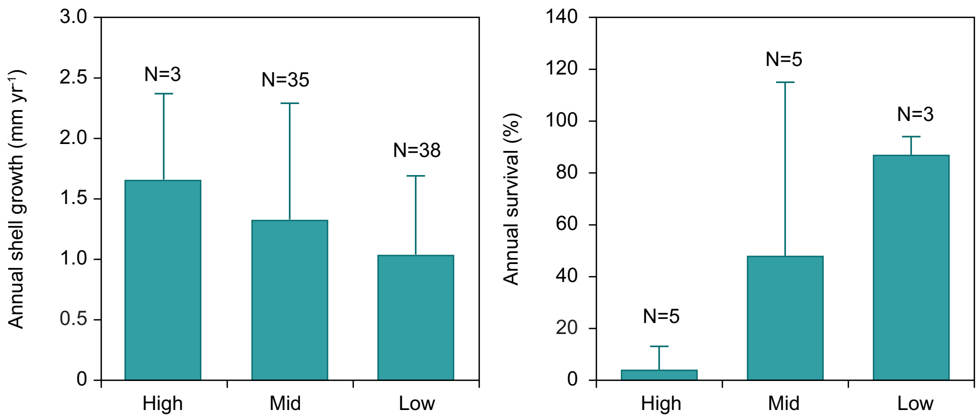

Figure 5.25 Left panel: average annual shell growth rates in experimental cages mounted at three different elevations in the intertidal zone (MWL + 0.5 m, MWL, MWL – 0.5 m). N indicates total number of surviving individuals. Right panel: average survival in 5 experimental cages mounted at each of three different elevations. N indicates the number of experimental cages available.

Table 5.3 Summery statistics from the temperature loggers inside experiment cages. Average values (± SD) from 3-4 loggers at each intertidal elevation is given.

	High	Mid	Low
Median	0.92 ± 0.12	1.13 ± 0.05	1.44 ± 0.15
5% Percentil	–1.31 ± 0.09	–1.26 ± 0.09	–1.19 ± 0.05
95% Percentil	13.20 ± 0.17	12.76 ± 0.08	12.85 ± 0.16
Minimum	–3.70 ± 1.63	–5.01 ± 1.00	–2.81 ± 0.36
Maximum	28.42 ± 4.36	22.75 ± 1.73	21.51 ± 2.49
No. obs. > 20°C	105 ± 50	19 ± 13	12 ± 17

Table 5.4 Summary of the duration of air exposure for each tidal elevation.

	High	Mid	Low
Average air exposure (hr)	8.25	6.46	4.91
Max. air exposure (hr)	22.17	7.16	5.67
Annual air exposure (%)	65	52	40

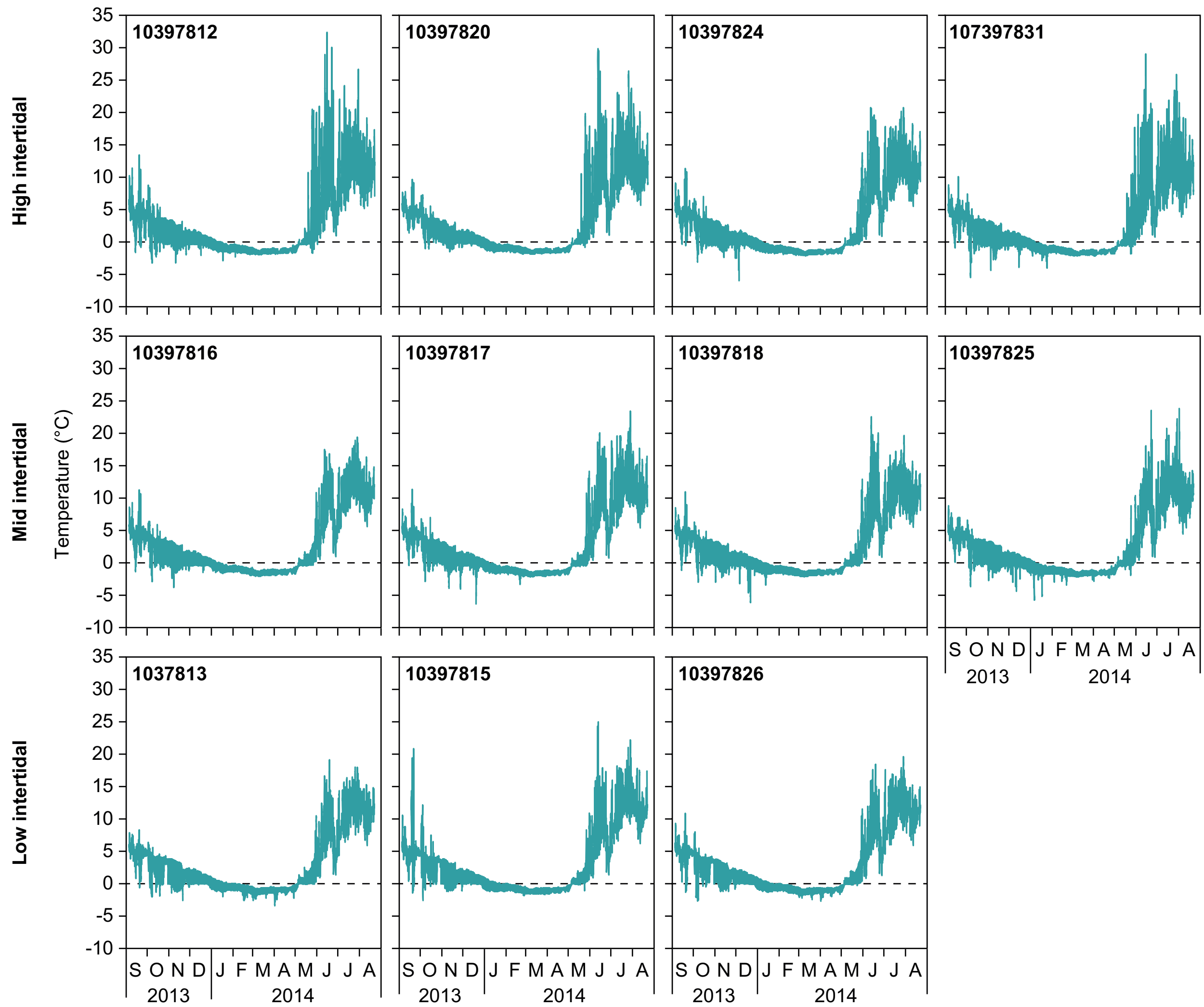

Figure 5.26 Data from individual data loggers placed inside experimental cages together with 15 Mytilus *spp. Cages were placed one year at three intertidal elevations. Loggers recorded temperature every 15 minutes.*

ing extreme temperatures, the minimum temperatures were also similar – from –2.8 to –5.0 °C. We did not record temperatures near the lower thermal limit of *Mytilus* (approximately minus 12-14 °C) in any of the cages. The similarity in minimum temperatures is likely attributed to the presence of sea ice in winter. The maximum temperature was high in the upper intertidal zone (28 °C) compared to 21 °C in the lower intertidal zone.

Higher maximum temperature, combined with longer air exposure, could explain the lower survival in the upper intertidal zone (table 5.4). However, there are obviously other factors involved. This is especially apparent in the mid intertidal zone where variation between the five replicate cages ranged from 0 to 100 % survival with no differences in temperatures to explain this difference. But it is striking that due to the effect of an ice foot in winter which modulates low winter temperatures, high temperatures in summer appear to be a significant stress factor. Intertidal mussels in Ireland have been reported to have an upper lethal temperature of 32 °C. Further work is needed to determine the upper lethal temperature of the specimens in Kobbefjord, and to assess how peaks in summer temperatures in combination with desiccation may contribute to a high stress level in the sub-arctic intertidal zone.

5.6 Seabirds

Two key seabird colonies in the vicinity of Nuuk are included in the MarineBasic programme. Additional seabird colonies in the Nuuk area have been visited since

Table 5.5 Breeding seabirds (pairs (P), individuals (I) or Apparently Occupied Nests (AON)) at Qeqertannguit since 2006.

Year	2006		2007		2008		2009		2010		2011		2012		2013		2014	
Species	**No.**	**Unit**	**No.**	**Unit**	**No.**	**Unit**	**No.**	**Unit**	**No.**	**Unit**	**No.**	**Unit**	**No.**	**Unit**	**No.**	**Unit**	**No.**	**Unit**
Black-legged kittiwake	45	AON	45	AON	20	AON	55	AON	42	AON	80	AON	0	AON	1	AON	8	AON
Iceland gull SE side	118	AON	82	AON	33	AON	40	AON	31	AON	31	AON	11	AON	17	AON	17	AON
Iceland gull NW side	–	AON	**	AON	12	AON	19	AON	13	AON	20	AON	9	AON	16	AON	0	AON
Great black-backed gull	46	P	38	P	44	P	24	P	40	P	17	P	16	P	18	P	17	P
Lesser black-backed gull	10	P	11	P	25	I	21	I	27	I	18	I	1	I	7	I	4	P
Glaucous gull	10	P	14	P	13	P	5	P	4	P	2	P	6	P	16	P	6	P
Herring gull	-	P	1	I	2	P	1	P	0	P	0	P	1	P	0	P	0	P
Arctic tern	150-220	I	150	I	0	I	150	I	54	I	50	I	50-100	I	0	I	0	I
Arctic skua	2	P	2	P	2	P	2	P	2	P	0	P	2	P	2	P	0	P
Black guillemot	615	I	562	I	689	I	637	I	790	I	1047	I	708	I	388	I	313	I
Red-throated diver	1	P	1***	I	1	P	1	P	0	P	0	P	0	P	0	P	0	P
Red-breasted merganser	*		4	P	3	P	0	P	1	P	0	P	0	P	0	P	0	P

*Observed
**These birds are included in number for SE birds
***Seen at coast, but lake was dry and no nest visible

2007. The seabird counts from MarineBasic are reported annually to the Greenland Seabird Colony Database maintained by the Department of Bioscience, Aarhus University.

Qeqertannguit (colony code: 64035)

Qeqertannguit in the interior parts of Godthåbsfjord (figure 5.1) is a low-lying island and holds the largest diversity of breeding seabirds in the Nuuk district. Especially surface feeders such as gulls, *Laridae*, kittiwake, *Rissa tridactyla*, and arctic tern, *Sterna paradisaea*, are usually well represented at the site (table 5.5). The steep cliff in the middle of the southeast-facing side of the island (kittiwake and Iceland gull, *Larus glaucoides*) and a smaller cliff on the northwest-facing side (Iceland gull) were counted from the sea using a boat as platform. Black guillemot, *Cepphus grille*, is present on the water around the island and is also counted using the boat as a platform. Counts of the remainder of the island were conducted by foot using direct counts of Apparently Occupied Nests (AON) or territorial behaviour as a criterion of breeding pairs. This year the island as well as the SE colony were observed and photographed from boat on 10 June.

Other birds observed during the walk (not considered breeding and not systematically counted), included a raven, *Corvus corax*, 19 snow buntings, *Plectrophenax nivialis*, four Lapland buntings, *Calcarius lapponicus*, five northern wheatears, *Oenanthe oenanthe*, two rock ptarmigans, *Lagopus muta*, and a nesting purple sandpiper, *Calidris maritima* with three eggs and one chick. The number of black guillemot around the island was estimated to 313 individuals.

Arctic tern was not observed on the island on 10 June and no nests were found (table 5.5). Complete absence of Arctic tern on Qeqertannguit was also recorded in 2008 and 2013. Small and mid-sized colonies of Arctic tern in Greenland are known to fluctuate considerably in population size and years of complete failure seem to occur regularly, but the reason is poorly understood.

This year a small number of kittiwakes was observed on the southeast side of the island. 15 individuals and eight apparent nests were counted. In 2011, numbers of breeding kittiwake peaked with 80 pairs, but the colony has had very few observed nests since. The number of Iceland gull on the SE side has remained at 17, the same number as in 2013. No nesting Iceland gulls were observed on the northwest side. Thus 2014 had the fewest observed number of nesting Iceland gull reported so far.

Qeqertannguit is influenced by legal egg harvesting (great black-backed gull (*L. marinus*) and glaucous gull, *L. hyperboreus*, prior to 31 May). Illegal egg harvesting (illegal species such as kittiwake, Iceland gull, lesser black-backed gull (*L. fuscus*), herring gull (*L. argentatus*) and egg harvesting after 31 May) has been reported

Table 5.6 Counts of breeding seabird at Nunngarussuit since 2006. Counts in Pairs are marked (P), and the remaining counts are of Individuals.

Year	2006	2007	2008	2009	2010	2011	2012	2013	2014
Species	No.	No.	No.	No.	No.	No.	No.	No.	No.
Guillemot unspecified	694	–			–	514	375	654	437
Brünnich's guillemot	–	705	388	475	–	–	–	–	–
Common guillemot	–	87	36	47	–	–	–	–	–
Guillemots on the water	2–300	450	450	–	–	500	2–400	–	300
Glaucous gull	20	14	14	12	–	11	4 (P)	–	18
Great black-backed gull	5	5	2	5	–	4	2 (P)	–	–
Northern fulmar	23	13	17	11	–	21	10 (P)	20	4

several times since the start of the monitoring programme.

Nunngarussuit (colony code: 63010)

Nunngarussuit is located approx. 40 km south of Nuuk (figure 5.1). The north-facing cliff wall of the small island holds the only colony of guillemots, *Uria* sp., in the Nuuk district. The colony includes both Brünnich's (*Uria lomvia*) and common guillemot (*U. aalge*). These alcids are deep divers preying on fish and large zooplankton. Photo counts of birds present on the cliff were conducted from the sea (boat) on 7 July (table 5.6). The number of guillemots (both species) on the cliff was 437 individuals, which is less than in 2013. The number of guillemots on the water was estimated to be around 300. It should be noted that the birds were quite nervous and took flight before the boat was within 3-400 metres of the colony. Also observed at the colony were 18 glaucous gulls.

In order to address the proportion of the boreal distributed common guillemot versus the arctic Brünnich's guillemot in the colony, an analysis of digital photographs is usually performed. This is interesting in the context of climate change where the proportion of common guillemot could be expected to increase in a warmer climate (table 5.6). Due to the distance and the quality of the photos, the two species could not be distinguished and the analysis was not performed this year.

Other seabird observations south of Nuuk

Simiutat consists of three small islands. The following was observed:

Simiutat (63011) 7 July: Four puffins (*Fratercula arctica*), three black guillemots, one pair of great black-backed gull, two pairs of glaucous gull, ten female common eiders (*Somateria mollissima*) – four of them with ducklings.

Simiutat (63012) 7 July 7: 24 puffins, eight guillemots (*Uria sp.*), approx. 30 black guillemots, ten common eiders and two male harlequin ducks. 20 glaucous gull as well as 13 great black-backed gulls of unknown breeding status were seen on the island. Two Canada geese (*Branta canadensis*) were observed on the island.

Simiutat (63013) 7 July : 35 glaucous gulls, 11 great black-backed gulls, 26 resting great cormorants (*Phalacrocorax carbo*), one pair of Canada geese with six ducklings, and 11 northern fulmar (*Fulmarus glacialis*).

"The Puffin Island" at Ravneøerne (63020) 15 July: 288 puffins around the island, one razorbill, four common guillemots, 38 black guillemots, 39 common eiders, four harlequin ducks, one great cormorant and one Canada goose.

Qarajat Qeqertaat (63019) 7 July: This site consists of two islands with breeding common eiders:

West island: 23 nests of common eiders (one nest with cold eggs). Average of 3.8 eggs/chicks per non-empty nest. Additionally 26 eiders (22 ♀ and 4 ♂ with 2 broods ~ 9 ducklings) were resting on the water. Otherwise 165 black guillemots, four purple sandpipers, five great black-backed gulls and 10-12 young Iceland or glacous gulls. Two nests of gulls with one and two eggs were found.

East island: 29 nests of common eider. Average of 3.4 eggs per nest with eggs. Additionally one nest with one egg was abandoned and ten empty nests were found. Otherwise 216 black guillemots around the island, one purple sandpiper and one pair of Arctic skua (*Stercorarius* *parasiticus*) (one light and one dark morph), 11 great black-backed gulls and 50 mixed glaucous and Iceland gulls flying above the island. Five gull's nests were found, with a variety of eggs and chicks.

5.7 Marine mammals

West Greenland is a summer feeding ground for an estimated 3200 humpback whales, *Megaptera novaeangliae* (Heide-Jørgensen *et al.* 2012). Most of them stay on the off-shore banks, but some visit the fjords and bays to feed on zooplankton and capelin *Mallotus villosus* (Heide-Jørgensen and Laidre 2007). Some of these whales have a high degree of site fidelity to Godthåbsfjord and return year after year to feed but also new individuals visit the fjord annually (Boye *et al.* 2010). In the MarineBasis monitoring programme, we use photo-identification to estimate the number of humpback whales feeding in Godthåbsfjord each summer and the turnover of whales during a season to understand how much these top-predators eat and thus affect the Godthåbsfjord ecosystem.

Photo-identification is a technique used to identify individual animals from photographs showing natural markings such as scars, nicks and coloration patterns (Katona *et al.* 1979). The technique can, in combination with mark-recapture analysis, be used for estimating abundance of marine mammals in specific areas. Photo-identification is also used to investigate residence time (i.e. how long the animals stay in a given area) and site fidelity (i.e. individuals returning to an area in different years) (e.g. Bejder and Dawson 2001). In humpback whales, the ventral side of the fluke is used for identification as the tail contains individual colour patterns, which in a way is comparable to human fingerprints. Photo-identification pictures were taken with a 350 EOS Canon camera with a 300 mm Canon lens. In addition to dedicated surveys, guides on the local whale tourist boats and the public kindly contributed with identification-photos. The dedicated surveys were carried out twice a week depending on the weather from May to October 2013 from small research boats. Only a single survey was conducted in 2014 due to personnel limitation. The rest of the photos from this given period were sent in by locals and tourist.

A total of 88 and 18 ID pictures were collected in Godthåbsfjord in 2013 and 2014, respectively. Of the 33 identified whales in 2013, 36 % had been identified previously (2007-2012) in the fjord and 27 % of the whales identified in 2013 had also been identified in 2012. Of the 10 identified whales in 2014, 60 % had been identified previously (2007-2013) and all of these were also present in 2013. In the period 2007-2014 a total of 619 ID photos have been collected and with these, a total of 101 individual whales have been identified in Godthåbsfjord so far (table 5.7).

May and early June are the months where most whales are seen in the fjord (figure 5.27 and 5.28) likely due to an influx of whales on their northward

Table 5.7 Humpback whale site fidelity to Godthåbsfjord in 2007-2014. Percentage of whales (within 2007-2014), identified in a given year and re-identified the following year in brackets.

				No. of whales seen in each subsequent year						
Year	**No. of photos**	**ID**	**N**	**2008**	**2009**	**2010**	**2011**	**2012**	**2013**	**2014**
2007	49	20	20	8 (40)	6 (40)	7 (27)	5 (24)	5 (19)	5 (15)	2 (20)
2008	143	20	12		6 (40)	10 (38)	7 (33)	9 (33)	8 (24)	4 (40)
2009	38	15	8			7 (27)	6 (29)	8 (30)	4 (12)	2 (20)
2010	68	26	13*				9 (43)	9 (33)	9 (27)	3 (30)
2011	130	21	10*					10 (37)	8 (24)	3 (30)
2012	85	27	13*						9 (27)	5 (50)
2013	88	33	21							6 (60)
2014	18	10	4*							
Total	**619**	**172**	**101**							

*Contains individuals photographed in the fjord prior to 2007
ID number of whales identified the given year
N the number of new individuals the given year

Figure 5.27 Greenland Institute of Natural Resources putting transmitters on humpback whales in Godthåbsfjord near Nuuk. (Photo: Anders Møller).

migration. Sightings drop during summer and reach a minimum in August. In September, sightings increase again which correspond the time where the whales commence their southward migration. The individuals with the highest degree of site fidelity are also the individuals that stay within the fjord for the longest periods of time during the feeding period and are therefore encountered more often (Boye *et al.* 2014). In Godthåbsfjord, between 10 and 33 individuals has been photographed each year.

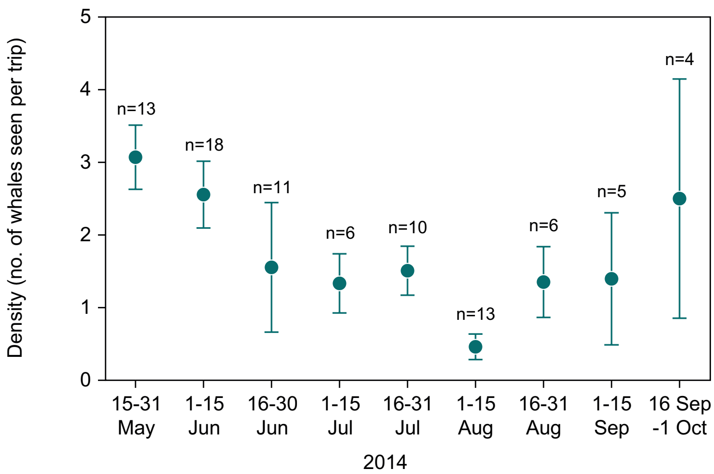

Figure 5.28 Density of whales with SE. Most whales are spotted during late spring and early autumn. n = effort by the authors on the water in days in the given period (figure from Boye et al. *2014).*

6 Research projects

6.1 The influence of icebergs, glacial meltwater and suspended sediments on iron and nutrient concentrations in a Greenlandic fjord

Mark Hopwood, Doug Connelly, Kristine Arendt, Thomas Juul-Pedersen, Mark Stinchcombe and Lorenz Meire

In addition to influencing the physical structure of the water column in Greenland's fjords, glacial meltwater can exert a strong influence on nutrient budgets. Glaciers can supply dissolved organic carbon (Barker *et al.* 2006; Bhatia *et al.* 2013; Hood *et al.* 2009), dissolved Si (Azetsu-Scott & Syvitski 1999) and the micronutrient Fe (Bhatia *et al.* 2013; Gerringa *et al.* 2012; Statham *et al.* 2008) to adjacent lakes and coastal waters. In May and August 2014, we collected samples for macronutrient (nitrate, phosphate and dissolved Si) concentrations, dissolved organic carbon (DOC) and dissolved Fe samples along Godthåbsfjord.

Comparison of the two transects, the first before the annual meltwater season commenced and the second at peak meltwater discharge, allowed us to determine the effects of meltwater input on fjord nutrient budgets and the export of nutrients to coastal ecosystems. Freshwater samples from accessible runoff streams and melted icebergs were also analysed in order to assess how changes in freshwater flux will affect nutrient biogeochemistry in Greenland's fjords (figure 6.1).

Fe is of specific interest because of the potential for Fe export from Greenland to offshore ecosystems where Fe can be a limiting or co-limiting nutrient. Some authors have argued that increasing meltwater from the Greenland Ice Sheet will increase the flux of Fe to offshore ecosystems (Bhatia *et al.* 2013; Hawkings *et al.* 2014). We, however, have challenged this hypothesis because the physical circulation around Greenland's fjords is unfavourable for export of micronutrients away from the Greenland Ice Sheet (Hopwood *et al.* 2015). Our data from May and August 2014 are the first to investigate Fe movement through Greenland's fjords and our results support the argument that Fe export is not enhanced by increasing freshwater input. Dissolved and total Fe concentrations were almost identical at the mouth of Godthåbsfjord in May and August despite the presence of freshwater plume due to meltwater input along the fjord in August.

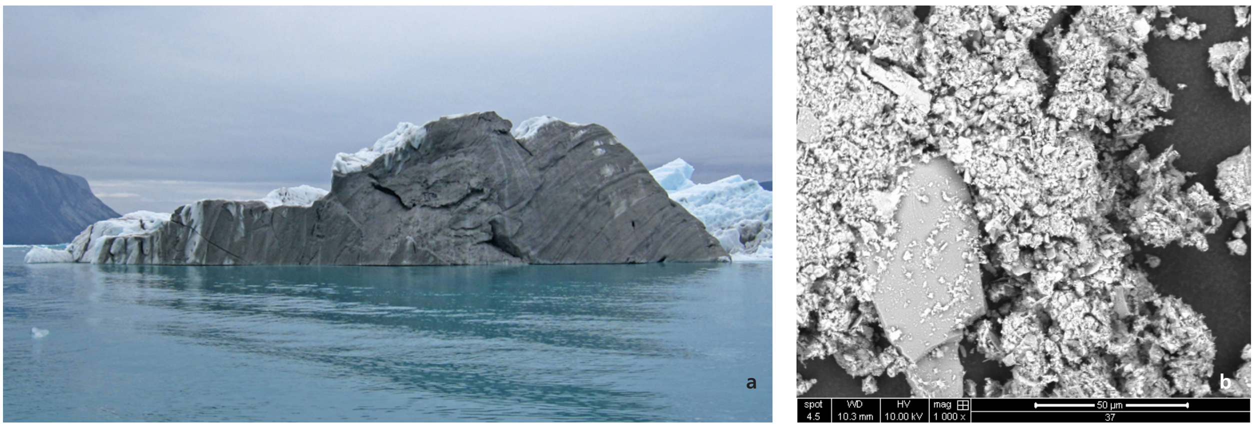

Figure 6.1 Iceberg with a surface coating of glacial flour. Scanning electron microscopy image of glacial flour collected from iceberg within Godthåbsfjord.

Figure 6.2 Marie is making a log book of a stream site on the north shore of Langesø. Photo: Ole Geertz-Hansen.

6.2 Food web structures of low Arctic lakes and streams

Marie Buchardt

The aim of this study was to analyse food webs of low Arctic lakes and streams in Kobbefjord to elucidate the role of fish in food web structuring. This we did by examining whether fish feed similarly across different lake habitats and whether the presence of fish affects stream food webs, potentially creating top-down control (figure 6.2). Our hypotheses were that: (1) fish, due to their mobility, feed similarly across different habitats, thereby coupling the habitats of the lake, and (2) the presence of fish decreases the number of food sources exploited by invertebrates (thus narrowing the food web). We examined this by analysing the content of the stable isotopes ^{13}C and ^{15}N of food web components, giving information on food items (^{13}C) and at which trophic level the sampled organism was placed in the food web (^{15}N).

Lakes: The results for the lakes are reported in the "Lakes" section of the present BioBasis report. It was found that Arctic char occupied two trophic levels of the lake food webs and that it changes trophic position at a fork length of approx. 20 cm. Arctic char > 20 cm exploited the same carbon sources despite being caught in different habitats of the lake. The smaller Arctic char (< 20 cm) fed on similar resources in the shallow Langesø, but in the deeper Badesø there was a difference in food sources between lake zones.

Streams: Use of Layman metrics on the isotope data from 14 streams showed that the invertebrates in the fishless streams exploited a greater range of the food sources present and were more differentiated in their isotopic niche.

Conclusions: Large Arctic char in Badesø and Langesø foraged in more than one habitat and were therefore able to move energy and thus couple the habitats. However, smaller Arctic char were only able to couple habitats in the shallow and smallest lake (Langesø). In the streams, we found that the presence of fish narrowed the invertebrate food webs due to top-down control, which led to a behavioural change of invertebrates to avoid predators.

Torben L. Lauridsen, Aarhus University, Department of Bioscience was main supervisor and Ole Geertz-Hansen, Greenland Natural Resource Institute, co-supervisor. The master thesis was defended on 29 May 2015.

7 Disturbances in the study area

Maia Olsen

The study area at Kangerluarsunnguaq/Kobbefjord is situated approx. 20 km south-east of Nuuk and can be reached by boat within half an hour. It is a public area and admittance is free to anyone.

Public disturbance falls in the following categories:

- Visits by boat in the head of the fjord – no landing.
- Visits by boats in the head of the fjord – people take a short walk inland and returns within a few hours or less.
- Visits by boats in the head of the fjord – people go on land and spend the night in a tent close to the coast.
- Hiking through the area – there is a hiking route from Nuuk to the inland passing through the area.
- Visits by snow mobile – during winter people visit the area from Nuuk.
- The electrical power transmission line between Nuuk and the hydro power plant in Kangerluarsunnguaq/Buksefjord runs through the area.
- Ordinary flights by fixed winged aircrafts passing over the study area in cruising altitude or in ascent or descent to or from Nuuk.
- Helicopter flights at cruising altitude passing over the study area or following the transmission line at low altitude.
- Helicopter flights visiting the climate stations for maintenance – once or twice during the season.

There have been only few interactions between visitors in the study area and the different setups and the cabin. In July, a large group of people camped in a number of tents in the area between the bridge and the BioBasis gas-flux setup for one night. Foxes have moved and laid droppings in the pitfall traps. The cabin has undergone repair necessitating a number of visits from craftsmen.

The monitoring programmes themselves have brought disturbance to the area, i.e. transportation between Nuuk and the head of the fjord, housing of personnel, walking between study plots and around study plots. Especially around the permanent plots in the *Empetrum* heaths and the fens have signs of wear. Furthermore, the wear around and between the BioBasis gas-flux measuring plots has become increasingly noticeable. The area close to the cabin, where most visitors put up their tents, is showing signs of wear as is the trail between the boat landing site and the cabin.

Transportation between Nuuk and the study site in Kangerluarsunnguaq/Kobbefjord has been conducted on an irregular basis, but during most of the season there was transportation two to three days a week (Tuesdays and Thursdays, or Mondays, Wednesdays, and Fridays). During most of the season the cabin was used temporarily by two to four persons.

Walking around the study plots has had a wearing effect on the vegetation and it should be considered to mark permanent trails between study sites and study plots.

In conclusion, it is estimated that monitoring activities only had minor impact on the vegetation and terrain.

8 Logistics

Henrik Philipsen

In 2014, the Greenland Institute of Natural Resources (GINR) Logistics section took care of the transport and maintenance work related to NuukBasic in Kobbefjord in co-operation with experienced people from the NuukBasic programmes.

The 2014 field season in Kobbefjord started on 14 January and ended on 14 November. In this period 49 scientists and logistics staff had 265 man-days and 56 man-days respectively, in the study area.

The transportation of logistics staff, technicians, scientists, visitors and guests from Nuuk to the research area in Kobbefjord was carried out by GINR's boats "Erisaalik" and "Aage V. Jensen II Nuuk". The boats were donated by the Aage V. Jensen Charity Foundation in 2005 and 2007. The total number of sailing days to Kobbefjord used by Logistics, BioBasis, GeoBasis and ClimateBasis were 74 in 2014. MarinBasis used 28 sailing days from 20 January to 17 December to sail to study areas in Kobbefjord and Godtshåbsfjord.

In 2013/2014 the winter was hard, but it was possible to sail to the bottom of Kobbefjord with GINR's boat "Erisaalik" in January. From early February until late May there inner 2-5 km of Kobbefjord was covered with ice. In March and April, NuukBasis labourers were disembarked at the edge of the ice from where they walked or used skies to get to the cabin and study area. From 3 June until 14 November there was no sea ice in Kobbefjord.

33 official and other guests made visits to the research area in Kobbefjord in 2014:

18 July: GEM Evaluation group with Steve Albon, professor, The James Hutton Institute, Scotland; Kim Holmén, international director, Norwegian Polar Institute, Norway; Jörn Thiede, professor, St. Petersburg State University, Russia and Henning Thing, senior advisor, Niels Bohr Institute, Denmark.

25 August: Freja and Jakob Bendtsen, Alfa Film, Denmark; Henrik Egede Lassen, Zoomedia, Denmark.

27 August: Mette Fabricius Skov, chairman of Aage V. Jensen Charity Foundation together with Jens Haugbyrd and Dorte Mette Jensen; Klaus Nygård, director, GINR; Søren Rysgård, professor, Arctic Research Centre, Aarhus University; Peter Schmidt Mikkelsen, administrative employee, Arctic Research Centre, Aarhus University.

10 September: 1 teacher and 9 journalist students from Greenland; Dorte Søgård, cand.scient., PhD, GINR and 7 PhD students.

26 September: two French freelance journalists.

NuukBasic scientists who do not live in Nuuk were accommodated in the GINR's Annex and Biologstationen where they spent a total of 178 nights. Accommodation in the cabin and tents in Kobbefjord was 87 in total.

The buildings are raised in 2008 and 2009 and are donated by the Aage V. Jensen Charity Foundation.

The cabin has a ramp for skidoo, catwalk, terrace and 11 m² storing room under the living room. The cabin is fitted with an entrance, laboratory with hot and cold water, bathroom with earth closet and shower, living room with kitchen, four berths and a heating oven.

The generator hut is equipped with a ramp, working bench, vice and tools.

The cabin and the generator hut were tar painted in 2014. Due to mould around the back entrance of the cabin, a larger repair work and replacement of timber and sealing of the doorframe were done in 2014. Drip caps were attached to the outside window frames on the northern gable.

Water supply came from the nearby river and was connected from mid-June until late September. Electric power was delivered from two portable 3 and 4 kW gasoline generators from 2008 and 2012 and a 5 kW diesel generator. One new 3 kW gasoline generator was bought in 2014.

Communication to Nuuk was done using Iridium satellite telephones while local communication to boats and others used portable VHF-radios. Two portable VHF-radios were ruined and four new ones were bought.

In 2014, the gasoline consumption for generators was 514 liters. The heating oven inside the cabin used 60 liters of diesel. The four diesel barrels were placed on pallets.

Freshwater consumption was 6450 liters in 2014. A drainpipe for grey household water was connected from early June until late September.

All kinds of daily household and toilet garbage – in total 500 kg – were returned to Nuuk during the season. A larger clean-up were done in the terrain and on 7 August a bonfire were made at the shoreline of burnable leftovers. Plastic and metal leftovers were sailed to Nuuk.

There were five operational days with the snowmobile in March and April. Unfortunately, the snowmobile rolled out and over a steep slope and it had several damages. The snowmobile was repaired in the cabin in September and October and is useable again.

Five helicopter trips were made by Air Greenland to the area in 2014. On 20 and 22 May, three scientists from Asiaq – Greenland Survey made a trip to a nearby glacier; on 17 to 19 July, three technicians from Asiaq – Greenland Survey performed maintenance work at the climate stations; on 28 July, four scientists from Asiaq – Greenland Survey again made a trip to the nearby glacier.

9 Acknowledgements

MarineBasis wish to acknowledge the crew on board the R/V Sanna for their valuable assistance during this year's May cruise. We also thank Thomas Krogh, Jens Weinell, Louise Mølgaard, Gabriela Garcia, Rebecca Scheuerlein, Maia Olsen, Lars Heilmann, Flemming Heinrich, Kunuk Lennert, Sofie R. Jerimiassen, Signe Jeremiassen, Jørgen Sethsen, Andrzej Witkowski and Marek Zajaczkowski for field and technical assistance. We would also like to acknowledge Paul Batty, Morten S. Frederiksen, Anna Haxen, Winnie Martinsen, Peter Bondo Christensen, Carsten Egevang, Bo Bergstrøm and Ditte M. Mikkelsen for their contribution to the programme in previous years.

10 Personnel and visitors

Compiled by Lillian Magelund Jensen

Anders Dan-Nielsen, Asiaq – Greenland Survey, Greenland
Antoine Frere, freelance journalist, France
Antti Lauri, University of Helsinki, Finland
Aqissiaq Jerimiassen, Asiaq – Greenland Survey, Greenland
Bastien Labat, freelance camera man, France
Birger Poppel, University of Greenland, Greenland
Birger Ulf Hansen, Department of Geosciences and Natural Resource Management, University of Copenhagen, Denmark
Bjarni Sigurdsson, Agricultural University of Iceland, Iceland
Carl Isaksen, Greenland Institute of Natural Resources, Greenland
Dorte Krause-Jensen, Aarhus University, Denmark
Dorte Mette Jensen, Aage V. Jensens Fonde, Denmark
Dorte Søgaard, Greenland Institute of Natural Resources, Greenland
Dorthe Petersen, Asiaq – Greenland Survey, Greenland
Ejgil Gravesen, Greenland
Emil Nielsen, Asiaq – Greenland Survey, Greenland
Eric Collins, University of Alaska Fairbanks, USA
Evan Firth, University of Washington, USA
Flemming Heinrich, Greenland Institute of Natural Resources, Greenland
Freja Bendtsen, Alphafilm, Denmark
Gitte Korff, Auditor general, Denmark
Hans Ole Jensen, Greenland Institute of Natural Resources, Greenland
Harry Lankreijer, Lund University, Norway
Heidi Sørensen, Greenland Institute of Natural Resources, Greenland
Helge Adam Møller, Controller and Auditor general, Denmark
Henning Thing, Danish Energy Agency, Denmark
Henrik Egede-Lassen, Zoomedia, Denmark
Henrik Lund, Greenland Institute of Natural Resources, Greenland
Henrik Philipsen, Greenland Institute of Natural Resources, Greenland
Henrik Thorup, Controller and Auditor general, Denmark
Horst Machguth, ARTEK – Center for Arktisk Teknologi – DTU, Denmark
Ingibjörg Jónsdóttir, University of Iceland, Iceland
Ivali Lennert, Institute of Natural Resources, Greenland
Jacob Bendtsen, Alphafilm, Denmark
Jakob Abermann, Asiaq – Greenland Survey, Greenland
Jens Frederik Rasmussen, Auditor general, Denmark
Jens Gottlieb, Asiaq – Greenland Survey, Greenland
Jens Haugbyrd, Aage V. Jensens Fonde, Denmark
Jessica Scheick, Asiaq – Greenland Survey, Greenland
John Iacozza, University of Manitoba, Canada
Jonathan N. K. Petersen, Asiaq – Greenland Survey, Greenland
Jørgen Broberg, Greenland Institute of Natural Resources, Greenland
Jörn Thiede, St. Petersburg State University, Russia
Josephine Nymand, Greenland Institute of Natural Resources, Greenland
Katrine Raundrup, Greenland Institute of Natural Resources, Greenland
Kim Holmén, Norwegian Polar Institute, Norway
Kim Jesper Jørgensen, Ministry of Defence, Denmark
Klaus Nygaard, Greenland Institute of Natural Resources, Greenland
Knud Kreutzmann, Greenland Institute of Natural Resources, Greenland
Krista Kenyon, University of Manitoba, Canada

Kristine Arendt, Greenland Institute of Natural Resources, Greenland
Lars Heilmann, Greenland Institute of Natural Resources, Greenland
Lennart Damsbo-Andersen, Controller and Auditor general, Denmark
Lise Buchardt, Aarhus University, Denmark
Lise Lotte Sørensen, Aarhus University, Denmark
Louise Holm Christensen, Asiaq – Greenland Survey, Greenland
Magnus Forsberg, Asiaq – Greenland Survey, Greenland
Maia Olsen, Greenland Institute of Natural Resources, Greenland
Majbritt Westring Sørensen, Asiaq – Greenland Survey, Greenland
Malene Simon, Greenland Institute of Natural Resources, Greenland
Malik Naamansen, Asiaq – Greenland Survey, Greenland
Maria L. Burup, Department of Geosciences and Natural Resource Management, University of Copenhagen, Denmark
Marie Buchardt, Aarhus University, Denmark
Mark Hopwood, University of Southampton, England
Martin Blicher, Greenland Institute of Natural Resources, Greenland
Mathias Madsen, Department of Geosciences and Natural Resource Management, University of Copenhagen, Denmark
Melisa Larsen, Asiaq – Greenland Survey, Greenland
Mette Fabricius Skov, Aage V. Jensens Fonde, Denmark
Mikhail Paramonov, University of Helsinki, Finland
Morten Birch Larsen, Greenland Institute of Natural Resources, Greenland
Naja O. Lennert, Greenland Institute of Natural Resources, Greenland
Ole Geertz-Hansen, Greenland Institute of Natural Resources, Greenland
Peder Larsen, Controller and Auditor general, Denmark
Per Hangaard, Asiaq – Greenland Survey, Greenland
Peter Hegelund, Institute of Natural Resources, Greenland
Peter Schmidt Mikkelsen, Institute of Natural Resources, Greenland
Qunaaq Møller, Greenland Institute of Natural Resources, Greenland
Rane Willerslev, Aarhus University, Denmark
Rasmus Egede, Asiaq – Greenland Survey, Greenland
Shelly Carpenter, University Of Washington, USA
Søren Rysgaard, Greenland Institute of Natural Resources, Greenland
Stefan Wacker, Asiaq – Greenland Survey, Greenland
Steffen Noe, Estonian University of Life Sciences, Estonia
Steve Albon, the James Hutton Institute, Scotland
Stine Kjær Petersen, Institute of Natural Resources, Greenland
Torben R. Christensen, University of Lund, Sweden & Greenland Climate Research Centre, Greenland
Wendy Loya, Greenland Institute of Natural Resources, Greenland
Yu Jia, Greenland Institute of Natural Resources, Greenland

4 painters, for painting the cabin
8 journalist students, 2 teachers, University of Greenland, Nuuk Greenland
11 persons, The Nordic Council of Ministers, Climate and Air Pollution Group (KoL), Denmark
2 persons from Arctic Command, Defence Command, Denmark

11 Publications

Compiled by Lillian Magelund Jensen

Scientific papers

Boye, T.K., Simon, M.J. and Witting, L. 2014. How may an annual removal of humpback whales from Godthaabsfjord, West Greenland, affect the within-fjord sighting rate? Journal of Cetacean Research and Management 14: 51-56.

Kjeldsen, K. K., Mortensen, J., Bendtsen, J., Petersen, D., Lennert, K. and Rysgaard, S. 2014. Ice-dammed lake drainage cools and raises surface salinities in a tidewater outlet glacier fjord, west Greenland. Journal of Geophysical Research: Earth Surface 119. doi:10.1002/2013JF003034.

Krawczyk, D. W., Witkowski, A., Waniek, J. J., Wroniecki, M. and Harff, J. 2014. Description of diatoms from the Southwest to West Greenland coastal and open marine waters. Polar Biology. doi: 10.1007/s00300-014-1546-2.

Mortensen, J., Bendtsen, J., Lennert, K. and Rysgaard, S. 2014. Seasonal variability of the circulation system in a west Greenland tidewater outlet glacier fjord, Godthåbsfjord (64°N). Journal of Geophysical Research: Earth Surface. doi: 10.1002/2014JF003267.

Riisgaard, K., Swalethorp, R., Kjellerup, S., Juul-Pedersen, T. and Nielsen, T.G. 2014. Trophic role and top-down control of a subarctic protozooplankton community. Marine Ecology Progress Series 500: 67-82.

Sejr, M. K., Krause-Jensen, D., Dalsgaard, T., Ruiz-Halpern, S., Duarte, C. M., Middelboe, M., Glud, R. N., Bendtsen, J., Balsby, T. J. S., and Rysgaard, S. 2014. Seasonal dynamics of autotrophic and heterotrophic plankton metabolism and P_{CO2} in a subarctic Greenland fjord. Limnology and Oceanography 59(5): 1764-1778. doi: 10.4319/lo.2014.59.5.1764.

Swalethorp, R., Malanski, E., Agersted, M. D., Nielsen, T.G. and Munk, P. 2014. Structuring of zooplankton and fish larvae assemblages in a freshwater influenced Greenlandic fjord: influence from hydrography and prey availability. Journal of Plankton Research. doi:10.1093/plankt/fbu099.

Swalethorp, R., Kjellerup, S., Malanski, E., Munk, P. and Nielsen, T.G. 2014. Feeding opportunities of larval and juvenile cod (*Gadus morhua*) in a Greenlandic fjord: temporal and spatial linkages between cod and their preferred prey. Marine Biology 161: 2831-2846. doi:10.1007/s00227-014-2549-9.

Teglhus, F. W., Agersted, M. A., Arendt, K. E. and Nielsen, T. G. 2014. Gut evacuation rate and grazing impact of the krill *Thysanoessa raschii* and *T. inermis*. Marine Biology. doi: 0.1007/s00227-014-2573-9.

Reports

Juul-Pedersen, T., Arendt, K.E., Mortensen, J., Krawczyk, D. W., Rysgaard, S., Retzel, A., Nygaard, R., Burmeister, A., Krause-Jensen, D., Marbà, N., Olesen, B., Sejr, M.K., Blicher, M.E., Meire, L., Geertz-Hansen, O., Labansen, A. L., Boye, T. and Simon, M. 2014. The Marin Basic programme 2013. In: Jensen, L.M. and Christensen, T.R. (eds.) 2014. Nuuk Ecological Research Operations, 7th Annual Report 2013, Aarhus University, DCE – Danish Centre for Environment and Energy. 94 pp.

Juul-Pedersen, T. and Hindrum, R. (eds). 2014. Circumpolar Biodiversity Monitoring Programme Marine Steering Group. 2014. Arctic Marine Biodiversity Monitoring Plan Annual Plan 2013: Annual Report on the Implementation of the Circumpolar Biodiversity Monitoring Programme's Arctic Marine Biodiversity Monitoring Plan (CBMP-Marine Plan). CAFF Monitoring Report No.12. CAFF International Secretariat, Akureyri, Iceland. ISBN: 978-9935-431-33-2.

Juul-Pedersen, T. 2014. Arctic Marine Biodiversity Monitoring Plan Greenland, 2013 Implementation. National one page update. Conservation of Arctic Flora and Fauna (CAFF).

Søgaard, D.H. 2014. Biological activity and calcium carbonate dynamics in Greenland sea ice – Implication for the inorganic carbon cycle. PhD thesis. Greenland Climate Research Centre and Department of Biology, University of Southern Denmark. Greenland Institute of Natural Resources, 148 pp.

Presentation at symposiums, workshops, meetings and conferences

Arendt, K.E. 2014. Introduction to Marine Ecology. Management of Natural Resources in Greenland, Ilisimatusarfik, 5 May. Nuuk, Greenland.

Arendt, K.E., Juul-Pedersen, T. and Sejr, M. 2014. Linking ocean-fjord-glacier interactions with pelagic biodiversity around Greenland. Arctic Biodiversity Congress, 2-5 December, Trondheim, Norway.

Juul-Pedersen, T. 2014. Arctic Regional Workshop to Facilitate the Description of Ecological or Biological Significant Marine Areas (EBSAs), 3-7 March, Helsinki, Finland.

Juul-Pedersen, T. 2014. Circumpolar Biodiversity Monitoring Programme (CBMP) – Annual Marine Steering Group and Expert Network Meeting, host and co-chair. 30 September – 2 October, Nuuk, Greenland.

Juul-Pedersen, T. 2014. Remote Sensing Needs Assessment Workshop for the Pan-Arctic, 1 December, Trondheim, Norway.

Juul-Pedersen, T. and Hindrum, R. 2014. CBMP Marine: Effects of stressors and drivers of relevance to biodiversity. Session Chairs. Arctic Biodiversity Congress, 2-5 December, Trondheim, Norway.

Krawczyk, D., Arendt, K. E., Juul-Pedersen, T., Mortensen, J., Blicher, M., Sejr, K., Jakobsen, H., Witkowski, A. and Rysgaard, S. 2014. What drives micro-plankton (phytoplankton) community structure and species diversity in offshore waters and fjords in Greenland? Arctic Biodiversity Congress, 2-5 December, Trondheim, Norway.

Mortensen, J. 2014. Coastal time series, ICES WGOH, 1-3 April, Hamburg, Germany.

Mortensen, J., Bendtsen, J. and Rysgaard, S. 2014.Circulation and heat sources for glacial melt in a west Greenland fjord, Arctic Change 2014, 8-12 December, Ottawa, Canada.

General information

Arendt, K.E. and Christensen, E. 2014. Smeltevand giver særegent liv i Nuup Kangerlua. Aktuel Naturvidenskab 1: 8-10.

Arendt, K.E. and Christensen, E. 2013. Det kribler og krabler i fjorden. Polarfronten 4: 12-13.

Søgaard, D. H. 2014. Climate Change workshop for Greenland High School teachers. September 11, Nuuk, Greenland.

Søgaard, D.H. 2014. Natural science day for students from Greenland High School. October 24, Nuuk, Greenland.

New publications

Ekici, A., Beer, C., Hagemann, S.; Boike, J., Langer, M., Hauck, C. 2014. Simulating high-latitude permafrost regions by the JSBACH terrestrial ecosystem model. Geosci. Model Dev. 7: 631-647. www.geosci-model-dev.net/7/631/2014/ doi:10.5194/gmd-7-631-2014.

Mbufong, H.N., Lund, M., Aurela, M., Christensen, T.R., Eugster, W., Friborg, T., Hansen, B.U., Humphreys, E.R., Jackowicz-Korczynski, M., Kutzbach, L., Lafleur, P.M.; Oechel, W.C., Parmentier, F.J.W., Rasse, D.P., Rocha, A.V., Sachs,T. van der Molen, M.M. and Tamstorf, M.P. 2014. Assessing the spatial variability in peak season CO_2 exchange characteristics across the Arctic tundra using a light response curve parameterization. Biogeosciences Discuss. 11: 6419-6460. www.biogeosciences-discuss.net/11/6419/2014/ doi:10.5194/bgd-11-6419-2014.

12 References

Compiled by Lillian Magelund Jensen

Azetsu-Scott, K. and Syvitski, J.P.M. 1999. Influence of melting icebergs on distribution, characteristics and transport of marine particles in an East Greenland fjord. Journal of Geophysical Research 104(C3): 5321. doi:10.1029/1998JC900083.

Barker, J.D., Sharp, M.J., Fitzsimons, S.J. and Turner, R.J. 2006. Abundance and dynamics of dissolved organic carbon in glacier systems. Arctic Antarctic and Alpine Research 38(2): 163-172. doi:10.1657/1523-0430(2006)38[163:aado do]2.0.co;2.

Bay, C., Aastrup, P., and Nymand, J. 2008. The NERO line – A vegetation transect in Kobbefjord, West Greenland. National Environmental Research Institute, Aarhus University, Denmark. NERI Technical Report No. 693, 40 pp.

Bejder, L. and Dawson, S. 2001. Abundance, residency and habitat utilisation of Hector's dolphins (*Cephalorhynchus hectori*) in Porpoise Bay, New Zealand. New Zealand Journal of Marine and Freshwater Research 35: 277-287.

Bhatia, M.P., Das, S.B., Xu, L., Charette, M.A., Wadham, J.L. and Kujawinski, E.B. 2013. Organic carbon export from the Greenland ice sheet. Geochimica Et Cosmochimica Acta 109: 329-344. doi:10.1016/j.gca.2013.02.006.

Bhatia, M.P., Kujawinski, E.B., Das, S.B., Breier, C.F., Henderson, P.B. and Charette, M.A. 2013. Greenland meltwater as a significant and potentially bioavailable source of iron to the ocean. Nature Geoscience 6(4): 274-278.

BioBasis, chapter 4 in Jensen, L.M., and Christensen, T.R. (eds.) 2014. Nuuk Ecological Research Operations, 7th Annual Report, 2013. Aarhus University, DCE – Danish Centre for Environment and Energy. 94 pp.

Boye, T.K., Simon, M.J. and Madsen, P.T. 2010. Habitat use of humpback whales in Godthåbsfjord, West Greenland, with implications for commercial exploitation. Journal of the Marine Biological Association of the United Kingdom 90: 1529-1538.

Boye, T.K., Simon, M. J. and Witting, L. 2014. How may an annual removal of humpback whales from Godthaabsfjord, West Greenland, affect the within-fjord sighting rate? Journal of Cetacean Research and Management 14: 51-56.

Cappelen, J. 2014. Greenland – DMI Historical Climate Data Collection 1873-2013 – with Danish Abstracts, DMI, Technical report 14-04.

Fortes, M.D. and Lüning, K. 1980. Growth rates of North Sea macroalgae in relation to temperature, irradiance and photoperiod. Helgoländer Meeresunters 34: 15-29.

Gerringa, L.J.A., Alderkamp, A.-C., Laan, P., Thuroczy, C.-E., De Baar, H.J.W., Mills, M.M. and Arrigo, K.R. 2012. Iron from melting glaciers fuels the phytoplankton blooms in Amundsen Sea (Southern Ocean): Iron biogeochemistry. Deep-Sea Research Part II: Topical Studies in Oceanography: 71-76: 16-31. doi:10.1016/j.dsr2.2012.03.007.

Hansen, B.U., Iversen, K.M., Tamstorf, M.P., Sigsgaard, C., Fruergaard, M., Højlund, S., Lund, M., Raundrup, K., Mastepanov, M., Falk, J.M., Ström, L., Westergaard, A., Rasmussen, B.H. and Christensen, T.R. 2010. Nuuk Basic: The GeoBasis Programme. In Jensen, L.M. and Rasch, M. (eds.). Nuuk Ecological Research Operations, 3rd Annual Report, 2009. National Environmental Research Institute, Aarhus University, Denmark, pp. 17-28.

Hansen B.U., Pedersen, S.H., Iversen, K.M., Tamstorf, M.P., Sigsgaard, C., Fruergaard, M., Højlund, S., Lund, M., Raundrup, K., Mastepanov, M., Ström, L., Westergaard-Nielsen, A., Rasmussen, B.H. and Christensen, T.R. 2011. Nuuk Basic: The GeoBasis Programme. In Jensen, L.M. and Rasch, M. (eds.).

Nuuk Ecological Research Operations, 4th Annual Report, 2010. National Environmental Research Institute, Aarhus University, Denmark, pp. 19-29.
Hansen, B.U., Hill, K., Pedersen, S.H., Christensen, L.H., Tamstorf, M.P., Sigsgaard, C., Fruergaard, M., Lund, M., Raundrup, K., Mastepanov, Westergaard-Nielsen, A. and Christensen, T.R. 2012. Nuuk Basic: The GeoBasis Programme. In Jensen, L.M. (ed.). Nuuk Ecological Research Operations, 5th Annual Report, 2011. National Environmental Research Institute, Aarhus University, Denmark, pp. 19-32.
Hansen, B.U., Christensen, L.H., Tamstorf, M.P., Lund, M., Højlund, S., Burup, M.L., Raundrup, K., Mastepanov, M., Westergaard-Nielsen, A. and Christensen, T.R. 2013. Nuuk Basic: The GeoBasis Programme. In Jensen, L.M. and Rasch, M. (eds.). Nuuk Ecological Research Operations, 6th Annual Report, 2012. National Environmental Research Institute, Aarhus University, Denmark, pp. 17-32
Hansen, B.U., Christensen, L.H., Tamstorf, M.P., Lund, M., Højlund, S., Burup, M.L., Raundrup, K., Mastepanov, M., Westergaard-Nielsen, A. and Christensen, T.R. 2014. Nuuk Basic: The GeoBasis Programme. In Jensen, L.M. and Christensen, T.R. (eds.). Nuuk Ecological Research Operations, 7th Annual Report 2013. National Environmental Research Institute, Aarhus University, Denmark, pp. 19-33.
Hawkings, J.R., Wadham, J.L., Tranter, M., Raiswell, R., Benning, L.G., Statham, P.J. and Telling, J. 2014. Ice sheets as a significant source of highly reactive nanoparticulate iron to the oceans. Nature Communications 5(3929). doi:10.1038/ncomms4929.
Heide-Jørgensen, M.P. and Laidre, K.L. 2007. Autumn space-use patterns of humpback whales (*Megaptera novaeangliae*) in West Greenland. Journal of Cetacean Research and Management 9: 121-126.
Heide-Jørgensen, M.P., Laidre, K.L., Hansen, R.G., Burt, M.L., Simon, M., Borchers, D.L., Hansen, J., Harding, K., Rasmussen, M., Dietz, R. and Teilmann, J. 2012. Rate of increase and current abundance of humpback whales in West Greenland. Journal of Cetacean Research and Management 12: 1-14.
Hood, E., Fellman, J., Spencer, R.G.M., Hernes, P.J., Edwards, R., D'Amore, D. and Scott, D. 2009. Glaciers as a source of ancient and labile organic matter to the marine environment. Nature, 462: 1044-1047. doi: 10.1038/nature08580.
Hopwood, M.J., Bacon, S., Arendt, K., Connelly, D.P. and Statham, P.J. 2015. Glacial meltwater from Greenland is not likely to be an important source of Fe to the North Atlantic. Biogeochemistry. doi:10.1007/s10533-015-0091-6.
Høgslund, S., Sejr, M.K., Wiktor Jr., J., Blicher, M.E. and Wegeberg, S. 2014. Intertidal community composition along rocky shores in South-west Greenland: a quantitative approach. Polar Biology 37: 1549-1561. doi:10.1007/s00300-014-1541-7.
Iversen, K. M., Højmark, S. and Thorsøe, K. 2008. The ClimateBasic programme. In Jensen, L.M. and Rasch, M. (eds.). Nuuk Ecological Research Operations, 1st Annual Report, 2007. National Environmental Research Institute, Aarhus University, Denmark, pp. 13-18.
Jensen, L.M. and Rasch, M. (eds.) 2009. NERO – Nuuk Ecological Reseach Operations. 2nd Annual Report 2008. Roskilde, National Environmental Research Institute, Aarhus University. 80 pp.
Jensen, L.M. and Rasch, M. (eds.) 2008. NERO – Nuuk Ecological Reseach Operations. 1st Annual Report 2007. Copenhagen, Danish Polar Center, Danish Agency for Science, Technology and Innovation, Ministry of Science, Technology and Innovation. 112 pp.
Katona, S.K., Baxter, B., Brazier, O., Kraus, S., Perkins, J. and Whitehead, H. 1979. Identification of humpback whales by fluke photographs. The behavior of marine mammals. In Winn, H.E. and Olla, B.L. (eds.). Behavior of marine mammal science. Volume 3. Cetaceans. Plenum press, New York, NY, pp 33-44.
Mønster, T. 2013. Betydningen af klimaforandringer for vækst og dybdeudbredelse af *Callitriche hamulata* i lavarktiske søer i Grønland. MSc Thesis, Aarhus University, Denmark, 54 pp.
Pernosky, M.A., Hangaard, P. and Larsen, M. 2012. ClimateBasis Monitoring Program Nuuk Basic, 2011. Asiaq Report no. 2012-05. 40 pp
Statham, P.J., Skidmore, M. & Tranter, M. 2008. Inputs of glacially derived dissolved and colloidal iron to the coastal

ocean and implications for primary productivity. Global Biogeochemical Cycles 22(3). doi:10.1029/2007gb003106.
Tamstorf, M.P., Iversen, K.M., Hansen B.U., Sigsgaard, C., Fruergaard, M., Højlund, S., Andreasen, R.H., Mastepanov, M., Falk, J.M., Ström, L. and Christensen, T.R. 2009. Nuuk Basic: The GeoBasis Programme. In Jensen, L.M. and Rasch, M. (eds.). Nuuk Ecological Research Operations, 2nd Annual Report, 2008. National Environmental Research Institute, Aarhus University, Denmark, pp. 18-25.
Åberg, P.A. 1992a. A demographic study of two populations of the seaweed *Ascophyllum nodosum*. Ecology 73: 1473-1487.
Åberg, P.A. 1992b. Size-based demography of the seaweed *Ascophyllum nodosum* in stochastic environments. Ecology 73: 1488-1501.
Aastrup, P., Nymand, J., Raundrup, K., Lauridsen, T.L., Krogh, P.H., Schmidt, N.M., Illeris, L. & Ro-Poulsen, H. 2009. NuukBasic. Conceptual design and sampling procedures of the biological programme of NuukBasic. National Environmental Research Institute, Aarhus University. 70 pp. NERI Technical Report No. 745. http://www.dmu.dk/Pub/FR745.pdf

Appendix

Regular years	Jan	Feb	Mar	Apr	May	Jun	Jul	Aug	Sep	Oct	Nov	Dec
1	1	32	60	91	121	152	182	213	244	274	305	335
2	2	33	61	92	122	153	183	214	245	275	306	336
3	3	34	62	93	123	154	184	215	246	276	307	337
4	4	35	63	94	124	155	185	216	247	277	308	338
5	5	36	64	95	125	156	186	217	248	278	309	339
6	6	37	65	96	126	157	187	218	249	279	310	340
7	7	38	66	97	127	158	188	219	250	280	311	341
8	8	39	67	98	128	159	189	220	251	281	312	342
9	9	40	68	99	129	160	190	221	252	282	313	343
10	10	41	69	100	130	161	191	222	253	283	314	344
11	11	42	70	101	131	162	192	223	254	284	315	345
12	12	43	71	102	132	163	193	224	255	285	316	346
13	13	44	72	103	133	164	194	225	256	286	317	347
14	14	45	73	104	134	165	195	226	257	287	318	348
15	15	46	74	105	135	166	196	227	258	288	319	349
16	16	47	75	106	136	167	197	228	259	289	320	350
17	17	48	76	107	137	168	198	229	260	290	321	351
18	18	49	77	108	138	169	199	230	261	291	322	352
19	19	50	78	109	139	170	200	231	262	292	323	353
20	20	51	79	110	140	171	201	232	263	293	324	354
21	21	52	80	111	141	172	202	233	264	294	325	355
22	22	53	81	112	142	173	203	234	265	295	326	356
23	23	54	82	113	143	174	204	235	266	296	327	357
24	24	55	83	114	144	175	205	236	267	297	328	358
25	25	56	84	115	145	176	206	237	268	298	329	359
26	26	57	85	116	146	177	207	238	269	299	330	360
27	27	58	86	117	147	178	208	239	270	300	331	361
28	28	59	87	118	148	179	209	240	271	301	332	362
29	29		88	119	149	180	210	241	272	302	333	363
30	30		89	120	150	181	211	242	273	303	334	364
31	31		90		151		212	243		304		365

Day of Year

Leap years	Jan	Feb	Mar	Apr	May	Jun	Jul	Aug	Sep	Oct	Nov	Dec
1	1	32	61	92	122	153	183	214	245	275	306	336
2	2	33	62	93	123	154	184	215	246	276	307	337
3	3	34	63	94	124	155	185	216	247	277	308	338
4	4	35	64	95	125	156	186	217	248	278	309	339
5	5	36	65	96	126	157	187	218	249	279	310	340
6	6	37	66	97	127	158	188	219	250	280	311	341
7	7	38	67	98	128	159	189	220	251	281	312	342
8	8	39	68	99	129	160	190	221	252	282	313	343
9	9	40	69	100	130	161	191	222	253	283	314	344
10	10	41	70	101	131	162	192	223	254	284	315	345
11	11	42	71	102	132	163	193	224	255	285	316	346
12	12	43	72	103	133	164	194	225	256	286	317	347
13	13	44	73	104	134	165	195	226	257	287	318	348
14	14	45	74	105	135	166	196	227	258	288	319	349
15	15	46	75	106	136	167	197	228	259	289	320	350
16	16	47	76	107	137	168	198	229	260	290	321	351
17	17	48	77	108	138	169	199	230	261	291	322	352
18	18	49	78	109	139	170	200	231	262	292	323	353
19	19	50	79	110	140	171	201	232	263	293	324	354
20	20	51	80	111	141	172	202	233	264	294	325	355
21	21	52	81	112	142	173	203	234	265	295	326	356
22	22	53	82	113	143	174	204	235	266	296	327	357
23	23	54	83	114	144	175	205	236	267	297	328	358
24	24	55	84	115	145	176	206	237	268	298	329	359
25	25	56	85	116	146	177	207	238	269	299	330	360
26	26	57	86	117	147	178	208	239	270	300	331	361
27	27	58	87	118	148	179	209	240	271	301	332	362
28	28	59	88	119	149	180	210	241	272	302	333	363
29	29	60	89	120	150	181	211	242	273	303	334	364
30	30		90	121	151	182	212	243	274	304	335	365
31	31		91		152		213	244		305		366

Greenland Ecosystem Monitoring

Greenland Ecosystem Monitoring (GEM) is an integrated monitoring and long-term research programme on ecosystem dynamics and climate change effects and feedbacks in Greenland.

ClimateBasis Programme

The GEM ClimateBasis Programme studies climate and hydrology providing fundamental background data for the other GEM programmes.

GeoBasis Programme

The GEM GeoBasis Programme studies abiotic characteristics of the terrestrial environment and their potential feedbacks in a changing climate.

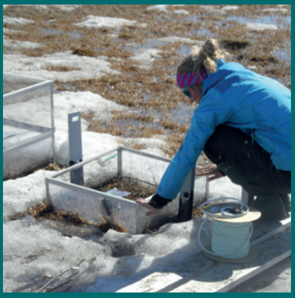

BioBasis Programme

The GEM BioBasis Programme studies key species and processes across plant and animal populations and their interactions within terrestrial and limnic ecosystems.

MarineBasis Programme

The GEM MarineBasis Programme studies key physical, chemical and biological parameters in marine environments.

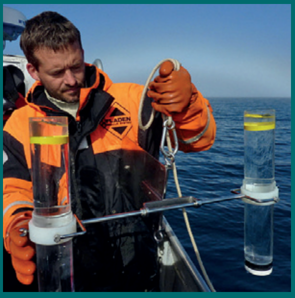

GlacioBasis Programme

The GEM GlacioBasis Programme studies ice dynamics, mass balance and surface energy balance in glaciated environments (only at Zackenberg Research Station).

AARHUS UNIVERSITY

ASIAQ

GEUS

Grønlands Naturinstitut
Pinngortitaleriffik • Greenland Institute of Natural Resources

DTU Technical University of Denmark

UNIVERSITY OF COPENHAGEN